



ISSN 1454-8518

**ANNALS  
OF THE UNIVERSITY OF  
PETROȘANI**  
*ELECTRICAL ENGINEERING*  
**VOL. 13 (XXXX)**

**UNIVERSITAS PUBLISHING HOUSE  
PETROȘANI - ROMANIA 2011**

ISSN 1454-8518

**EDITOR OF PUBLICATION**

Prof. Dr. Eng. Ioan-Lucian BOLUNDUȚ, Email: ibol@upet.ro

**ADVISORY BOARD**

**Prof. Dr. Eng. Alexandru BITOLEANU** - University of Craiova, *Romania*; **Prof. Dr. Eng. Stanislaw CIERPISZ** – Silesian University of Technology, *Poland*; **Prof. Dr. Eng. Tiberiu COLOȘI** - Technical University of Cluj-Napoca, *Romania*; **Acad. Prof. Dr. Eng. Predrag DAŠIĆ** - High Technological Technical School, Krusevac, *Serbia and Montenegro*, **Dr. Eng. Nicolae DAN**- Dessault Systems Simulia Corp., Providence, *USA*; **Assoc. Prof. Dr. Daniel DUBOIS** - University of Liège, *Belgium*; **Prof. Dr. Eng. Ion FOTĂU** - University of Petroșani, *Romania*; **Dr. Eng. Emilian GHICIOI**, INCD INSEMEX Petroșani, *Romania*; **Prof. Dr. Eng. Vladimir KEBO** -Technical University of Ostrava, *Cehia*; **Prof. Dr. Eng. Vladimir Borisovich KLEPIKOV**– National Technical University of Kharkov, *Ukraine*; **Assoc. Prof. Dr. Eng. Ernő KOVÁCS** - University of Miskolc, *Hungary*; **Prof. Dr. Eng. Gheorghe MANOLEA** - University of Craiova, *Romania*; **Prof. Dr. Eng. Radu MUNTEANU** - Technical University of Cluj-Napoca, *Romania*; **Assoc. Prof. Dr. Dan NEGRUT** University of Wisconsin-Madison, *USA*; **Prof. Dr. Eng. Mihai PĂSCULESCU** - University of Petroșani, *Romania*; **Acad. Prof. Dr. Eng. Ghenady PIVNYAK** – National Mining Uninersity of Ukraine, *Ukraine*; **Prof. Dr. Eng. Aron POANTĂ** - University of Petroșani, *Romania*; **Prof. Dr. Eng. Emil POP** - University of Petroșani, *Romania*; **Prof. Dr. Eng. Flavius Dan ȘURIANU** – “Politehnica” University of Timișoara, *Romania*; **Prof. Dr. Eng. Willibald SZABO** – “Transilvania” University of Brașov, *Romania*; **Prof. Dr. Eng. Alexandru VASILIEVICI** – “Politehnica” University of Timișoara, *Romania*.

**EDITORIAL BOARD****Editor-in-chief:**

**Prof. Dr. Eng Ion FOTĂU** University of Petroșani  
**Assoc. Prof. Dr. Eng. Susana ARAD** University of Petroșani

**Associate Editor:**

**Assoc. Prof. Dr. Eng Corneliu MÂNDRESCU** University of Petroșani  
**Assoc. Prof. Dr. Eng. Nicolae PĂTRĂȘCOIU** University of Petroșani  
**Assoc. Prof. Dr. Eng. Ilie UȚU** University of Petroșani

**Editor Secretary:**

**Assist. Dr. Eng. Florin Gabriel POPESCU** University of Petroșani  
**Lecturer Dr. Eng. Bogdan SOCHIRCA** University of Petroșani

**Editorial office address:** 20 University Street, 332006 Petroșani, Romania, Phone: +(40) 254 542 580; +(40) 254 542 581; Fax: +(40) 254 543 491, Contact person: **Susana ARAD**, e-mail: [susanaarad@yahoo.com](mailto:susanaarad@yahoo.com).

This publication is distributed worldwide to 28 countries.

## CONTENTS

<b>Ilie Uțu, Maria Daniela Stochițoiu, Applications of power electronics in electromechanical drives from mining plants.....</b>	<b>5</b>
<b>Adrian Ioan Toma, Florin Gabriel Popescu, Constantin Leon Pană, Dynamic compensation of the reactive energy for electric arc furnace used in steel factory.....</b>	<b>11</b>
<b>Brana Liliana Samoila, Teodor Tăbăcaru, Solar panel control system.....</b>	<b>17</b>
<b>Titu Niculescu, Study of electro-dynamics forces in short circuit regime using matlab-simulink software.....</b>	<b>23</b>
<b>Adrian Ioan Toma, Florin Gabriel Popescu, Brana Liliana Samoila, Teodora Mititica, Use the carbon and oxygen injection for reducing the electric energy consumption at electric arc furnace, UHP type.....</b>	<b>29</b>
<b>Maria Daniela Stochițoiu, Ilie Uțu, Energetical ground oltenia - the electrical energy consumption and some problems about environment protection in lignite open pits.....</b>	<b>37</b>
<b>Teodor Tabacaru, Brana Liliana Samoila, Repairs of a.c. induction motors.....</b>	<b>43</b>
<b>Roxana Bubatu, Emil Pop, Camelia Barbu, E-Learning Technique In Human Resource.....</b>	<b>49</b>
<b>Corneliu Mândrescu, Olimpiu Stoicuța, The Stability Improvement Of Sensorless Vector Control System Of Induction Motor.....</b>	<b>55</b>
<b>Nicolae Pătrășcoiu, Adrian Marius Tomuș, Angular Speed Measurement Using Fpga Technology.....</b>	<b>71</b>
<b>Camelia Barbu, Roxana Bubatu, Adrian Dinoiu, Lorand Bogdanffy, Designing, Modeling And Simulation Of A Pico-Hydro Power Plant Controller.....</b>	<b>77</b>
<b>Angela Egri, Vali-Chivuta Sirb, Software Application Application For Determining The Minimum Trip Length On Map .....</b>	<b>83</b>



## **APPLICATIONS OF POWER ELECTRONICS IN ELECTROMECHANICAL DRIVES FROM MINING PLANTS**

**ILIE UȚU<sup>1</sup>, MARIA DANIELA STOCHITOIU<sup>2</sup>**

**Abstract:** Starting from the electric energy consumption decrease, the paper takes into account modern electric drive systems using power electronic devices. The paper treats winding machine converter feed drive systems and some measurements about the nonsinusoidal regime caused by these drive systems. Also, it takes into account some controlled drive system for the bucket wheel excavators.

**Keywords:** electric drive systems, voltage harmonic, current harmonic, electric energy quality, data acquisition, PWM converter.

### **1. INTRODUCTION**

Impetuous development and continuous electricity consumption, is an important feature, as it is based on obtaining high productivity and superior capitalization human and material potential of a country. A fundamental flaw in the current situation is reached disparities worldwide between energy needs and availability of primarily for solid and liquid fuels.

In this context, the importance of coal as a source of energy and raw materials, and mining becomes more evident.

Of the many issues regarding equipment in mining in this paper deepened use of new types of electric drives by applying power electronics as a measure to reduce electricity consumption.

### **2. USING POWER ELECTRONICS EQUIPMENT IN MINING UNDERGROUND**

Due to the development of power electronics and benefits posed by static converter drives, engine (speed control widely, starting and braking on favorable terms, simple

---

<sup>1</sup> *Associate Professor Eng., Ph.D. at the University of Petrosani*

<sup>2</sup> *Associate Professor Eng., Ph.D. at the University of Petrosani*

automation operating system) has been the use of such drives in machines of underground mining. An important category of energy-intensive equipment is the extraction plants.

Meet extraction plants operated dc motor fed through bridge rectifiers completely ordered phase.

These systems can be operated with one motor or two motors (Fig. 1) mounted on the same shaft and are powered by two fully controlled three-phase bridge rectifier. To reduce the harmonic rectifiers are supplied from AC power through two transformers, one in connection  $\Delta/\delta$  and the other in connection  $Y/\delta$ . In both cases separate excitation motor is powered by a rectifier assembly as seen in figure.

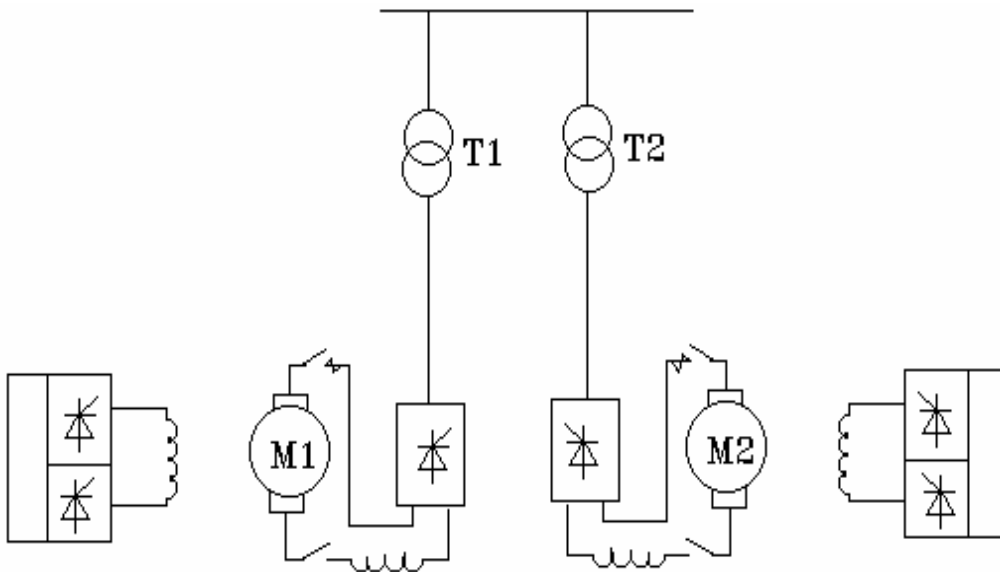


**Fig.1.** Winding machine with two DC motors.

The main disadvantage of these drives is the introduction of the harmonics in the network that introduced the current harmonics of orders:

$$v = k \cdot p + 1; k = 1, 2, \dots \quad (1)$$

and voltage:

$$v = k \cdot p; k = 1, 2, \dots \quad (2)$$

In fig. 2.a and 2.b presents the harmonic spectrum of phase current at steady for a drive system with one and two motor, high spectrum from measurements made using a data acquisition board.

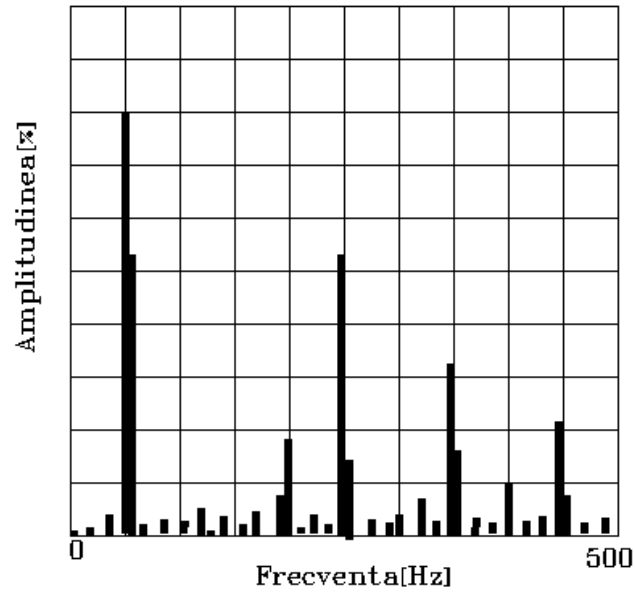


Fig.2.a. Harmonic spectrum of current to drive with one motor

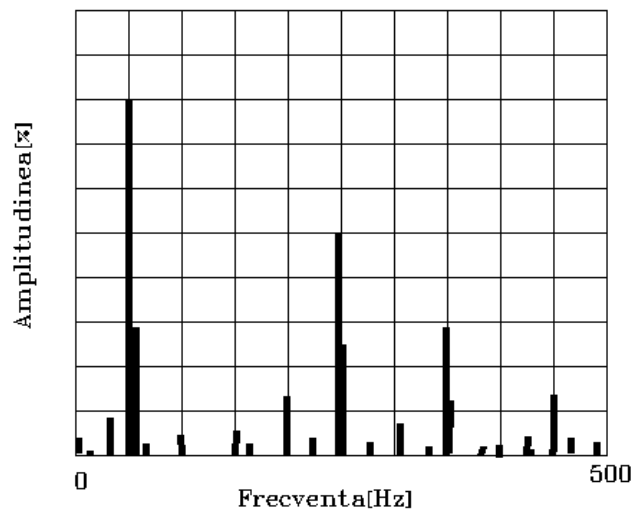


Fig.2.b. Harmonic spectrum of current to drive with two motors

Static converters are also used to drive the fans and compressors. Their electric drive is made with excitation synchronous motors fed through static rectifiers.



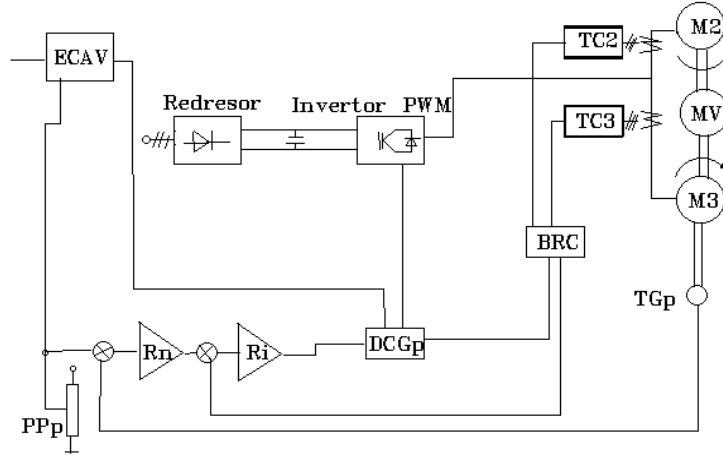


Fig.4. Inverter drive scheme

For bucket wheel drive you can use asynchronous motor connected in cascade. If the modification bucket wheel speed in the same way as pivot speed drive the scheme can use the superstructure is driven cascade induction motor and swivel mechanism PWM inverter with speed control unit together.

A modern solution is to drive the induction motor and static frequency converter (see Figure 5). Prescribed speed chain set open, insert the block BI integrator via  $U_n^*$ .

Block integrator output voltage rectifier is controlled simultaneously through  $U_{E\alpha}^*$  size and frequency inverter via  $U_f^*$  size. Minimum operating voltage,  $U_{fmin}$  is set by the potentiometer P2.

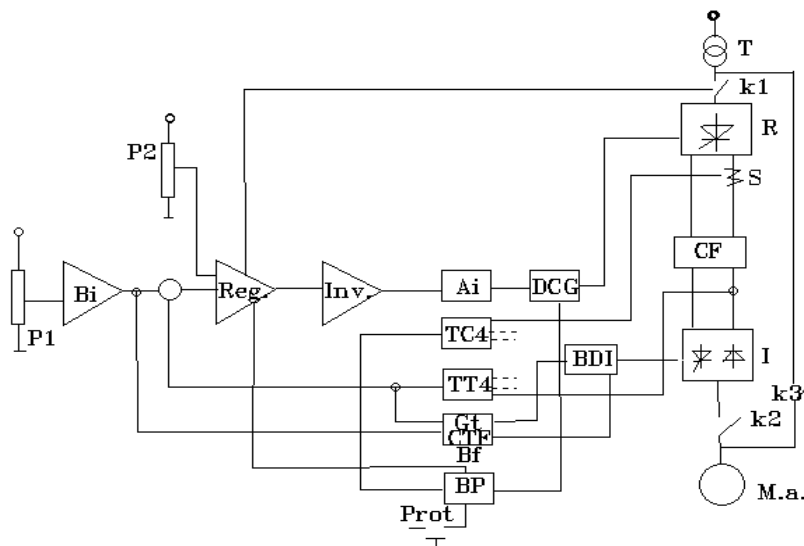


Fig.5. Scheme operated by static frequency converter

---

#### 4. CONCLUSIONS

Using the static converter in underground and open pits we obtain high performances for the electric drives. But, as we know, the static converter has great disadvantages by increases the distortions running in electric networks.

From studies over the years concluded that the best extraction facilities are equipped with DC drives, even if the initial investment is higher.

Following these conclusions were switched to using DC motors extraction facilities commissioned to new installations and replacing drives with obsolete motors from old wells.

DC electric drives were used in the old mines, but the generator-motor system. This type of operation is obsolete, requiring a large number of rotating electrical machines.

Modern solution is the electric drive rectifier-DC motor. The only major drawback of this type of operation is the deforming regime introduced by the rectifier system to be reduced or eliminated whenever possible.

The distorting regime cause power losses in mining plants, because of using static converter motor drive. These losses charged unreasonably selling price of coal delivered to beneficiaries.

The question is to eliminate these drawbacks through a systematic approach to the problems posed deforming regime. To tackle deforming effect is necessary theoretical knowledge parameter characterizing this system: distortion factors, form factor, ripple factor, the harmonics, etc.

#### REFERENCES

- [1]. **Chiuță, I.** Compensarea regimului energetic deformant. Editura Tehnică, București, 1989.
- [2]. **M.D. Marcu, D. Borca,** *Convertoare statice în acționări electrice.* Editura Topoexim, București, 1999.
- [3]. **Marcu M.D., Popescu F.G., Samoilă B.L.** *Modeling and simuling power active filter using method of generalized reactive power theory.* Proceedings of the IEEE International Conference on Computer Science and Automation Engineering (CSAE 2011), Shanghai, China.
- [4]. **Popescu F.G., Marcu M.D., Stepanescu I.** *Analiza calității energiei electrice dintr-o linie tehnologică de la E.M. Roșia.* SIMPRO 2008, Petroșani 16-17 Octombrie.
- [5]. **Popescu F.G., Marcu M.D., Orban M.D.** *Simulation software for static rectifiers and static switch controllers.* Annals of University of Petrosani, Electrical Engineering, Vol. 11, Petroșani 2009.
- [6]. **Popescu F.G.** *Contribuții privind analiza regimului deformant și reducerea acestuia în carierele de lignit.* Teză de doctorat, Petroșani 2011.
- [7]. **Tunsoiu, Gheorghe.** - Acționări electrice. Editura Didactica si Pedagogica, București, 1982.
- [8]. **Uțu, I.** Reducerea consumului de energie electrică în acționările electrice de mare putere din industria minieră. Teză de doctorat, Petroșani 1998.

## DYNAMIC COMPENSATION OF THE REACTIVE ENERGY FOR ELECTRIC ARC FURNACE USED IN STEEL FACTORY

ADRIAN IOAN TOMA<sup>1</sup>, FLORIN GABRIEL POPESCU<sup>2</sup>,  
CONSTANTIN LEON PANĂ<sup>3</sup>

**Abstract:** Demands for increased steel production and rules for network disturbances have, together with increasing cost of energy, made reactive power compensation a profitable solution in the steel industry. A modern and cost efficient steel melting process demands a stable and steady voltage support for the Electric Arc Furnace. With dynamic reactive power compensation, the random voltage variations characterized by an arc furnace are minimized.

The minimized voltage variations are achieved by continuously compensating the reactive power consumption from the arc furnace.

**Keywords:** electric arc, furnace, power transformer, electric system, charge, melting.

### 1. INTRODUCTION

The furnace type EBT is a high power electric furnace in which an electric arc are primed between the electrodes. The electrical arc has a nonlinear resistance, which leads to a non-sinusoidal voltage-current characteristic. Due to the dynamic behavior of the arc during the melting process, an EAF is a major sources of perturbations on a high voltage network with a low short-circuit capacity [1], [2], [3]. The perturbations are of random nature and encompass a frequency range from DC to a few hundreds of Hz.

Variation of currents according to short-circuit power supply network causing reactive power variation, which in turn causes voltage changes. Voltage variation disrupts the operation of other electric melting furnaces and other electrical equipments in the industrial or the public electricity grid.

In contrast to other types of loads which are usually operated by voltage steps, EAF

---

<sup>1</sup> *PhD. Student Eng. at University of Petrosani*

<sup>2</sup> *Ph.D. Assistant Eng. at University of Petrosani*

<sup>3</sup> *PhD. Lecturer Eng. at University of Petrosani*

produce random flicker which cannot be easily calculated with standard curves and methods.

## 2. ELECTRICAL MEASUREMENTS AND ANALYTICAL DETERMINATIONS CARRIED OUT ON STEEL MILL ARCELORMITTAL HUNEDOARA

The analyzed EAF attends the Electric Steel Shop no.2 from ArcelorMittal Steel Hunedoara. This type of furnace, with O<sub>2</sub> and CH<sub>4</sub> supplement and continuous operation, has a reduced energy specific consumption and high productivity.

*Table 1 Measurement performed at 220/30kV substation OE2 from ArcelorMittal Hd*

Ora	P MW	Q MVAR	S MVA	cos -	Q (0.92) MVAR	Q MVAR	Q (0.94) MVAR	Q MVAR
1	42	40	58.0	0.72	17.9	22.1	15.2	24.8
2	34	33	47.4	0.72	14.5	18.5	12.3	20.7
3	48	46	66.5	0.72	20.5	25.6	17.4	28.6
4	12	11	16.3	0.74	5.1	5.9	4.4	6.6
5	10	9	13.5	0.74	4.3	4.7	3.6	5.4
6	47	45	65.1	0.72	20.0	25.0	17.1	27.9
7	63	62	88.4	0.71	26.8	35.2	22.9	39.1
8	47	44	64.4	0.73	20.0	24.0	17.1	26.9
9	48	49	68.6	0.70	20.5	28.6	17.4	31.6
10	45	42	61.6	0.73	19.2	22.8	16.3	25.7
11	50	49	70.0	0.71	21.3	27.7	18.2	30.9
12	41	41	58.0	0.71	17.5	23.5	14.9	26.1
13	47	45	65.1	0.72	20.0	25.0	17.1	27.9
14	43	41	59.4	0.72	18.3	22.7	15.6	25.4
15	46	46	65.1	0.71	19.6	26.4	16.7	29.3
16	54	54	76.4	0.71	23.0	31.0	19.6	34.4
17	53	51	73.6	0.72	22.6	28.4	19.2	31.8
18	47	43	63.7	0.74	20.0	23.0	17.1	25.9
19	8	6	10.0	0.80	3.4	2.6	2.9	3.1
20	15	15	21.2	0.71	6.4	8.6	5.4	9.6
21	50	48	69.3	0.72	21.3	26.7	18.2	29.9
22	65	60	88.5	0.73	27.7	32.3	23.6	36.4
23	47	46	65.8	0.71	20.0	26.0	17.1	28.9
24	37	35	50.9	0.73	15.8	19.2	13.4	21.6
<b>Total</b>	999	961	1386	-	425.6	535.4	362.6	598.4
<b>minim</b>	8.0	6.0	10.0	<b>0,70</b>	3.4	2.6	2.9	3.1
<b>maxim</b>	65.0	62.0	88.5	<b>0,80</b>	27.7	35.2	23.6	39.1
<b>medie</b>	41.6	40.0	57.8	<b>0,72</b>	17.7	22.3	24.6	15.4

After the measurements performed at 220/30 kV substation OE2 for 24 hours result the medium power factor: 0.72.

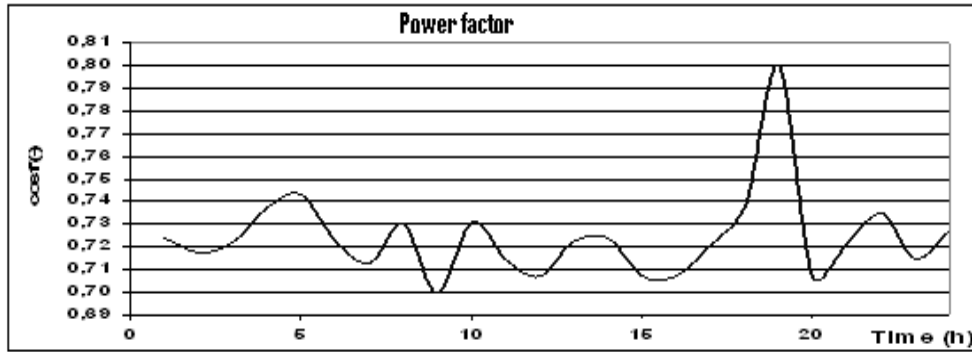


Fig.1 The variation of power factor

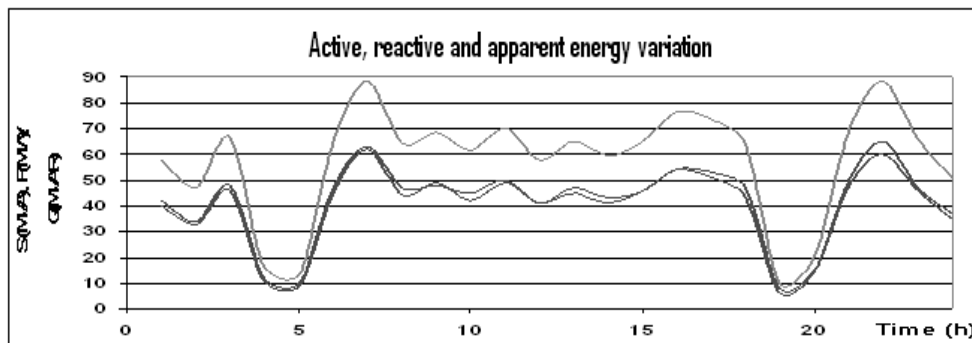


Fig.2 The variation of active, reactive and apparent energy

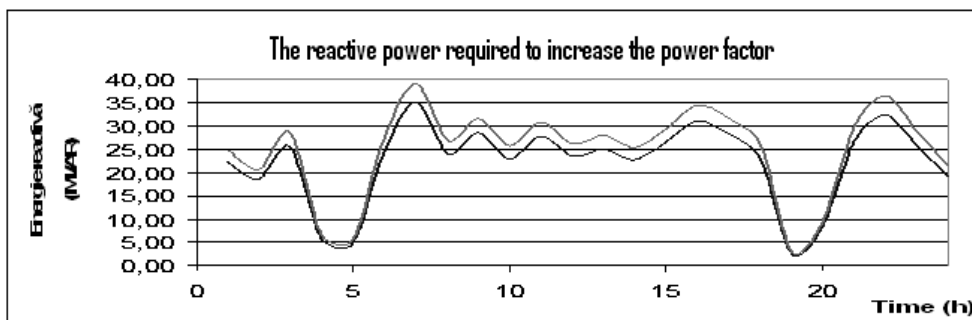


Fig. 3 The reactive power required to increase the power factor from 0.72 to 0.92 or 0.94

Electrical measurements performed at 30 kV voltage level and the analytical procedure revealed that the resultant load is a resistive-inductive character pronounced.

The analysis shows that the power factor and hourly energy: active, reactive and apparent varies widely during the melting on the electric arc furnace.

### 3. DYNAMIC REACTIVE POWER COMPENSATION AND HARMONIC DISTORTION AND HARMONIC DISTORTION MITIGATION IN OE2 220/33 kV ELECTRIC STATION

A Static VAR Compensator (or SVC) is an electrical device for providing fast-acting reactive power on high-voltage electricity transmission networks. The SVC generates reactive power which compensates the variations of reactive power and stabilizes the power factor [4].

A rapidly operating Static VAR Compensator (SVC) can continuously provide the reactive power required to control dynamic voltage swings under various system conditions and thereby improve the power system transmission and distribution performance. In addition, an SVC can mitigate active power oscillations through voltage amplitude modulation [5],[6].

The operating principle of SVC's is based on the following equality:

$$Q_{\text{load}} + Q_{\text{TCR}} - Q_{\text{FC}} = 0 \quad (1)$$

where:

- $Q_{\text{load}}$  is the reactive power absorbed by the electric arc furnace
- $Q_{\text{TCR}}$  is the reactive power thyristor controlled reactor
- $Q_{\text{FC}}$  is the reactive power harmonic filters.

In other words, the sum of the existing reactive network node where the SVC has to be fitted to be zero, a condition perfectly feasible if used thyristor to control inductors.

SVC's are built up to 200 MVAR power thyristors and the ordered coil can be mounted directly to the 30 kV voltage levels.

The SVC filter circuit's component is designed to filter harmonics. The carefully adjusting the resonant frequency filter circuits reduce THD. For 50 Hz the filters act as a capacitor that compensates the reactive power.

Reactance of the magnetic core has a number of advantages over other magnetic cores of the impedance in the air, such as:

- does not radiate a magnetic field outside the yoke
- has reduced dimension;
- has low power loss;
- is resistant to corrosion;
- not maintenance required even in polluted environments.

The parameters for SVC's sizing are considered the following:

- $S = 80$  MVA (consider both consumers EAF-EBT and LF)
- $\cos \varphi = 0,94$
- $Q = 65$  MVAR (consider both consumers EAF-EBT and LF)

Fluctuations in voltage coming from the system can not be compensated with SVC's.

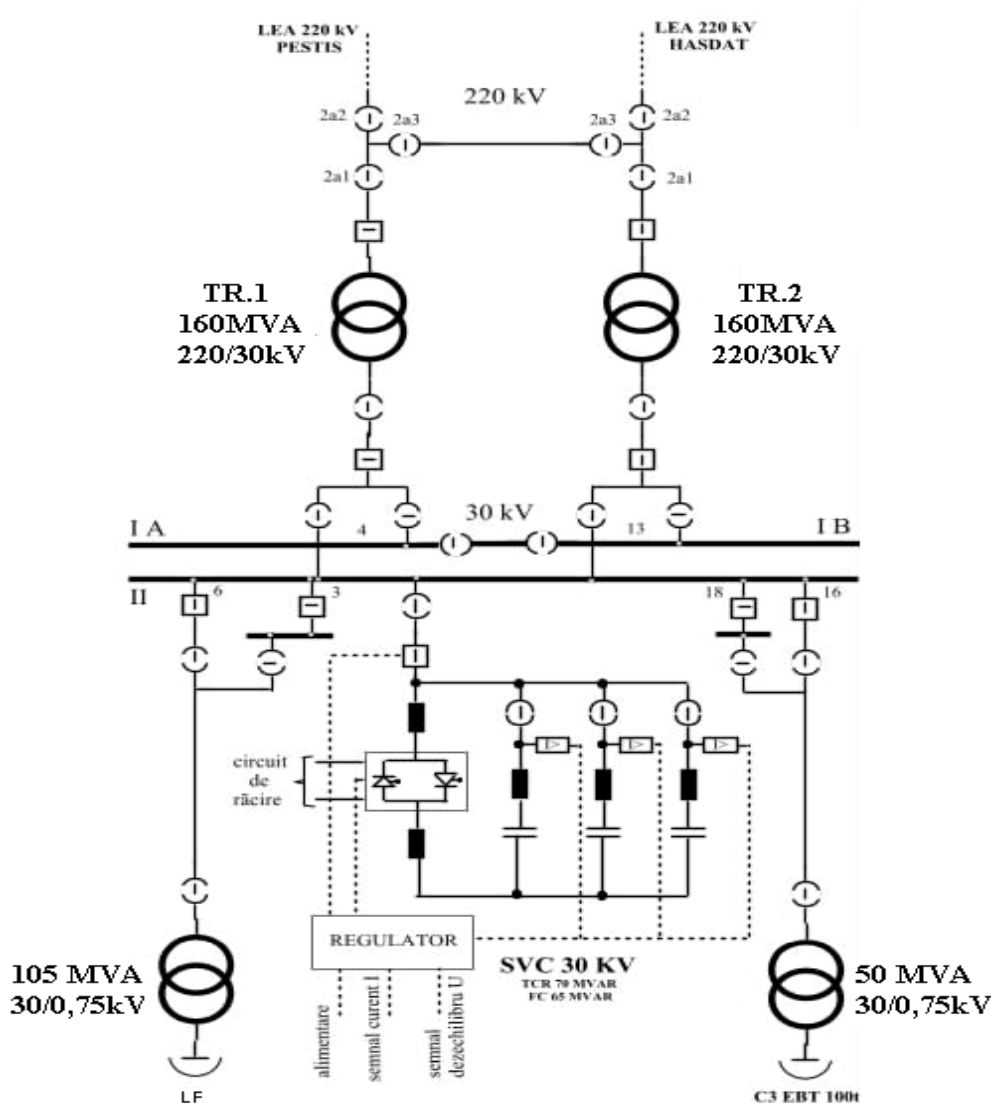


Fig. 4 The block diagram for SVC

SVC target is to compensate the reactive power consumed within 15 minutes interval after which the active and the reactive power are registration and then calculate penalties for to low power factor.

---

#### 4. CONCLUSIONS

The benefits of an SVC can be seen within a steel plant as a stable power factor in spite of varying loads at the plant, and externally when the disturbances do not affect the supplying grid.

Proposed technical solution to implementation of SVC has the following advantages:

- reduces the voltage fluctuations;
- reduce the flicker phenomenon;
- reduce the weight of harmonics;
- is fast reactive power compensation;
- reduce power losses;
- reduces the reactive power bill;
- lower maintenance costs;
- improves the voltage local by local reactive power production leading to increased efficiency;
- increased load capacity active power energy plants;
- not required operating personnel;
- specific cost is lower than the value of synchronous compensators with the capacitor (compared in the EUR / kVAR);
- ensure continuous power factor adjustment to achieve optimal compensation;
- can be located outdoors;
- have a long service life;
- does not introduce harmonics in the network;
- the investment pays for itself in short period (one year and three months).

#### REFERENCES

- [1]. **Arad, S.**, *Electrotehnologii*,. Ed. FOCUS Petroșani, ISBN 978-973-677-140-8, 2008
- [2] **Arad, S., Marcu, M., Pasculescu, D. Petrilean, C.**, *Aspects of the electric arc furnace control*, Proc. Of Int. Sympon Advanced Engineering & Applied Management, CD, Faculty of Engineering Hunedoara, SI, pp 33- 38, ISBN 978-973-0-09340-7, 2010
- [4]. **Chapman D.**, *Ghid de Aplicare - Calitatea Energiei Electrice*, Copper Development Association, 2001.
- [5]. **Chiuță I., Conecini I.**, *Compensarea regimului energetic deformant*, Editura Tehnică, București, 1989.
- [6]. **Chong H., Huang A. Q.**, *Filed Data-based Study on Electric Arc Furnac Flicker Mitigation*, IEEE Transactions on Industry Applications, USA, 2006.
- [7]. **Chong H., Huang A. Q., White L., Ingram M.**, *Design of an Ultra-capacitor Enegy Storage System (UESS) for Power Quality Improvement of Electric Arc Furnaces*, IEEE Transactions on Industry Applications, 2008.
- [8]. **Pană L., Marcu M.D., Uțu I.** *Evaluarea puterii optime a transformatoarelor electrice pe baza criteriului pierderilor minime de energie in exploatare*. Lurările științifice ale simpozionului internațional "Universitaria ROPET 2008", Petroșani.
- [9]. **Uțu I., Marcu M.D.** *Monitoring of the Voltage and Current Harmonics in Electric Networks*. Annals of the University of Craiova, 2010.

## SOLAR PANEL CONTROL SYSTEM

BRANA LILIANA SAMOILA<sup>1</sup>, TEODOR TABACARU<sup>2</sup>

**Abstract:** This paper deals with solar panels control systems, meant to orient it towards the sun in order to maximize the electric energy. This kind of panels are used especially for low consumption isolated consumers. When designing the control system, we used the multibody systems method, which allowed us to accomplish the orientating articulated mechanisms.

**Key words:** control, photovoltaic element; solar panel; energy; orientation; guiding.

### 1. GENERAL CONSIDERATIONS ABOUT SOLAR ENERGY

The solar energy can be used with high efficiency and low investments to prepare the hot water, heat the houses and water in the pools.

The solar energy is non-polluting, inexhaustible, ecological and safe. It doesn't produce waste and it doesn't release polluting gases.

More than two millennia ago, it seems that the people of Syracuse focused the sun light using mirrors and they pointed it to the Roman invader navy, setting it on fire.

In 1849, the first photoelectric cell was made. After 10 years, the first solar cell was accomplished, producing electricity.

In 1904, the German physicist Philipp Lenard found out the first explanation for the photoelectric effect, being rewarded with the Nobel price in physics in 1905.

Albert Einstein, in 1905, solved the problem explaining the dual character of the light on the basis of the quantum theory. He acknowledged that the maximum kinetic energy of an electron is independent of the light intensity, depending only of the light wavelength, respectively of its frequency. In 1921, he got the Nobel price for his research concerning the photovoltaic effect. The first solar cell, as we know it today, was manufactured in the Bell Company laboratories, where the researchers noticed that

---

<sup>1</sup> Associate Professor, Eng., PhD, University of Petroșani, Romania

<sup>2</sup> Associate Professor, Eng., PhD, University of Petroșani, Romania

a silicon rectifier delivered a higher current when it was exposed to the sunlight.

Solar cells kept improving along the next years. During the 70's, mineral oil products increasing price quickened the research on the solar cells, leading to cells with an efficiency of about 20 % [4], [6], [9].

## 2. ORIENTABLE SOLAR PANELS DESIGN

There were a few characteristics that we had to establish when starting the design, such as:

- meteorological data;
- the photovoltaic system configuration;
- the solar panel type;
- the panel obliquity, without the guiding-orienting system;
- the inverter type.

The inverter type is chosen by the program, once the panel has been defined.

The photovoltaic panels work at a maximum efficiency when the incoming Sun rays are perpendicular to their cells. Maintaining the module perpendicular to the incoming sunlight means that the module intercepts the maximum amount of sunlight [10].

That's why, no matter the panel type, the guiding-orientating systems increase the solar energy flux that reaches a panel, by a certain percentage. Comparing to an immobile panel, orientated by 45°, simulation showed that the orientating system appreciate the solar energy by 29.3%.

The efficiency of the photovoltaic conversion is less influenced by the panel orientation (on an average of about 4.1%) and can be correlated with the collateral effects of the orientation, especially with the panel surface thermal regime. The panel active material becomes an important factor.

The electric energy generated by photovoltaic conversion using orientated panels is by 35% higher, comparing to the immobile panels, oriented by 45°, due to the conversion efficiency improvement.

The efficiency of the entire photovoltaic system increases by 4.5%.

We used the Multibody Systems Method (MBS) [7], [8] to model the mechanisms involved in the panel orientating movement. This method considers the mechanism as a multibody system, defined as an assembly of rigid bodies, submitted to geometrical and kinematical restrictions [1],[5].

The orientated solar panel we manufactured is shown in fig. 1.

The electric scheme is divided in: supply; command and detection; control.

We took into account the practical considerations related to the signal filtration and interferences, layout width and thermal dissipation [2], for each section.



**Fig.1** Orientated solar panel

The stand-by consumption was minimized ( $< 1 \text{ mA}$ ) by activating the necessary parts only by software commands.

The electronic scheme is shown in fig. 2.

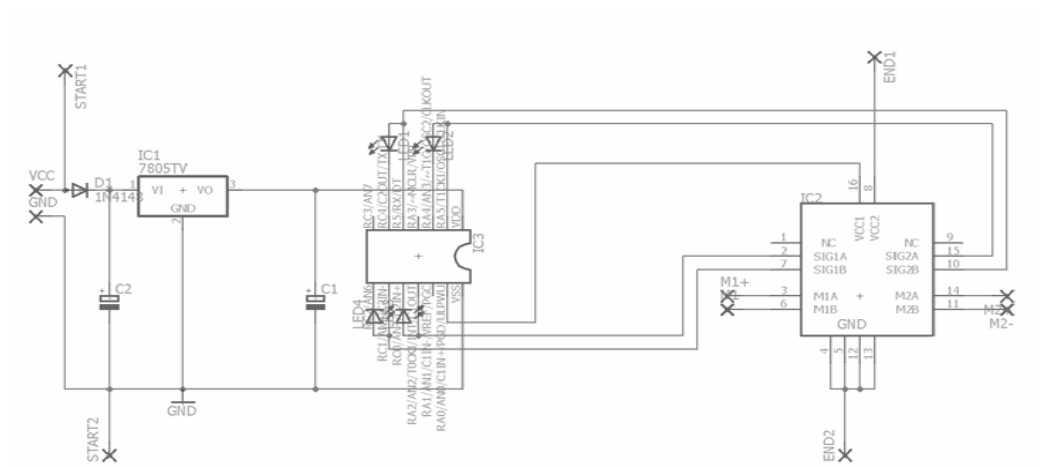


**Fig. 2** Solar panel orientating system control electronic scheme

The circuit was primarily achieved on a breadboard, for tests, and then it was designed in Eagle.

The number of components was reduced as much as possible, considering a bulk production, without affecting the system functionality.

---

The algorithm configuration is made by reprogramming the microcontroller. A RS232 connection on the TTL logical level is all along activated for attending the performances.

The supply and filtration part is based on a single LM7805 integrated circuit, to take over the input voltage of 8-36 V and to stabilize it at 5 V. For practical reasons, we considered a supply voltage level between 10 and 15 V, specific for working on batteries with Pb, acid electrolyte or gel. We considered also a 24 V voltage for systems with two actuators in series, but, usually, actuators of 12 V are used. In order to protect the circuit against the drop in voltage, specific for autonomous regime, a few hundreds of microfarad capacitor is placed at the input of the integrated circuit.

The most probable failure cause of the voltage stabilizer LM7805 is an inverted voltage on its input and/or output voltage higher than the input one. A 1N4148 rapid diode insures the fact that, if a fall of voltage occurs, other circuits with the same supply will not determine the quick disruption of the capacitor and/or the stabilization integrated circuit breakdown. The 5 V voltage is further on used for the processor and the logical command supply.

The device is meant to command a solar panel orientating system, on two axes (azimuth and elevation) [3]. Taking into account that both orientating motors are d.c. ones and they need sense changing, two complete H bridges are provided.

We analyzed several implementation possibilities of the H bridges:

1. final command by bipolar transistors, which is characterized by low cost, possible high currents, but the circuit is complicated;
2. final command by MOSFET transistors and anticipatory command by bipolar transistors – high currents, incorporated diodes for certain models, but the circuit is complicated as well;
3. final command by MOSFET transistors and anticipatory command by specialized integrated circuits (MOSFET driver) which appears to be the best solution, with all possible protections but the price is the highest and the scheme is not simplified;
4. electromechanical relays which bring along advantages like: very high currents, simplified scheme, but also disadvantages: long dead time, attrition, quite high price.
5. integrated circuit, which is a completely integrated solution, with all kind of protections, simple design, steady transitions, but quite expensive.

We chose the last solution because of its advantages and availability of the components (SGS L293 Half-H driver).

The buffer amplifier is controlled by the microcontroller, so that the stand-by consumption is null and the usual current is 30 mA.

The circuit can be achieved with almost any kind of Microchip 16F controllers, the difference being made by certain details concerning the available set of instructions.

The serial connection, used to get the troubleshooting data, is emulated with a timer that reproduces the necessary delay to get the transfer rate of 9600bps, correcting the cumulated errors.

The 4 LED's were meant to measure the luminosity difference on 2 axes, X and Y (azimuth and elevation) (Fig. 2).

In the debug mode, the LED's show the implicitly activated output, that is the motor work sense and axis.

The microcontroller and the sensors have a dark threshold to orientate the panel to the Est when the debug mode is deactivated. The microcontroller makes a periodical polling on the sensors (especially in the debug mode), alternatively by the two axes. It commands the output when the difference between two LED's exceeds a certain threshold, needing to redirect the panel.

In the debug mode, the reverse inhibit algorithm (or PID controller) which helps to stabilize the panel on a direction without unnecessary movements, is not activated. That means that the motors work more often, continuously trying to get the panel to the bright point. It is an unwanted effect, leading to needless energy consumption.

The incident light measurement is based on the LED's characteristic of changing its capacitance when it is illuminated. Using the measured values, two diodes on the same axis are compared. We can find out if the motor has to move and in which sense, with a PID (proportional, integral, derivative) algorithm. This kind of algorithm is used to optimize the current resources, eliminating the useless actions of the actuators.

Depending on the action taken in the previous step, the processor actuates the requested output and sense during 100 ms. The measured values and the decision taken in the step 2 are written on the serial port for troubleshooting and algorithm optimization. The system gets to a stand-by state, for a predefined period of time. When, for a certain period of time, the darkness is detected, the microcontroller takes the decision to change the panel azimuth to the East, to ensure that in the morning the panel is oriented towards the sun, even if the batteries are run down.

The main results of using the guiding-orientating system that we achieved are summarized in tables 1 and 2.

**Table 1 The orientated solar panel efficiency (IP – immobile panel; OP – orientated panel)**

No.	P <sub>i</sub> [W]	Solar energy input [kWh]		Output energy [kWh]		Panel efficiency [%]		System efficiency [%]	
		IP	OP	IP	OP	IP	OP	IP	OP
1	40	10955.1	14172.5	635.5	860.5	6.6	6.8	5.8	6.1
2	50	10128	13102.4	763.2	1033.1	8.6	8.9	7.5	7.8

Comparing measured values for an orientated panel and an immobile one, we found that: the input solar energy is about 30% higher and the output energy increases by 35%, when using orientation systems. So, the panel efficiency is enhanced by more than 3%.

**Table 2 The orientating system influence on the energy conversion**

No.	P <sub>i</sub> [W]	$\Delta E_{\text{radiation}}$ [%]	$\Delta E_{\text{electric}}$ [%]	$\Delta \eta_{\text{pv}}$ [%]	$\Delta \eta_{\text{system}}$ [%]
1	40	29.36897	35.41175	3.030303	5.172414
2	50	29.36809	35.36426	3.488372	4.000000

### 3. CONCLUSIONS

We identified the main demands specific to the conversion systems orientation and their parameters. Using the MBS method, we accomplished the orientating articulated mechanisms structural analysis in one and two axes systems.

Starting from the existing mechanisms, we generated new structural graph variants, extended to morphological ones. Most of the structural solutions that we proposed can be adapted with few changes for one-axis orientation systems.

We used a self-manufactured orientation controlled photovoltaic panel to charge two batteries of 12V, 14.4Ah, which had to insure a gasification boiler control equipment and pumps supply continuity. Such a heating station is used in out-of-way houses, where the electric energy supply is often broken. We made our research trying to find a solution to keep working the installation.

We designed this control equipment and run tests to check whether it works properly. The results were more than satisfactory.

### REFERENCES

- [1]. **Alexandru P.** *Proiectarea functionala a mecanismelor*, Lux Libris Publishing House, Brasov, pp. 78-165, 1999.
- [2]. **Athientis A. K., Santamouris M.** *Thermal analysis and design of passive solar buildings*, James&James, London, pp. 8-11, 2002.
- [3]. **Cotfas D. T., Cotfas P., Ursutiu D., Samoila C.** *The implementation of a biaxial monitoring system for the maximum of the solar radiation*, Symposium on remote Engineering and Virtual Instrumentation, Maribor, 2006.
- [4]. **Danescu A., Bucurenciu S., Petrescu S.** *Utilizarea energiei solare*, Technical Publishing House, Bucharest, pp. 121-189, 1980.
- [5]. **Dudita F., Diaconescu D., Gogu G.** *Mecanisme articulate*, Technical Publishing House, Bucharest, 1989.
- [6]. **Howell D.**, *Your solar energy home*, Pergamon Press, New York, 1986.
- [7]. **Lester A., Myers D.R.** *A method for improving global parameter measurement by modeling responsivity functions*, Solar Energy, pp. 322-331, 2006.
- [8]. **Myers D.** *Solar radiation modeling and measurements for renewable energy applicaions: data and model quality*, Energy, pp. 1517-1531, 2005.
- [9]. **Sen Z.** *Progress in energy and solar energy in progress and future research trends*. Combustion Science, pp. 367-416, 2004.
- [10]. **Stepanescu I., Fotău I., Popescu F.G., Stepanescu A., Marc O., Bjorn G.** *Future distributed generators in the Jiu Valley*. SIMPRO 2010, Petroșani 14-15 Octombrie.

## STUDY OF ELECTRO-DYNAMICS FORCES IN SHORT CIRCUIT REGIME USING MATLAB-SIMULINK SOFTWARE

TITU NICULESCU<sup>1</sup>

**Abstract:** The paper presents a study of electrodynamic forces using MATLAB-SIMULINK software. The single-phase short circuit, and the three-phase short circuit are presented and for these situations the graphical correlation between these forces and time are presented, using MATLAB-SIMULINK software for transitory phenomena. Simulation models and theoretical basements are presented also.

**Keywords:** simulation, circuit, conductor, three phase, electrodynamic forces, model.

### 1. SINGLE-PHASE SHORT CIRCUITS

These electrodynamic forces result in the distribution and transport of electric energy with two conductors, and with three conductors when the short circuit occurs between three conductors.

The expression of electrodynamic forces for the transitory regime is:

$$F = CI^2(e^{-\lambda t} - \cos \omega t)^2 \quad (1)$$

where  $\lambda$  is the equivalent time constant, and:

$$C = \frac{\mu_0}{2\pi} \cdot \frac{l}{a} \cdot \varphi_{CD} \cdot \varphi\left(\frac{a}{l}\right) \quad (2)$$

In the expression (2) is a function which depends by Dwight's diagrams, and:

---

<sup>1</sup> *PhD. Associate Professor Eng. University of Petroșani*

$$\varphi\left(\frac{a}{l}\right) = \sqrt{1 + \frac{a^2}{l^2}} - \frac{a}{l} \tag{3}$$

where “l” is the length of the conductors and “a” is the distance between these.

**1.1. The circuit simulation model**

The explicit function (1) conducts to the simulation model from (Fig.1), which generated the explicit diagram for dependence between electro-dynamic force and time (Fig.2). The explicit diagrams were obtained for specific values of the circuit parameter as follows:

$$R = 100\Omega; L = 2H; l = 100m; a = 0.5m; \varphi_{CD} = 0.8; I = 100A.$$

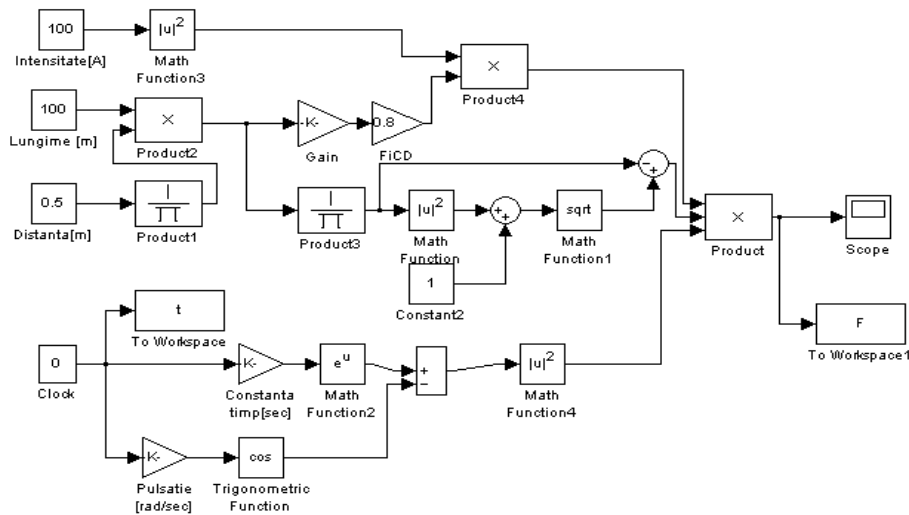


**Fig.1.** The Simulink model for single-phase short circuit

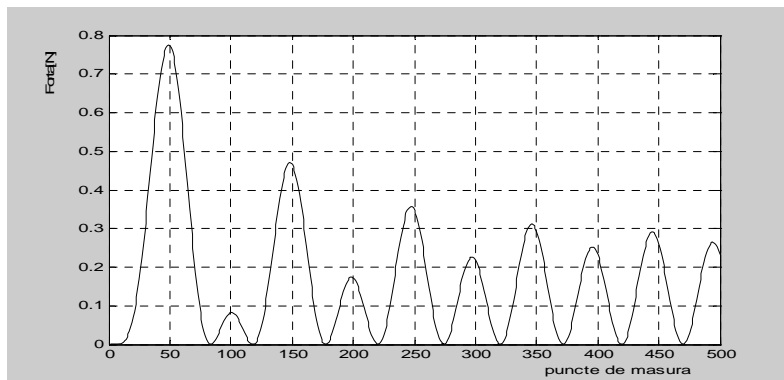


**Fig.2.** The force diagram

## 2. THREE-PHASE SHORT CIRCUITS

The electrodynamic forces appear in the transport and distribution of energy in three-phase systems. Short circuit is made between the three active conductors of the system.

### 2.1. The force exerted on the median conductor

If a short circuit between conductors is made of three phase system, electrodynamic force acting on the median conductor:

$$F_m = C \cdot i_1 \cdot (i_2 - i_3) \quad (4)$$

with the expressions currents in the three conductors:

$$\begin{cases} i_1 = \hat{I} \cdot \left[ e^{-\lambda t} \cdot \sin \alpha + \sin(\omega t - \alpha) \right] \\ i_2 = \hat{I} \cdot \left[ e^{-\lambda t} \cdot \sin\left(\alpha + \frac{2\pi}{3}\right) + \sin\left(\omega t - \alpha - \frac{2\pi}{3}\right) \right] \\ i_3 = \hat{I} \cdot \left[ e^{-\lambda t} \cdot \sin\left(\alpha - \frac{2\pi}{3}\right) + \sin\left(\omega t - \alpha + \frac{2\pi}{3}\right) \right] \end{cases} \quad (5)$$

The force exerted on the median conductor is obtained by inserting expressions currents of relations (5) in (4):

$$\begin{aligned} F_m &= C \cdot \hat{I}^2 \cdot \left[ e^{-\lambda t} \cdot \sin \alpha + \sin(\omega t - \alpha) \right] \cdot \left[ e^{-\lambda t} \cdot \sin\left(\alpha + \frac{2\pi}{3}\right) + \right. \\ &\quad \left. \sin\left(\omega t - \alpha - \frac{2\pi}{3}\right) - e^{-\lambda t} \cdot \sin\left(\alpha - \frac{2\pi}{3}\right) - \sin\left(\omega t - \alpha + \frac{2\pi}{3}\right) \right] = \\ &= C \cdot \hat{I}^2 \cdot \left[ e^{-\lambda t} \cdot \sin \alpha + \sin(\omega t - \alpha) \right] \cdot \left\{ e^{-\lambda t} \cdot \left[ \sin\left(\alpha + \frac{2\pi}{3}\right) - \right. \right. \\ &\quad \left. \left. - \sin\left(\alpha - \frac{2\pi}{3}\right) \right] + \sin\left(\omega t - \alpha - \frac{2\pi}{3}\right) - \sin\left(\omega t - \alpha + \frac{2\pi}{3}\right) \right\} = \\ &= C \cdot \hat{I}^2 \cdot \left[ e^{-\lambda t} \cdot \sin \alpha + \sin(\omega t - \alpha) \right] \cdot \left[ e^{-\lambda t} \cdot \left( -\frac{1}{2} \cdot \sin \alpha + \right. \right. \\ &\quad \left. \left. \frac{\sqrt{3}}{2} \cdot \cos \alpha + \frac{1}{2} \cdot \sin \alpha + \frac{\sqrt{3}}{2} \cdot \cos \alpha \right) - \frac{1}{2} \cdot \sin(\omega t - \alpha) - \right. \end{aligned}$$

$$\left[ \frac{\sqrt{3}}{2} \cdot \cos(\omega t - \alpha) + \frac{1}{2} \cdot \sin(\omega t - \alpha) - \frac{\sqrt{3}}{2} \cdot \cos(\omega t - \alpha) \right]$$

and finally, the relationship becomes:

$$F_m = \sqrt{3} \cdot C \cdot \hat{I}^2 \cdot [e^{-\lambda t} \cdot \sin \alpha + \sin(\omega t - \alpha)] \cdot [e^{-\lambda t} \cdot \cos \alpha - \cos(\omega t - \alpha)] \tag{6}$$

The maximum force occurs for the angle  $\alpha = \frac{\pi}{4}$ . The final force expression is:

$$F_m = \frac{\sqrt{3}}{2} \cdot C \cdot \hat{I}^2 \cdot [e^{-\lambda t} + \sin \omega t - \cos \omega t] \cdot [e^{-\lambda t} - \sin \omega t - \cos \omega t] \tag{7}$$

The simulation model of force is presented in Fig. 3 and the diagram generated by this in Fig.4.

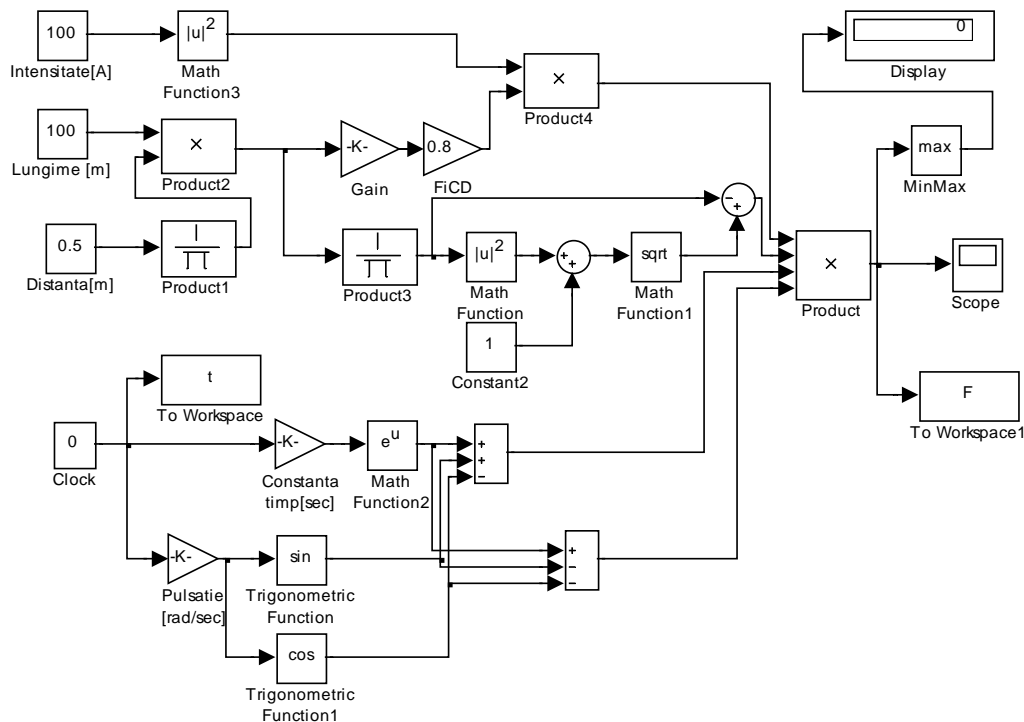


Fig.3 The Simulink model for three-phase short circuit, median conductor

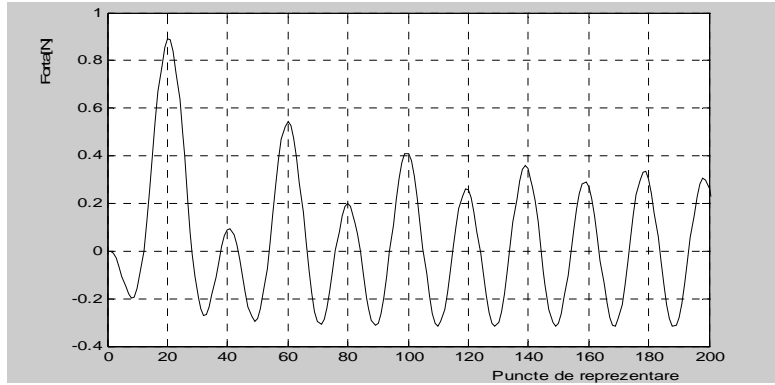


Fig.4. The force diagram

### 2.2. The force exerted on the side conductor

If a short circuit between the conductors of three phase system occurs, electro-dynamics force acting on the side conductor is:

$$F_l = C \cdot i_1 \cdot \left( i_2 + \frac{i_3}{2} \right) \quad (8)$$

If you apply the previous reasoning, this force becomes:

$$F_l = -\frac{\sqrt{3}}{4} \cdot C \cdot \hat{I}^2 \cdot \left[ e^{-\lambda t} \cdot \sin \alpha + \sin(\omega t - \alpha) \right] \cdot \left[ e^{-\lambda t} \cdot (\sqrt{3} \cdot \sin \alpha - \cos \alpha) + \sqrt{3} \cdot \sin(\omega t - \alpha) + \cos(\omega t - \alpha) \right] \quad (9)$$

The simulation model of force is presented in Fig. 5 and the diagram generated by this in Fig.6.

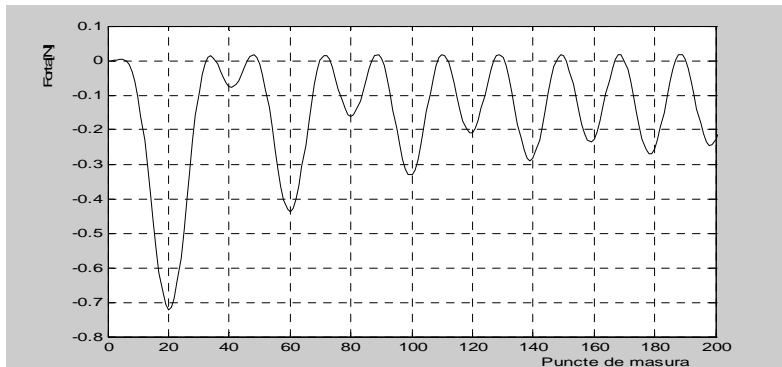


Fig.6. The force diagram

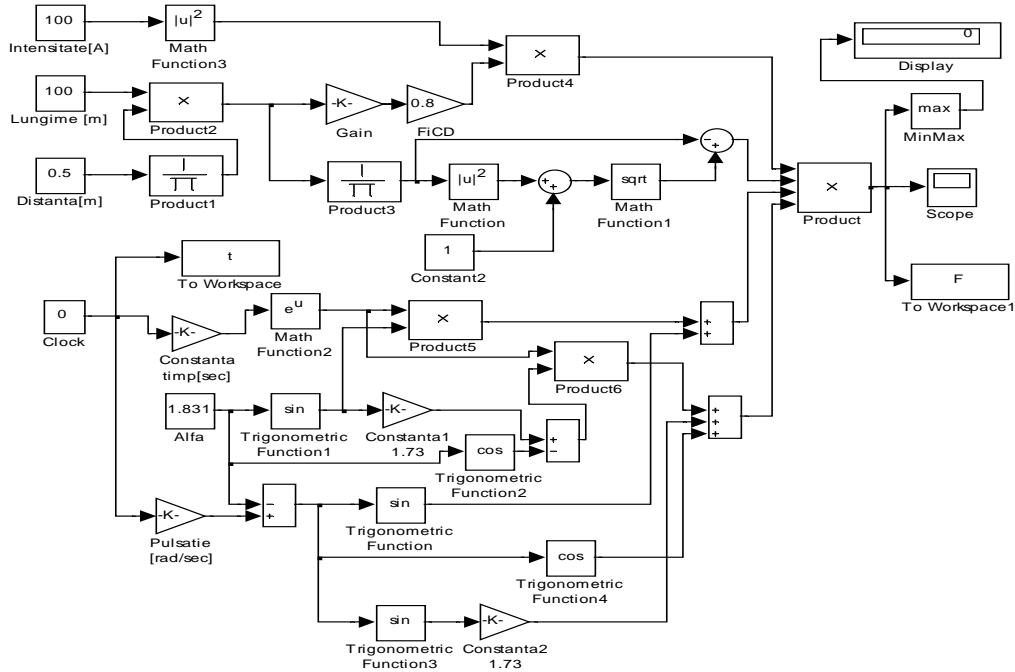


Fig.5. The Simulink model for three-phase short circuit, side conductor

Simulation models have been designed so that input quantities are grouped separately to be modified and thus allow study of the influence of each input parameter on electrodynamic forces for each situation.

#### REFERENCES

- [1]. Ghe. Hortopan. *Aparate electrice*, E.D.P., București, 1980.
- [2]. I. Ghinea, Firțeanu V.,- *MATLAB calcul numeric, grafică*, Editura Teora 1994.
- [3]. S. Halunga-Fratu, O. Fratu. *Simularea sistemelor de transmisiune analogice și digitale folosind mediul MATLAB/SIMULINK*, Editura MATRIXROM București 2005.

## USE THE CARBON AND OXYGEN INJECTION FOR REDUCING THE ELECTRIC ENERGY CONSUMPTION AT ELECTRIC ARC FURNACE, UHP TYPE

ADRIAN IOAN TOMA<sup>1</sup>, FLORIN GABRIEL POPESCU<sup>2</sup>, BRANA  
LILIANA SAMOILĂ<sup>3</sup>, TEODORA MITITICA<sup>4</sup>

**Abstract:** The paper presents a study of the electric arc furnace who using Carbon-Jet and Oxygen-Jet to reduce specific consumption of energy.

Electric arc furnaces (EAF) play an important and increasing role in modern steel work concepts. The ability to precisely control the temperature and chemistry of the batch make EAF an ideal choice for producing high-grade steel for the recycling of scrap. Of the steel made today 36% is produced by the EAF route and this share will increase to 50 by 2030. The EAF has been studied for many years, but it is still difficult to complete representation.

**Keywords:** electric arc, furnace, oxygen, carbon, injection, charge, melting

### 1. INTRODUCTION

The Eccentric Bottom Tapping is a ultra high power electric furnace in which the electric arc is primed between the electrodes and charge (direct action) [1], [2]. EBT furnaces have intake of oxygen during preparation, and specific fuel consumption is 450 ... 530 kWh / t of steel, smaller than other types of electric furnaces [3].

Foaming slag is used to increase the thermal efficiency of the furnace during refining, where the side walls are fully exposed to arc radiation [5]. A slag foam will rise and cover the arc, allowing the use of larger amounts of heat without increasing the thermal load on the furnace walls. In this phase of the steel, an electric arc covered by a slag foam had a higher efficiency in heat transfer. Slag foaming is achieved by injecting oxygen in liquid steel, in which case the iron is oxidized under the reaction:

---

<sup>1</sup> *PhD. Student Eng. at University of Petrosani*

<sup>2</sup> *Ph.D. Assistant Eng. at University of Petrosani*

<sup>3</sup> *Ph.D. Associate Professor Eng., at the University of Petrosani*

<sup>4</sup> *Ph.D. Assistant Eng. at University of Petrosani*



The gas output (CO) is a critical component for obtaining the slag foaming.

The Electric Steelwork No 2 belonging to ArcelorMital Hunedoara S.A. was equipped with an electric arc furnace EBT type that was designed to melting 100t of steel in 70 minutes to 1.600 °C. The EAF-EBT has equipment for oxygen and carbon injection.

## 2. THE EQUIPMENT FOR OXYGEN AND CARBON INJECTION

### 2.1. The Oxygen -Jet MK III

The Oxygen-Jet Mk III injector is an oxygen and natural gas injector. It was designed so that it can function both as a way supersonic oxygen injection and as a burner for heating and melting scrap steel inside a furnace. The nozzle is designed to provide a coherent supersonic jet of oxygen. A double ring of holes, the natural gas inside and outside the oxygen for burning phase, used for both the burner, and also to maximize the effect of the supersonic jet [4].

A normal cycle Oxygen-jet Mk.III work begins with an initial phase of the burner for a merger, followed by a second phase of the injection. The two phases can be described as follows:

- Phase burner, the methane and oxygen are injected to preheat the scrap inside the electric oven. Time for this operation is strictly related to the electric furnace melting process.

- Phase injection, the oxygen is injected. Time required for the injection phase is closely related to the electric furnace melting process.

All the phases described above and operational issues are controlled by the operator.

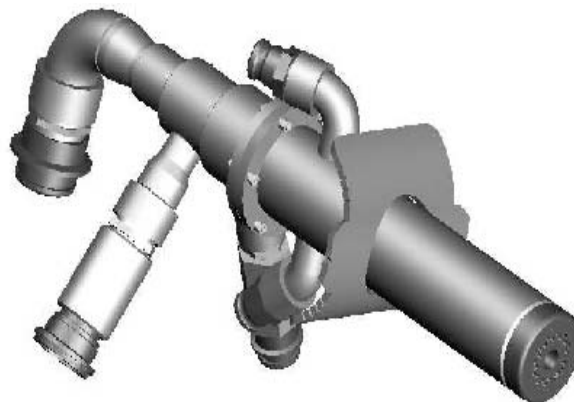


**Fig.1.** The Oxygen Jet

The oxygen injector is represented in the figure 1 and has the following components: the main body cooled, drum rear including sealing, OR sealing gaskets, and retainer valves.

The oxygen injector is designed for maximum methane gas flow of 500 Nm<sup>3</sup>/h at a pressure of 6 bar and a maximum flow of oxygen of 2200 Nm<sup>3</sup>/h at a pressure of 16 bar. In the burner regime the oxygen consumption is 900 Nm<sup>3</sup>/h and the methane gas consumption is 350 Nm<sup>3</sup>/h. In the supersonic regime the oxygen consumption is 1600 Nm<sup>3</sup>/h.

## 2.2. The Carbon -Jet MK III

The Carbon-Jet Mk III injector is an oxygen injector designed so that it can function as the injection of pulverized coal and oxygen to heat and melt scrap metal inside a furnace [4].

A normal cycle Carbon-jet Mk.III work begins with an initial phase of the burner for a merger, followed by a second phase of the injection, the two phases can be described as follows:

- Phase burner, the oxygen and gas are injected to preheat scrap in electric oven. Time for this operation is closely related to the electric furnace fusion;
- Phase injection, the oxygen is injected. Time required for the injection phase is closely related to the electric furnace fusion.

All the phases described above and operational issues are controlled by the operator.

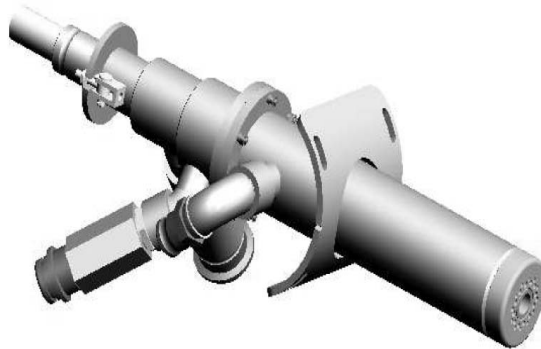


Fig.2. The Carbon-Jet

The carbon injector is represented in the figure 2 and has the following components: the main body cooled, drum rear including sealing, ceramist tube for injecting coal, OR sealing gaskets and retainer valves.

The carbon injector is designed for maximum methane gas flow of 500 Nm<sup>3</sup>/h at a pressure of 6 bar and a maximum flow of oxygen of 2200 Nm<sup>3</sup>/h at a pressure of 16 bar. In the burner regime the oxygen consumption is 900 Nm<sup>3</sup> / h, the methane gas

consumption is 350 Nm<sup>3</sup>/h and carbon consumption is 15-45 kg/min. In the supersonic regime the oxygen consumption is 1600 Nm<sup>3</sup>/h.

### 3. ANALYSIS THE POWER QUALITY PARAMETERS FOR EAF WITH AND WITHOUT OXYGEN AND CARBON INJECTION

The measurements, presented further, were achieved in the electric station of the Electric Steel Shop no.2 Mittal Steel Hunedoara. Were achieved two groups of measurements for the electric arc furnace supplied from the transformer with power of 105 MVA, 30/0.8kV: with and without Oxygen-Jet and Carbon-Jet.

In both situations, the measurements were achieved in the power transformer's primary. There were used voltage measuring transformers with the transformation ratio  $kU=300$  and current measuring transformers with the transformation ratio  $kI=400$ . For measuring the voltages L1, L2 and L3 were used three voltage transformers, and for measuring the currents were used only two current transformers on phases L1 and L3.

The measurements were achieved by means of the three-phase power quality analyzer CA 8334 (Chauvin-Arnoux, France, 2007) who gave an instantaneous image of the main characteristics of power quality for the analyzed furnace.

The values computed by the CA8334 for electric arc furnace without oxygen and carbon injection are presented in table 1.

*Table 1. The power quality parameters for EAF without oxygen and carbon injection*

Technological Phase			Melting			Active boiling	Pre-deoxidation
			Melting 1	Melting 2	Melting 3		
Parameter			7:10	7:42	7:58	8:05	8:39
			7:37	7:53	8:05	8:39	8:55
<b>Time</b>	effective	min	27	11	7	34	16
<b>F</b>	max	Hz	50	50	50.04	50.1	50
	min	Hz	49.97	49.97	49.96	49.97	49.97
<b>UTHD</b>	max	%	4.1	3.2	3.4	3.6	3.3
	min	%	0.8	2.4	2	0.7	0.1
<b>ATHD</b>	max	%	72	10	16	30	21
	min	%	2.5	5	4	3	2
<b>P</b>	max	MW	23.5	22.5	24	24	16
<b>Q</b>	max	MVAR	22	17	18.5	18.5	14.5
<b>S</b>	max	MVA	31	28	32	31	20
<b>cos φ</b>	max	-	0.81	0.81	0.81	0.8	0.5
	min	-	0.1	0.65	0.7	0.18	0.3

The values computed by the CA8334 for electric arc furnace with oxygen and carbon injection are presented in table 2.

**Table 2. The power quality parameters for EAF with oxygen and carbon injection**

Technological Phase			Melting			Active boiling	Pre-deoxidation
			Melting 1	Melting 2	Melting 3		
Parameter			7:08 7:23	7:27 7:32	7:50 7:58	7:58 8:10	-
<b>Time</b>	effective	min	15	18	8	12	-
<b>F</b>	max	Hz	50,16	50,20	50,1	50,1	-
	min	Hz	49,93	49,89	49,91	50,08	-
<b>UTHD</b>	max	%	8.6	8.92	11.4	9.6	-
	min	%	0.9	0.6	0.5	0.6	-
<b>ATHD</b>	max	%	11.96	72.28	84.76	66.08	-
	min	%	0.8	0.4	0.2	0.1	-
<b>P</b>	max	MW	29.85	30.82	30.1	30.01	-
<b>Q</b>	max	MVAR	31.1	32.5	34.32	29.95	-
<b>S</b>	max	MVA	37.1	38.5	39.8	40.66	-
<b>cos φ</b>	max	-	0.95	0.98	0.98	0.96	-
	min	-	0.38	0.18	0.11	0.4	-

The main parameters measured by the CA8334 analyzer were: TRMS AC phase voltages, and TRMS AC line currents; peak voltage, and current; active, reactive, and apparent power per phase; harmonics for voltages and currents up to the 50th order.

This analyzer provide numerous calculated values and processing functions in compliance with EMC standards in use (EN 50160, IEC 61000-4-15, IEC 61000-4-30, IEC 61000-4-7, IEC 61000-3-4).

The measured parameters for the EAF functioning without EAF injectors are compared with the parameters measured for the EAF functioning with oxygen and carbon injectors. The power factor is worsening, UTHD and ATHD are increasing and it requires the adoption of technological solutions to improve power quality.

#### 4. REDUCTION OF SPECIFIC CONSUMPTION AND MELTING TIME

Since specific energy consumption for the years 2003-2008 were situated well above the standards obtained in this type of furnace, it was necessary to implement measures to reduce both development time and specific energy consumption.

The specific consumption of electricity in the electric arc furnace 100 t, type EBT had a downward trend since 2009. For 2008, specific consumption of electricity was to 650.20 kWh/t, dropping to 620.15 kWh/t for 2009, once with the change of furnace transformer, which it was undersized and therefore did not allowed a sufficient loading. The time for melting was reduced from 70 min to 60 min, and the total time was decreased from 83 min to 73 min.

The time for melting is represented in the figure 3. Notice that time during the melting has a downward trend.

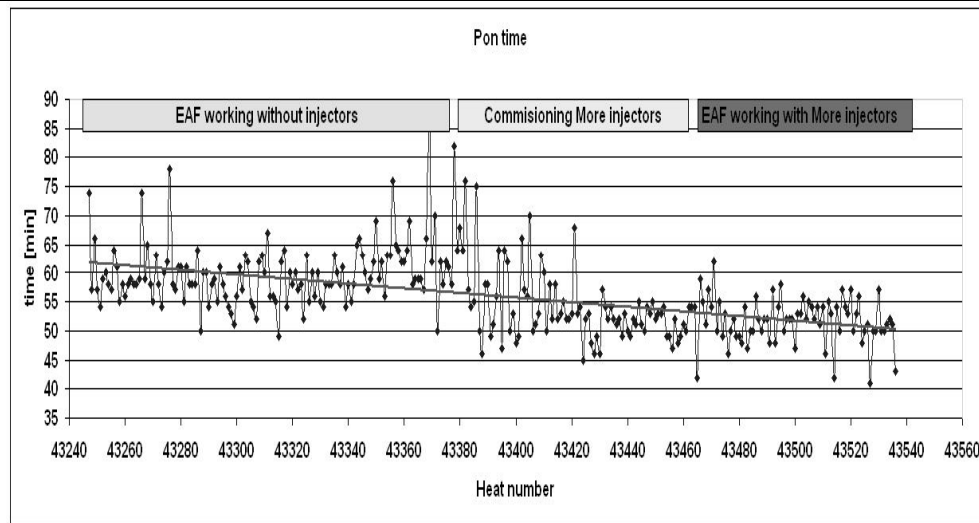


**Fig.3.** Time evolution for melting

The electrical energy specific consumption for melting is represented in the figure 4. Notice that electrical energy for melting has a downward trend.

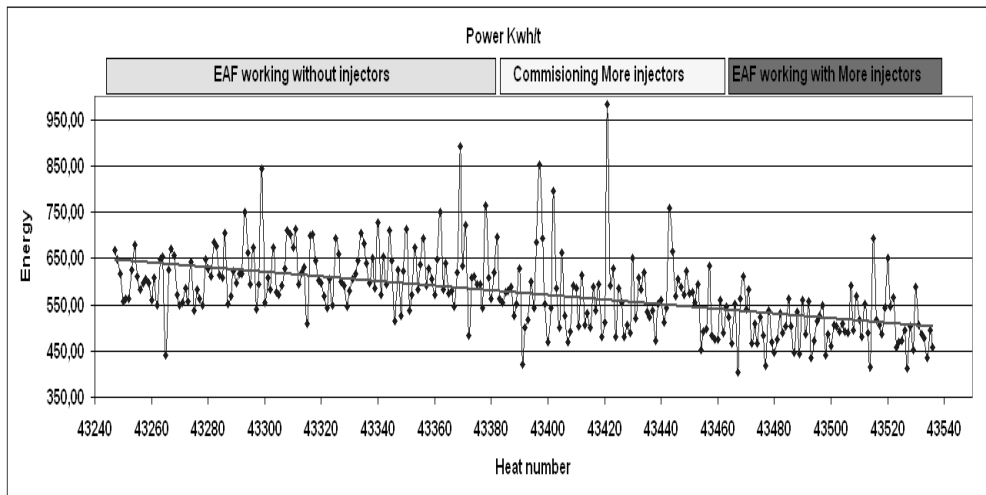


**Fig.4.** The specific consumption for melting

For 2010, consumption reached 510.8 kWh/t, once with the commissioning of Oxygen-Jet and Carbon-Jet, for an average of steel produced 109.5 t.

### 3. THE ECONOMIC CALCULATION

Was made an economic calculation to determine if is appropriate to use of oxygen and carbon injectors to the arc furnaces. In the economic analysis was taken into account the additional cost of oxygen and methane gas.

**Table 3. The calculation of additional oxygen consumption**

<b>Oxygen</b>	Oxygen normally consumed without injectors	15	mc/h
	Oxygen normally consumed with injectors	40	mc/h
	Difference	25	mc/h
	Additional consumption at 100 t	2,500	mc/h
	Oxygen price in Euro	0.15	Euro/mc
	Change rate	4.10	Ron/Euro
	Oxygen price (in Ron)	0.615	Ron/mc
	Additional oxygen price at 100 t	1,538	Ron/100t

In the table 3 is presented an economic calculation for the additional consumption of oxygen.

**Table 4. The calculation of additional methane gas consumption**

<b>CH4</b>	Gas normally consumed without injectors	7.50	mc/h
	Gas normally consumed with injectors	20	mc/h
	Difference	12.50	mc/h
	Additional consumption at 100 t	1,250	mc/h
	Methane gas price (for MWh)	71.98	Ron/MWh
	Methane gas price (for mc)	0.76	Ron/mc
	Additional methane gas price at 100 t	944.44	Ron/100t

In the table 4 is presented an economic calculation for the additional consumption of methane gas.

**Table 5. The calculation of electricity savings**

<b>Electric Energy</b>	Electrical energy consumed without injectors	600	kWh/t
	Electrical energy consumed with injectors	500	kWh/t
	Difference	100	kWh/t
	Electrical electricity savings at 100 t	10,000	kWh
	Electrical energy price (in Ron)	300.94	Ron/MWh
	Price for saving electrical energy at 100 t	3.009	Ron
	The economy at 100 t	527,46	Ron/100t
	The economy	5,27	Ron/t

In the table 5 is presented an economic calculation for the economy for electrical energy. Economic calculation shows that is obtain a benefit of 5.27 Ron/t if are using these injectors.

#### 4. CONCLUSIONS

The specific consumption of electricity in the electric arc furnace 100 t, type EBT had a downward trend after commissioning of oxygen-jet and carbon-jet for EAF

---

belonging to S.C. ArcelorMital Hunedoara S.A. The specific consumption of electricity decreases to 510.8 kWh/t from 620.15 kWh/t.

The time for melting was reduced from 70 min to 60 min, and the total time was decreased from 83 min to 73 min.

Economic calculation shows that is obtain a benefit of 5.27 Ron/t if are using these injectors and it is an important saving.

After the electrical measurements it was found that the power factor is worsening, and UTHD Requires ATHD it is increasing and the adoption of technological solutions to improve Power Quality.

#### REFERENCES

- [1] Arad, S. *Utilizarea energiei electrice*, Ed Focus, ISBN 978-973-677-140-8, 246 pg., 2010
- [2]. Ionescu G. T., *Indicatorii de calitate a energiei electrice și propuneri de nivele limită admise*, Energetica, nr.5, seria B, 1994.
- [3]. Popa I., “*Instalații electrice. vol. 1*”, Editura Mirton, Timișoara, 2000;.
- [4]. \*\*\*, *Instrucțiuni de lucru Oțelăria Electrică*, Cod IL-02, Ediția 1., Rev.5, 2007
- [5]. \*\*\*, PE 124/1993, *Normativ privind stabilirea soluțiilor de alimentare cu energie electrică a consumatorilor industriali și similari*, RENEL, București, 1993.
- [6]. \*\*\*, PE 143/1994, *Normativ pentru limitarea regimului nesimetric și deformant în rețele electrice*, RENEL, București, 1994.

## **ENERGETICAL GROUND OLTENIA - THE ELECTRICAL ENERGY CONSUMPTION AND SOME PROBLEMS ABOUT ENVIRONMENT PROTECTION IN LIGNITE OPEN PITS**

**MARIA DANIELA STOCHIȚOIU<sup>1</sup>, ILIE UȚU<sup>2</sup>**

**Abstract.** In the conditions of mondial economy globalization and the Romanian alignment of UE requirements, on the electrical energy market it is necessary to deliver services and productions at high quality level. Lignite sector is characterized by increasing technological careers due to rehabilitation technological lines landfill and improve career technology and infrastructure.

**Keywords:** Energetical ground, lignite open pits, specific consumption

### **1. INTRODUCTION**

EU develops ambitious energy policy, which covers all energy sources from fossil fuels (oil, gas and coal) to nuclear and renewable energy (solar, wind, geothermal, hydroelectric etc.).

In an economy increasing globalized a country's energy strategy is done in the context developments and changes taking place in the world. Total energy demand in 2030 will be about 50% higher than in 2007, and oil will be about 46% higher. Certain known oil reserves can sustain current levels of consumption only until 2040, and the gas until 2070, while world reserves of coal provides for more than 200 years even an increase in operating. It is estimated that about a quarter of primary energy needs, globally, will be covered by the coal.

The ideas about weak coal using ( lignite and charcoal) which exists in our country is used for producing the electrical energy in the thermoelectrical power plants (CTE) from National Energetic System.

The lignite production is not subsidized in Romania. The lignite consumption is about 30 mil. tone/year.

---

<sup>1</sup> *Associate Professor Eng., Ph.D. at the University of Petrosani*

<sup>2</sup> *Associate Professor Eng., Ph.D. at the University of Petrosani*

---

It is estimated that the lignite apport in assuring the energetical resources will be kept about (45-50)% till 2020. All countries seek to assure the energy necessary from own resources due to the high costs of energetical resources.

The coal deposits are estimated at 3,5 billion tonnes as about 2,7 billion tonnes of lignite and 1,5 billion tonnes are to be exploit. The lignite deposits are sufficient at the present and forecast consumption till 50 years.

Because for building the hydropower plants are necessary more investments (the rentable sources are already fitting out) and the necessary of hydrocarbons takes over the own production, so for a long period of time the coal and especially the lignite represents the base energetical resource in Romania.

The exploited lignite from Romania has a caloric power about 1600-1800 kcal/kg smaller than another lignite from Europe's countries, the Romanian lignite has an increase content of ash, so the CTE's Efficiency using lignite is weaker than the CTE's efficiency using hard coal or hydrocarbons.

Since 2013, the electricity sector responsible for most emissions EU CO<sub>2</sub> will face full auctioning from the purchase certificates CO<sub>2</sub> emissions.

The energy production based on lignite has the following advantages: the production costs are approximately the fuel oil production costs; diminution of hydrocarbons imports through its own resources using; the investments for lignite are smaller than nuclear energy investments at the same installed power; assuring the occupation work forces like an important social aspect; the dependence of electrical energy input is eliminated, it can even produce thermal energy in cogeneration; the environmental problems are solving with actual used technologies.

## **2. THE LIGNITE OPEN PITS – BIG ELECTRICAL ENERGY COSTUMERS**

### **2.1. Technical endowment, the electrical energy supply for the electrical costumers from lignite open pits**

After the last organizational restructure through the Energetical Ground (CE), the lignite open pits Jilt, Rovinari, Tismana, Pînoasa, Rosia, etc., have the exploitation and capitalization of lignite deposits objectives in assuring the coal consumption for thermal power plants from Oltenia ground which has an installed power of 3570 MW: Turceni (4x330MW), Rovinari (4x330 MW), Isalnita (2x315MW), Craiova (2x150 MW), which give about 32% of country's electrical energy. For lignite exploitation are used some methods in continuous flux using mechanized and automatic machines.

The surface mining adaptation at the economic market exactingness due to technological and mechanical machine from open pits and it is in dependence with the management, technical technological restructure.

In the exploitation process, the technological lines contain bucket wheel excavators (BWE) for four types, belt conveyers (BC) for five types and dumping machines (MH) for ten types having a large productivity and the other machines, together assure an hour capacity about 100.000 mc/h, a transport capacity about 400.000 mc/h and a dumping capacity about 150.000 mc/h.

## 2.2 The electrical energy consumption in the lignite open pits

The asynchronous motors in schortcut or induction motors are frequently used in electrical drives for open pits machines. The motor `s power are from 100 to 630 kW and the open pits costumers are supplied from transformer stations about 2x4MVA, 20/6 kV using different electrical cables.

The lignite exploitation became an energointensive process due to open pits machine`s dimensions (overdimensions) and underusing their capacity, even that from annual production about 90% is used in thermal power plants for electrical energy production. CE Turceni and CE Rovinari have a specific electric energy consumption about 5-6 kWh/m<sup>3</sup> which cost represent about (15-20)% from global exploitation expenditures. The diagram 1 shows the electrical energy consumption evolution.

**The electrical energy consumption in lignite open pits from CE**

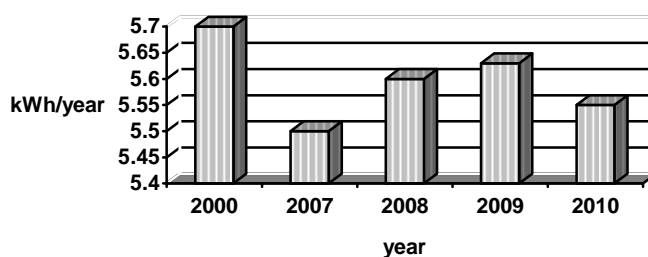


**Fig.1**

The causes which determ the waste electrical energy consumption are:

- the overdimensions and typify of electric drives groupes and technological lines with asynchronous motors (630 kW, 6kV, 71A, 980 ro/min) in underloading operations;
- the typify of drive stations for belt conveyers as gauge, drive models, rolls types and belt dependenceless on lenght or conveyer`s loading capacity;
- overdimensions of transformer stations (2x4MVA, 20/6 kV) but sometimes the installed power of these is about 13%, to a transformer of 4 MVA the iron losses are about 50MWh/year;
- uncorrelation between conveyers capacity from deposits with BWE`s and MH`s capacity;
- frequent starts/stops for technological lines, large period of time for transitory stage for start which determ electromagnetical energy losses;
- adjustable speed systems adsentee for BWE, BC, MH;
- bad quality for motors repairing;
- reactive energy compensation system`s absentee.

After a statistical analysis of using degree about excavators, transport and dumping capacities from CE Oltenia we can draw some conclusions:

- 
- the general indicator of using excavation capacities is about 11% in compare with 30% as should be;
  - the general indicator for belt conveyers is between 11%-13%;
  - the general using of trnasporter and dumping indicator is 5%;
  - an extended transport capacity determs larger costs with electrical energy, with electrical and mechanical maintenance, etc.
  - necessity for finding fialbe technical solutions in correlation with work existed capacity in open pits.

### **2.3 The electrical energy consumption diminuation in the lignite open pits from Oltenia Energetical Ground**

The lignite open pits activity is only justified in some conditions when the lignite costs are attractive in the market competition. To assure the lignite competition with another primary energy fuels it is necessary the correlation between transport, excavation activity with the market requests for increase the economic efficiency, increase the productivity and for reduction the stuff and energy consumption.

Electrical energy consumption is an important part on the lignite structure cost so it must achieve a detailed study about losses of energy and to establish a measurements plan. The following measurements and programme on short and average time are applied:

- limitation of peak loading which is based on the direct relations between programmed mechanical torque to be used and the effective mechanical torque;
- electromagnetical monitoring to determ some levels for electrical measurements to be used;
- the adjustable electrical drives used in the open pit's equipments through power electronics and adequated comand represent a method to diminuate the electrical energy consumption and the financial effort is not important because the actual motors are kept in function working with static converters;

Chemical and steel plants, waste burning stations and thermal power plants generate a large quantity of SO<sub>2</sub>, carbons and nitrogen oxides which produce acide rains, green house and reduce the thickness of ozone layer. The measurements recorded at couple of thermalpower plants outline important quantities of toxic oxides. The power plants are main pollution generation due to their technological processes, the nature of processed raw materials, the waste generated, the number of installations and the size of the affected landmass.

As well as any power plant has a negatice impact on environment, the thermal power plants together with ones that use solid fuels (lignite, hard coal, brown coal) affect all the environmental elements (air, water, soil, animals and plants).

That's why the content of environment protection laws (Directive 2001/80EC) and (H.G. nr.541/2003) which relates the power plants shall be applied all over the board from the power plant design stage to their final implementations.

After a development period during '67-'87 the thermal power plants with large burning coal installations suffered unexpected decline. The romanian economy was

capable of a sustained development program for power plants with capacity over 10.000 MW.

The large burning installations ( on coal) from thermal power plants are equip only with electrofilters. The electrofilters retain the burning gases powders thus reduce the dust emissions.

Nowadays, there is no thermal power plant equipped to assure sulfur dioxide pollution retain as the emission from power plants using coals are bigger than the limits imposed by environment protection laws.

The lignite open pits are integrated cost units of energy producers.

In Romania the lignite exploitation is not government subsidized. The average lignite consumption for 2010 is foreseen not to exceed the 2005 level. The lignite calorific power from Romanian pits is about 1600/1800 kcal/kg and this level is lower than in other european countries and has component around: ash 42%; humidity 44%, sulf contain 1,2%; volatile materials 20%. The efficiency of lignite burning plants is lower than for hard coal or hydrocarbon based installations.

The maximum levels for powder emission allowed by existing legislation for boilers are:

- for solid fuel 100mg/m<sup>3</sup> ;
- for liquid fuel 50mg/m<sup>3</sup> ;
- for natural gas 5mg/m<sup>3</sup> .

The already existing boilers the following values apply:

- 150mg/m<sup>3</sup> for boiler with load between 50-500MWt on solid fuel;
- 100mg/m<sup>3</sup> for boiler with load over 500MWt on solid fuel;
- 50mg/m<sup>3</sup> for boiler working on liquid fuel;
- 5mg/m<sup>3</sup> for boiler working on gases fuel.

Well developed countries budget important funds for research of the process towards development of performant technologies which would reduce such pollution.

#### **4. THE NEGATIVE IMPACT ABOVE C.E.ROVINARI AND TURCENI ENVIRONMENT EROSION**

##### **4.1The diminuation of powder emission**

To reduce these emissions levels the electric filters was reliabled and modernized following the neuniform distribution influence of gases speed above the electrostatic undusting efficiency; the optimisation of friction state in electrostatic undusting technology, etc. The polution emissions levels was reduced aplying these ideas.

The large coal burning installations about 1035 t/h was equipped with electrofilters where the level of polution emissions is shown in the below table (table 1).

Table 1

C.E. Group Poluant	U.M	ROVINARI				TURCENI	
		Group 3		Group 6		Group 1	
		test 1	test 2	test 1	test 2	test 1	test 2
CO <sub>2</sub>	%	16,9	10,25	12,9- 13,6	13,7- 14,3	10,4	10,2-11
CO	mg/m <sup>3</sup>	124	90	90-520	77-215	49-66	110
SO <sub>2</sub>	mg/m <sup>3</sup>	2291	2571- 1675	5233- 5877	3602- 3877	4314- 4438	4327- 4521
NO <sub>x</sub>	mg/m <sup>3</sup>	132	190-204	273-324	325-337	451-462	440

#### 4.2 The lignite open pits – important elements in the environment pollution

About ninety percent from the global lignite deposits from Romania are in the Oltenia basin where are the Rovinari, Motru, Jilt, Berbesti and Husnicioara open pits. The lignite is used for obtaining the thermal agent for heating some important cities and a small part is using for family consumption.

The lignite weight in Romania is from one to eight meters. Over 80% from lignite deposits are exploited in open pits and 15%-20% are exploited in ground mines.

The lignite open pits from Oltenia are equipped with technologies in continuous flux characterized by:

- the lignite deposits are excavated by bucket wheel excavators (BWE) with the following capacities 470 l, 1300 l, 1400 l, 2000 l and productivity about 1680 m<sup>3</sup>/h - 6500 m<sup>3</sup>/h;
- the belt conveyor has the productivity about 1400 -12500 m<sup>3</sup>/h ;
- the laying down machines have capacity about 2500 -12500 m<sup>3</sup>/h.

The biggest affected surfaces from mining industry in Oltenia are in Rovinari, Jilt, Motru basins. As well as in Oltenia, in the other lignite open pits from Romania are existing effected and eroded surfaces by the mining industry but the percent is about 10% from occupied and damaged surfaces in Oltenia. From the global agriculture surface affected by mining industry about 25% represent pastures and about 55% represent orchards and vines. From the surfaces belong to mining industry, 68% was destined for work fronts (deposits and sterile) and 32% was for social building, roads, access ways, etc.

There even appeared geomechanical phenomena like settles, ground slipes, qualitative and quality changes in water surfaces and in the air quality. The lignite open pits exploitation affects all the environment elements, specially soil, which determine the territorial reliability in places where the open pits are in development.

#### REFERENCES

- [1]. M.D. Orban, C. Popescu C. *Carierele de lignit din bazinul carbonifer al Olteniei, surse de energie primară pentru unele termocentrale din Romania*, MININVEST DEVA 2004.
- [2]. F.G. Popescu, M.D. Marcu, I. Stepanescu. *Analiza calității energiei electrice dintr-o linie tehnologică de la E.M. Roșia*. SIMPRO 2008, Petroșani 16-17 Octombrie.
- [2]. \*\*\* [www.enero.ro](http://www.enero.ro) *Strategia energetică a României pentru perioada 2007 – 2020*.
- [3]. \*\*\* [www.cenoltenia.ro](http://www.cenoltenia.ro).

## REPAIRS OF A.C. INDUCTION MOTORS

TEODOR TĂBĂCARU<sup>1</sup>, BRANA LILIANA SAMOILĂ<sup>2</sup>

**Abstract:** There are presented all the steps for full operation to repair the a.c. induction motors both stator, rotor and auxiliaries and some causes of winding failures in three-phase stators of these motors.

**Keywords:** repair, steps, tests, checking bearings and shaft, measurements, inspect, cleaning, failure causes.

The repair and refurbishments of an induction motor should include the following steps:

1. Perform a visual inspection to assess the general condition of the motor. Check for cracks, broken welds, and missing parts. Photographs are required in some cases prior to disassembly of the motor to document the motor construction and accessories.
2. Perform these tests on the stator windings and record the results:
  - Insulation resistance (IR) and polarization index (PI);
  - Winding resistances (terminal-to-terminal resistances).
3. Rotate the rotor manually, and check for any defects in the bearings and shaft.
4. Run the motor at no load. Measure and record the currents, vibration, bearing temperatures, and temperature rises.
5. Measure and record the rotor end play (axial and radial movement of the rotor in the bearings).
6. Dismantle the motor and remove the rotor.

### Stator Work

7. Clean the windings, using low-pressure steam, if they are contaminated with dust, oil or grease.

---

<sup>1</sup> *PhD. Associate Professor Eng. University of Petrosani*

<sup>2</sup> *PhD. Associate Professor Eng. University of Petrosani*

8. Dry the stator in an oven at a temperature of 105°C for a period of 6 h.
9. Take IR and PI tests.

Following steam cleaning and drying of the windings, the results of IR and PI tests should improve.

10. Inspect the motor cable insulation for cracks, overheating, and brittleness.
11. Inspect the stator insulation for cracks, brittleness, and puffiness.
12. Inspect the slot wedges and bracing system in the stator for looseness.
13. Inspect the laminations in the stator core for looseness, damage due to rotor rubbing, localized overheating, and blockage of the vent ducts.
14. If there are no defects in the core or windings of the stator, perform these tests on the stator windings and record the results:
  - Insulation resistance and polarization index tests,
  - Terminal-to-terminal resistances (winding resistances),
  - DC high-potential test,
  - Surge (impulse) test.

#### **Typical causes of winding failures in three-phase stators**

The life of a three-phase stator winding can be shortened dramatically when the motor is exposed to unfavorable operating conditions-electrical, mechanical or environmental.

The winding failures illustrated below are typical of what can happen in such circumstances.

They are shown here to help identify the causes of failure, so that, where possible, preventive measures may be taken.

A single-phase winding failure is the result of an open in one phase of the power supply to the motor (Fig. 1). The open is usually caused by a blown fuse, an open contactor, a broken power line, or bad connections.

Figures 2 to 6 illustrate insulation failures that typically are caused by contaminants, abrasion, vibration, or voltage surge.

Thermal deterioration of insulation in one phase of the stator winding can result from unequal voltage between phases. Unequal voltages usually are caused by unbalanced loads on the power source, a poor connection at the motor terminal, or a high-resistance contact (weak spring). A 1% voltage unbalance may result in a (6÷10) % current unbalance.

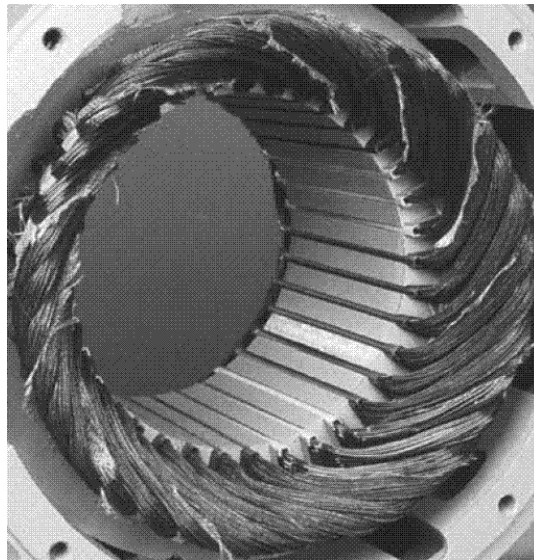


**Fig.1** Winding single-phase (Y-connected)

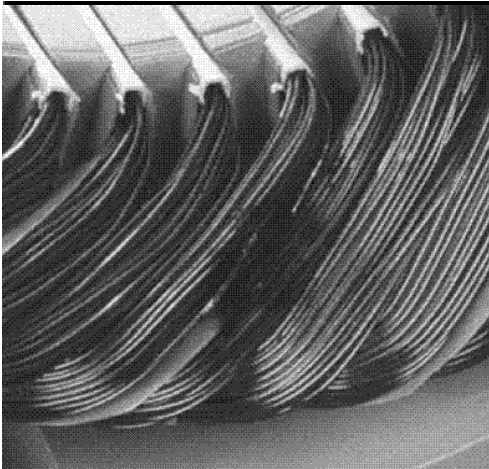


**Fig.2** Winding shorted phase to phase.

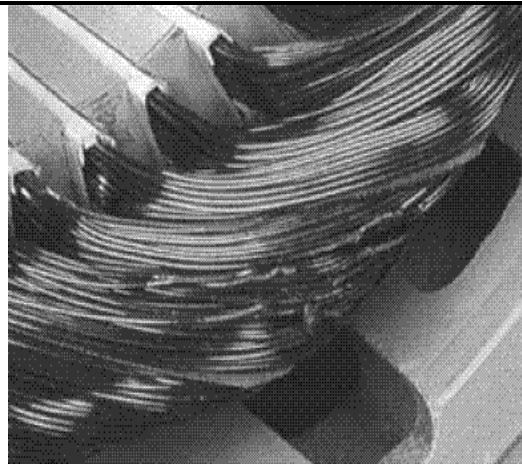


**Fig.3** Winding shorted turn to turn.



**Fig.4** Winding grounded at edge of slot.

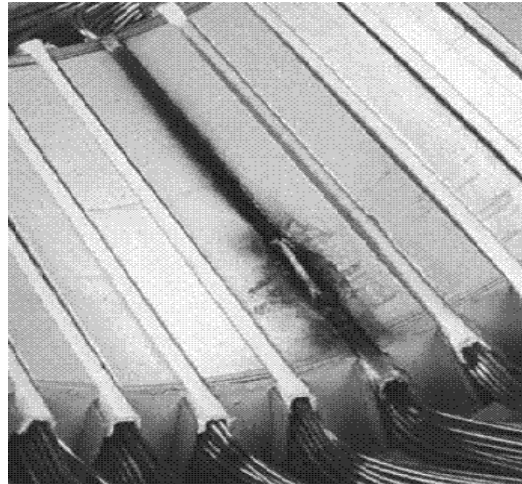


**Fig.5** Winding grounded in the slot.

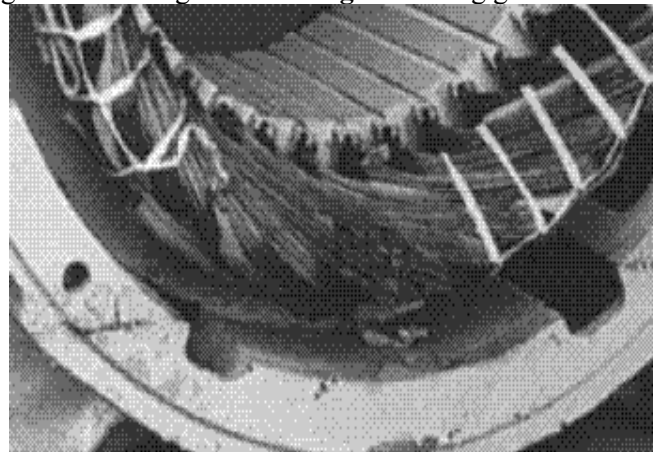


**Fig.6** Shorted connection.

Thermal deterioration of the insulation in all phases of the stator winding typically is caused by load demands exceeding the rating of the motor. (Fig.7). Undervoltage and overvoltage will result in the same type of insulation deterioration.

Severe thermal deterioration of the insulation in all phases of the motor normally is caused by very high currents in the stator winding due to a locked-rotor condition (Fig. 8). It may also occur as a result of excessive starts or reversals.

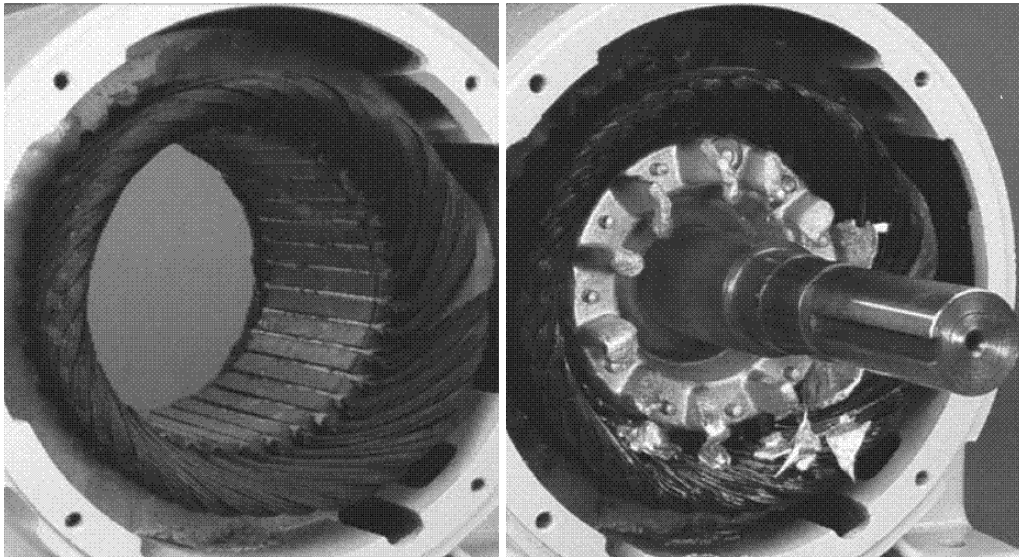


**Fig. 7** Winding damaged due to overload. **Fig. 8** Damage caused by locked rotor.

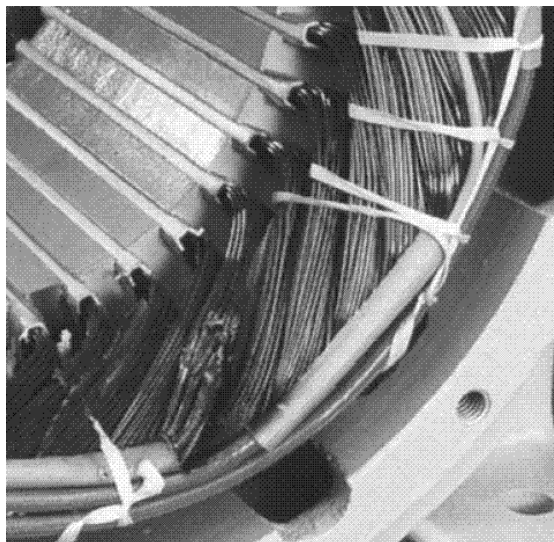


**Fig. 9** Winding damaged by voltage surge.

---

Insulation failures like the one shown in Fig. 9 usually are caused by voltage surges. Voltage surges are often the result of switching power circuits, lightning strikes, capacitor discharges, and solid-state power devices.

### **Rotor Work**

15. If there is a dust, grease, or oil contamination on the rotor, clean it with low-pressure steam.

16. Inspect the rotor laminations for looseness, cracks, and damage due to rubbing with the stator and localized overheating.

17. Inspect the rotor shaft fans of the motor for cracks. If there are signs of cracks, perform dye penetrant and ultraviolet light inspection.

18. Inspect the bars and end rings of the rotor for cracks, looseness, and localized overheating.

If there are signs of cracks, perform the manual rotation test as well as dye penetrant and ultraviolet light inspection.

19. Inspect the rotor shaft for cracks.

20. Mount the rotor on a lathe and measure the eccentricity of the shaft. The total indicated reading should be less than 0.0038 cm.

### **Bearings**

21. Inspect the bearings for cracks, wear, etc.

### **Oil and Water Heat Exchangers**

If heat exchangers are used, perform the following steps:

22. Perform chemical cleaning of the heat exchanger, using a weak acid solution.

23. Inspect the heat exchanger for erosion and corrosion.

24. Perform a hydrostatic pressure test to confirm the integrity of the heat exchanger. The pressure of the water during the test should be 1.5 times the design pressure of the heat exchanger.

25. If there is evidence of corrosion or erosion, perform an eddy current inspection on the tubes of the heat exchanger. All tubes that experienced a reduction of more than 50 % in the wall thickness should be plugged. If more than 10 % of the tubes have experienced a reduction in wall thickness of more than 50 %, consideration should be given to replace the heat exchanger.

### **Temperature Detectors**

26. Perform a visual and a functional check for all resistance temperature detectors (RTDs) and thermocouples used in the winding or bearings of the motor.

**Motor Repair**

27. All defective components should be repaired or replaced.

28. Perform all the tests listed in Tests and Acceptance Criteria for each sort of ac induction motor. The results of the tests should meet the acceptance criteria before the motor can be reassembled.

**Motor Rewind**

If the windings of the motor have serious damage, the motor should be rewound.

**REFERENCES**

[1]. **L. R. Higgins**, *Maintenance Engineering*, 5th ed., McGraw-Hill, New York, 1995;

[2]. **Tăbăcaru, T., Pădure, Al.**, *Exploatarea, întreținerea și repararea echipamentelor și mașinilor electrice*, Editura EDYRO PRESS, Petroșani, 2008.

## **E-LEARNING TECHNIQUE IN HUMAN RESOURCE**

ROXANA BUBATU<sup>1</sup>, EMIL POP<sup>2</sup>, CAMELIA BARBU<sup>3</sup>

**Abstract:** In this paper the trainings ways based on e-Learning for institutions and companies are introduced.

At the beginning of the paper the concepts of these types of education, the methods and possibilities, the advantages and disadvantages are analyzed. In the following, types of e-Learning for training and education, like: synchronous and asynchronous training, the structure of e-Learning courses etc. are presented.

At the end, the paper presents the curriculum components on an e-Learning application, which shows the advantages of this type of education especially for institutions and companies which invest in human resources.

**Keywords:** e-Learning, training, educational impact, asynchronous training.

### **1. E-LEARNING DEFINITIONS, CONCEPTS, METHODS AND MEANS**

#### **1.1. E-Learning Concepts**

E-Learning is the type of training where trainers use IT and Web technologies which considerably reduce the distance and the period of time allowing the trainee to prepare on their own pace using convenient stress free methods.

The benefit of using on-line courses to other methods of information providers, such as Word and PowerPoint online documents, is that e-Learning has been created as a dedicated software based on training concepts, presenting the information in several ways, allowing the access to explanations understood by everyone, eliminating redundant elements and replacing them with those understood, self-evaluation, self-correction, and teacher in education [1], [5].

Considering that an e-Learning course fully uses the internet and Web pages, these include all the basic characteristics of a Web site and are based on them for the realisation of an easy access to information. Consequently e-Learning resembles to the Web sites with an ergonomic and simple user interface, while e-Learning courses need to be simple but informative. Basic elements may be found on the starting page, such

---

as: the name of the course, the summary, the objectives and the navigation menu of the course. From the access to information point of view, it is ideal that any 4 level course architecture to be accessed by only three clicks. Such a course architecture usually contains 4 hierarchical levels [1].

Level 1: Called Course;

Level 2: Called Chapter;

Level 3: Called Pages;

Level 4: Called Subpages.

There are two ways of using e-Learning: the *synchronous* and the *asynchronous*.

- *Synchronous e-Learning* means that teachers and students meet at a pre-convened hour for the course.

- *Asynchronous e-Learning* means that students use the material they have at their disposal on the Web site, which is sufficient enough and may be used at any given time in any place, the relation with the teachers and colleagues being made on-line.

### **Synchronous e-Learning**

Synchronous e-Learning resembles classroom training but there still are a lot of differences between them. Usually the teacher and the students are together in an open conference where PowerPoint may be the most known presentation instrument but it also requires a web format delivery mechanism. For the courses taught in the classroom, probably, the most known transmission system is the shared board which may be used to see the content of the presentations and to allow the trainer to share the desktop with the students, by using a projector. Therefore the trainers control what is shown, heard and on the projected slides on the board, and through the question table made by the student, he can give answers, realising therefore the best communication by instant messages.

### **Asynchronous e-Learning**

Asynchronous e-Learning represents a guided student. The content is available on-line for the students, and it has to be full so that the reference study may be possible. Therefore, PowerPoint presentations are the poorest choices, a software content presenter and a lot of other instruments being necessary for understanding the course, for self-examinations, communication with the teacher and the colleagues, applications, etc.

The following is a presentation of the characteristics of the two e-Learning types from the point of view of their advantages and disadvantages.

Synchronous e-Learning:

- Is able to ensure teacher-student communication, both ways, which is essential for an adequate formation and an efficient evaluation, coordinated by a teacher who establishes and leads the programme;

- An important characteristic is the cost, which is larger than the asynchronous one, due to travelling costs, but the training duration is more reduced;

- 
- It is more efficient especially for the last minute information, because teachers may modify and adapt the presentation during the course;
  - There are professional courses, concentrated according to a time budget, but more expensive due to the need of a course trainer.

Asynchronous e-Learning is different in many ways from the synchronous one, the differences between them have to be considered when preparing the course:

- The main advantage of the asynchronous one is that the content of the course is supplied at a convenient time for the student, at his own pace, and if it is well done it meets all the needs;

- The asynchronous type does not require an instructor for each course. Although, for an efficient use, the material has to be, first of all, interesting and then provide a lot of information and be assisted by the tutor;

- When an asynchronous course is created, the authors has to consider all the students' arguments and questions possible in order to provide them with the expected answers, and the content to be available in all the circumstances;

- The course neither does it need an instructor nor for the trainees to travel, but it is elaborated more difficultly and it also more expensive;

- This type of courses may be used by companies as a resource of increasing their productivity;

- Trainees may be trained anywhere, even at home, all they need is time.

Synchronous e-Learning is more efficient when it is taught by an instructor, or if the company is able to organise the courses in certain geographical places or it affords to take the trainees to professional formation specialised training. Courses which are personalised are adequate to synchronous e-Learning candidates.

Asynchronous e-Learning distinguishes itself by providing training to the staff of companies such as: hospitals, plants, production plants, services, travelling staff, office staff, and unforeseeable schedule staff.

### 3. STRUCTURE OF E-LEARNING COURSES

Web type Courses, also called Web 2.0 have been lately developed for e-Learning professional formation combining the best Web design and design training techniques [2].

The characteristics of the course are the following:

- Ensure the training in the pre-established time;
- They are used a long term resource;
- The duration of the course is of 15 or 20 minutes;
- Easily runs on web browsers on any Pc or PDA;
- Have a specific architecture.

#### **Duration of a course**

Formation using an on-line course is completely different from classroom formation or even reading a book.

---

Here are a series of solutions regarding the minimisation of the duration of courses:

- The basic rule says that: a trainee needs 1 minute for each page.
- A chapter of the course needn't comprise more than 15-20 pages, therefore 15-20 pages per chapter.
- In order to create a functional course for a busy person, a first step is to divide the course in segments of 15-20 minutes each.
- Dividing a course in 5 chapters, each of 15-20 pages, allows the trainee to study a chapter per day and finish the course in one week. These have a feeling of fulfilment if they are able to finalise learning a course in a relatively short period of time.
- Longer courses are created in separate modules.

### **Courses Architecture**

A simple and efficient method for designing a course is to divide the structure material on 4 levels:

Level 1: The course

The first page presents the name of the course and a short summary. The summary may also be the training objective of the course or a high level general view composed of several phrases. The summary is very important because:

- Asynchronous learning does not have a trainer in front of the class to confirm if what is learned is the correct thing.
- The trainers are interested in training when they have a reference framework which may be composed of the objectives and a summary of the material to be studied.

Level 2: Chapters

Each chapter has a title and a summary or a list of learning objectives. Also, optionally, a list of the pages in the chapter may be given, for reaching more objectives:

- The books are divided on chapters and sub-chapters in order to help readers understand the material to be studied. The same reasoning is also applied to e-Learning.
- For the future, the trainees who have studied the course may also use a chapter and a direct information access guideline.

Other characteristics of the course, i.e. on an organisational course level in supporting the student, is to provide the course structure in a toolbar and a list of the chapters.

Level 3: Pages

The third level in the structure of the course is created by pages, figure 1, [3].

A content page should provide:

- A summary, because an easy way of beginning a new subject is provided to the course creators.

- The basic material also contains bookmarks helping the trainees to read attached journals making therefore a difference. The best thing is the journalistic style written material and which needs to be followed considering a series of details.
- Optional information is on the fourth level, and they are also called as drill-down elements. The detailed content should be provided only if the trainee wants to, the provision of optional information drill-down made by the page.

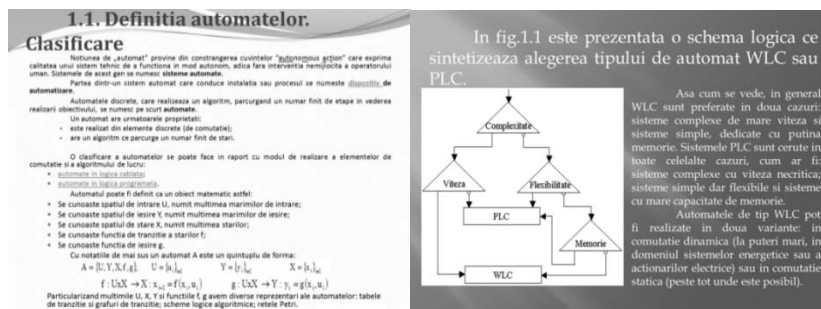


Fig. 1. The e-Learning Course

Another reason for using bookmarks is done considering the Web nature itself. Although a web page is not limited as a paper page or a PowerPoint screen, it may be scrolled easily enough in case it doesn't fit on the screen, but it becomes dull for the user. Therefore it is useful to divide the material in sequences, as such:

- The screen should comprise approximately 400 words or 30 text lines, in order to be easily displayed.
- Avoid using edit on multiple columns. It happens that the trainers forget to read the second column.

Level 4: Sub-pages

Level 4 subpages or drill-down page may be used to consolidate learning. These pages amend the marked element on the contents pages. Often, a course creator may use extra materials to create a course which contains more information accessed using the drill-down, figure 2.

Drill-down pages may be: an article, a link for a web resource, an exercise; a simulation, a movie and a test.

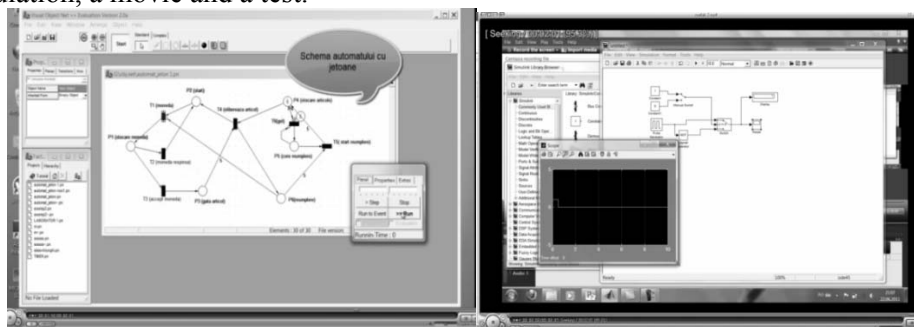


Fig. 2. A capture using Camtasia

---

Drill-down pages should be optionally accessed by the trainer. The display experience level of the trainees is different, and need to wait for each simulation series, even if they are not interested in order for them to continue the course.

#### 4. CONCLUSIONS

E-Learning has already become a new learning system, the characteristics of which are the following:

- It is appropriate for initial training of trainers as well as for continuous formation in institutions and commercial companies;
- This learning system ensures the most efficient professional formation considering the cost / quality ratio;
- Asynchronous e-Learning allows the formation and development of the human resource, launching or designing new projects.
- As a major disadvantage we may appreciate the hardware-software cost of the system and the difficulty in realising specific on-line courses.

#### REFERENCES:

- [1]. **ROSEN**, *E-learning 2.0 Proven Practices and Emerging Technologies to Achieve Results*;
- [2]. **Kay Lehman, Lisa Chamberlin**, *Making the Move to e-Learning. Putting Your Course On-line*;
- [3]. **E. POP, M. LEBA**, *Microcontrollers and Programmable Logic Controllers*, Editura Didactical and Pedagogical, Bucuresti 2003, ISBN 973-30-2070-2;
- [4]. **Allen, I.E., & Seaman, J.**(2007). *On-line nation: Five years of growth in on-line learning*. Needham, MA: Sloan-C;

## THE STABILITY IMPROVEMENT OF SENSORLESS VECTOR CONTROL SYSTEM OF INDUCTION MOTOR

Corneliu MÂNDRESCU<sup>1</sup>, Olimpiu STOICUȚA<sup>2</sup>

**Abstract:** In this paper we analyze the discrete time asymptotic stability of a vector control system for an induction motor with short-circuited rotor that contains in its loop an Extended Luenberger Observer. Estimator is designed so that it is stable at low speeds both in motor and in regenerating mode running. The studied control system is based on the direct rotor flux orientation method (DFOC) and the stability study is based upon the linearization theorem around the equilibrium points of the control system, emphasizing the estimated variation domain of the rotor resistance for which the control system remains asymptotically stable.

**Key words:** asymptotic stability, vector control system, induction motor.

### 1. INTRODUCTION

The direct control systems of rotor flux, sensorless type, of the induction motors' speed assume the estimation of the rotor speed and also the module and rotor flux position estimation. In case the excitation frequency becomes zero the rotor speed can not be estimated [7]. For this reason the low speed control systems' performances are weak. In order to improve the low speed performances nowadays there are different strategies.

So Y. Tamura and H. Kubota within their work [21], suggest a BIBO type stabilization solution of the ELO estimator and implicitly of the control system, based on the Ruth Hurwitz criteria. This method is based on the determination of the proportionality coefficient between the eigenvalues of the motor and the eigenvalues of the Luenberger observer based on an algorithm which ensures the BIBO stability of the ELO observer at very low speed both in motor and in regenerating mode running.

Another strategy, of increasing the performances of the control system at very low speed, is the one suggested by T. Hamajima in his work [15] or the one suggested

---

<sup>1</sup> Ph.D. Assoc. Professor, University of Petroșani, c\_mandrescu@yahoo.com

<sup>2</sup> Ph.D Assist. Professor, University of Petroșani, stoicuta\_olimpiu@yahoo.com

by M. Hinakkanen in his work [12]. So T. Hamajima suggests a stabilization solution for the control system based on a sliding-mode type adaptive observer. The adjustment is made depending on the estimated rotor speed and the estimated stator resistance. The solution proposed by M. Hinakkanen is based on another designing way of the Luenberger matrix. The solutions identical to those given M. Hinakkanen are presented in works [4], [5], [8], [13] and [16].

The newest strategy of increasing the performances of the low speed control system is the one suggested by [9]. This method is based on a Luenberger observer designed based on the relations proposed by Kubota in his work [6]. The proportionality coefficient between the eigenvalues of the motor and the eigenvalues of the observer is chosen based on a “look-up table” depending on the estimated speed and the estimated motor’s couple.

This work proposes a new strategy of choosing the proportionality coefficient between the eigenvalues of the motor and the eigenvalues of the Luenberger Observer. The relations that define the Luenberger gate are the same with the ones suggested by Kubota in his work [6]. The design strategy of the proportionality coefficient is made based on the Ruth Hurwitz criteria considering that the controller within the adaptive mechanism is an adaptive type one. The tuning of the controller is made depending on the proportionality coefficient between the eigenvalues of the motor and the eigenvalues of the Luenberger Observer [19].

Also in this work we present the tuning method of the controllers within the control system. The tuning of these controllers is based on the poles-zeroes method and also on the module and the symmetry criteria the Kessler variant.

These strategies of tuning are based on the research made in this way by Harnefors and Lee in tuning the current controllers [11], but also on the research made by Briz in tuning the flux controller [2], [3]. This paper approaches a difficult problem within vector driving systems for induction motors namely the discrete time asymptotic stability study in a Lyapunov manner [14], [17], and [18].

The difficulty is brought by the mathematical model of the nonlinear analyzed system that makes the Lyapunov stability analysis methods difficult to apply. The novelty of the paper consists in obtaining the method and the form of the linearized mathematical model on which the analysis of the asymptotic stability is made. The shape and structure of the mathematical model depends on the actual components within the analyzed control system and the way in which the state values are selected. Verifying the results is made by simulation using three induction motor types of different powers motor.

## 2. THE DESCRIPTION OF THE VECTOR CONTROL SYSTEM

The speed control system is a sensorless one; its block diagram is shown in figure 1. In figure 1, we marked with B2 the control block of the speed control system with direct orientation after the rotor flux and B1 is the Extended Luenberger observer.

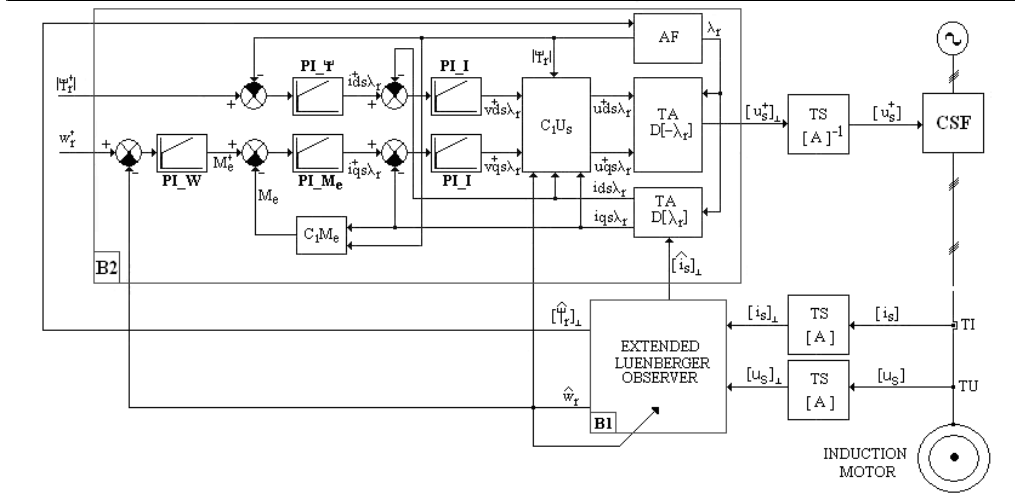


Fig. 1. The block diagram of the vectorial control system

In view of the analysis of the control system and also of its designing, we shall work out the following simplifying hypothesis:

- The static frequency converter (CSF) is assumed to contain a tension inverter.
- The static frequency converter is considered ideal so that the vector of the command measures is considered to be the input vector of the induction motor.
- The dynamic measure transducers are considered ideal.

For the study of the system's stability in the following we present the mathematical equations which define the main blocks of the control system:

- stator voltages decoupling block ( $C_1U_s$ ):

$$u_{ds\lambda_r}^* = (1/b_{11}^*) \cdot [b_{11}^* \cdot v_{qs\lambda_r}^* - h_1] ; \quad u_{qs\lambda_r}^* = (1/b_{11}^*) \cdot [b_{11}^* \cdot v_{qs\lambda_r}^* + h_2] \quad (1)$$

where:

$$h_1 = a_{13}^* \cdot \hat{\psi}_r + a_{31}^* \cdot \hat{i}_{qs\lambda_r}^2 / \hat{\psi}_r + z_p \cdot \hat{\omega}_r \cdot \hat{i}_{qs\lambda_r}$$

$$h_2 = a_{14}^* \cdot z_p \cdot \hat{\omega}_r \cdot \hat{\psi}_r + a_{31}^* \cdot \hat{i}_{ds\lambda_r} \cdot \hat{i}_{qs\lambda_r} / \hat{\psi}_r + z_p \cdot \hat{\omega}_r \cdot \hat{i}_{ds\lambda_r}$$

- PI flux controller ( $PI_\psi$ ) defined by the  $K_\psi$  proportionality constant and the  $T_\psi$  integration time:

$$dx_6/dt = \psi_r^* - \hat{\psi}_r ; \quad \dot{\hat{i}}_{ds\lambda_r}^* = (K_\psi/T_\psi) \cdot x_6 + K_\psi \cdot (\psi_r^* - \hat{\psi}_r) \quad (2)$$

- couple PI controller ( $PI_{M_e}$ ) defined by the  $K_M$  proportionality constant and the  $T_M$  integration time:

$$dx_7/dt = M_e^* - \hat{M}_e ; \quad \dot{\hat{i}}_{qs\lambda_r}^* = (K_M/T_M) \cdot x_7 + K_M (M_e^* - \hat{M}_e) \quad (3)$$

- mechanical angular speed PI controller (PI\_W) defined by the  $K_\omega$  proportionality constant and the  $T_\omega$  integration time:

$$dx_8/dt = \omega_r^* - \hat{\omega}_r; M_e^* = (K_\omega/T_\omega) \cdot x_8 + K_\omega(\omega_r^* - \hat{\omega}_r) \quad (4)$$

- current PI controller (PI\_I) defined by the  $K_i$  proportionality constant and the  $T_i$  integration time

$$dx_9/dt = i_{ds\lambda_r}^* - \hat{i}_{ds\lambda_r}; v_{ds\lambda_r}^* = (K_i/T_i) \cdot x_9 + K_i(i_{ds\lambda_r}^* - \hat{i}_{ds\lambda_r}) \quad (5)$$

$$dx_{10}/dt = i_{qs\lambda_r}^* - \hat{i}_{qs\lambda_r}; v_{qs\lambda_r}^* = (K_i/T_i) \cdot x_{10} + K_i(i_{qs\lambda_r}^* - \hat{i}_{qs\lambda_r}) \quad (6)$$

- flux analyzer (AF):

$$\hat{\psi}_r = |\hat{\underline{\psi}}_r| = \sqrt{\hat{\psi}_{dr}^2 + \hat{\psi}_{qr}^2}; \sin \lambda_r = \hat{\psi}_{qr}/|\hat{\underline{\psi}}_r|; \cos \lambda_r = \hat{\psi}_{dr}/|\hat{\underline{\psi}}_r| \quad (7)$$

- the calculus of the torque block (C<sub>1</sub>M<sub>e</sub>):

$$\hat{M}_e = K_a \cdot \hat{\psi}_r \cdot \hat{i}_{qs\lambda_r} \quad (8)$$

where:  $K_a = 3/2 \cdot z_p \cdot L_m^*/L_r^*$ ;  $z_p$  is the pole pairs number

The coefficients  $b_{11}^*, a_{13}^*, a_{14}^*, a_{31}^*$  are:  $b_{11}^* = 1/L_s^* \cdot \sigma^*$ ;  $a_{13}^* = L_m^*/L_s^* \cdot L_r^* \cdot T_r^* \cdot \sigma^*$ ;  $a_{14}^* = L_m^*/L_s^* \cdot L_r^* \cdot \sigma^*$ ;  $a_{31}^* = L_m^*/T_r^*$ ;  $\sigma^* = 1 - L_m^{*2}/L_s^* \cdot L_r^*$ ;  $T_r^* = L_r^*/R_r^*$

These coefficients are specific to the mathematical model stator currents – rotor fluxes of the induction motor and  $L_m^*$ ,  $L_s^*$ ,  $L_r^*$  and  $R_r^*$  are the mutual three-phase inductivity, the stator's total inductivity, rotor's total inductivity respectively the rotor identified phase resistance.

**The induction motor:** The stator currents – rotor fluxes model is given by the following equations:

$$\frac{d}{dt} \begin{bmatrix} i_s \\ i_r \end{bmatrix} = A_a \cdot \begin{bmatrix} i_s \\ i_r \end{bmatrix} + \begin{bmatrix} \beta_{11} \\ \beta_{31} \end{bmatrix} \cdot \underline{u}_s \quad (9)$$

where:  $A_a = \begin{bmatrix} \alpha_{11} - j \cdot \alpha_{12} \cdot \omega & \alpha_{13} - j \cdot \alpha_{14} \cdot \omega \\ \alpha_{31} + j \cdot \alpha_{32} \cdot \omega & \alpha_{33} + j \cdot \alpha_{34} \cdot \omega \end{bmatrix}$ ;  $i_r = i_{dr} + j \cdot i_{qr}$ ;  $\alpha_{11} = -\frac{1}{T_s \cdot \sigma}$ ;

$$\alpha_{12} = \frac{1 - \sigma}{\sigma}; \alpha_{13} = \frac{L_m}{L_s \cdot T_r \cdot \sigma}; \alpha_{14} = \frac{L_m}{L_s \cdot \sigma}; \alpha_{31} = \frac{L_m}{L_r \cdot T_s \cdot \sigma}; \alpha_{32} = \frac{L_m}{L_r \cdot \sigma};$$

$$\omega = z_p \cdot \omega_r; \alpha_{33} = -\frac{1}{T_r \cdot \sigma}; \alpha_{34} = \frac{1}{\sigma}; \beta_{11} = \frac{1}{\sigma \cdot L_s}; \beta_{31} = -\frac{L_m}{L_s \cdot L_r \cdot \sigma}.$$

The motion equation of the induction motor proper to the stator currents – rotor fluxes model, is:

$$d\omega_r/dt = K_{m1} \cdot (i_{dr} \cdot i_{qs} - i_{qr} \cdot i_{ds}) - K_{m2} \cdot \omega_r - K_{m3} \cdot M_r \quad (10)$$

where:  $K_{m1} = 3/2 \cdot z_p / J \cdot L_m$ ;  $K_{m2} = F/J$ ;  $K_{m3} = 1/J$ .

**The Extended Luenberger Observer:** The equations that define this observer are shown in the following relations:

$$\frac{d}{dt} \begin{bmatrix} \hat{i}_s \\ \hat{\psi}_{-r} \end{bmatrix} = A_b \cdot \begin{bmatrix} \hat{i}_s \\ \hat{\psi}_{-r} \end{bmatrix} + \begin{bmatrix} b_{11}^* \\ 0 \end{bmatrix} \cdot u_s + L \cdot (i_s - \hat{i}_s) \quad (11)$$

where:  $\hat{i}_s = \hat{i}_{ds} + j \cdot \hat{i}_{qs}$ ;  $\hat{\psi}_{-r} = \hat{\psi}_{dr} + j \cdot \hat{\psi}_{qr}$ ;  $A_b = \begin{bmatrix} a_{11}^* & a_{12}^* \\ a_{21}^* & a_{22}^* \end{bmatrix}$ ;  $L = \begin{bmatrix} l_{11} + j \cdot l_{12} \\ l_{21} + j \cdot l_{22} \end{bmatrix}$ ;

$$a_{11}^* = -\left(1/T_s^* \cdot \sigma^* + (1 - \sigma^*)/T_r^* \cdot \sigma^*\right); a_{12}^* = a_{13}^* - j \cdot a_{14}^* \cdot z_p \cdot \hat{\omega}_r;$$

$$a_{21}^* = a_{31}^*; a_{22}^* = a_{33}^* + j \cdot z_p \cdot \hat{\omega}_r; a_{33}^* = -1/T_r^*.$$

The coefficients of the Luenberger matrix are obtained from the proportionality condition between the motor's eigenvalues and the Luenberger observer's eigenvalues. After imposing this condition the Luenberger matrix is composed by the following coefficients [3]:

$$l_{11} = (1-k) \cdot (a_{11}^* + a_{33}^*); l_{12} = z_p \cdot \hat{\omega}_r \cdot (1-k); \quad (12)$$

$$l_{22} = -\gamma \cdot l_{12}; l_{21} = (a_{31}^* + \gamma \cdot a_{11}^*) \cdot (1-k^2) - \gamma \cdot l_{11}$$

where:  $\gamma = \sigma^* \cdot L_s^* \cdot L_r^* / L_m^*$ .

In order that the Extended Luenberger Observer to be completely defined, sequently we present the speed adjustment's mechanism law.

$$\begin{cases} dx_{14}/dt = e_a \cdot \hat{\psi}_{qr} - e_b \cdot \hat{\psi}_{dr} \\ \hat{\omega}_r = K_R/T_R \cdot x_{14} + K_R \cdot (e_a \cdot \hat{\psi}_{qr} - e_b \cdot \hat{\psi}_{dr}) \end{cases} \quad (13)$$

where:  $e_a = i_{ds} - \hat{i}_{ds}$ ;  $e_b = i_{qs} - \hat{i}_{qs}$ .

In these circumstances the sensorless control system shown in figure 1 is completely defined.

The paper deals with the analytical tuning controllers through the method of repartition of zeros - poles and the symmetry criteria and module Kessler instance.

Therefore, for the controllers composing block B2 of the speed control system the following analytical tuning formulas are used [1], [2], [5], [19], [20].

- Current controller:

$$T_i = -1/a_{11}^*; K_i = 1/(b_{11}^* \cdot T_{d1}^*) \quad (14)$$

- Flux controller:

$$T_{\psi} = T_r^* ; K_{\psi} = T_r^* / (2 \cdot L_m^* \cdot T_{d1}^*) \quad (15)$$

- Couple controller:

$$T_M = T_{d1}^* ; K_M = T_{d1}^* / (K_a \cdot |\psi_r^*| \cdot T_{d2}^*) \quad (16)$$

- Speed controller:

$$K_{\omega} = T_4 \cdot (1 + \rho^2) / (2 \cdot K_4 \cdot T_{d2}^*) ; T_{\omega} = 4 \cdot T_{d2}^* \cdot (1 + \rho^2) / (1 + \rho)^3 \quad (17)$$

where:  $\rho = T_{d2}^* / T_4$ ;  $K_4 = 1/F$  and  $T_4 = J/F$ .

In the above mentioned formulas,  $T_{d1}^*$  and  $T_{d2}^*$  are two time constancies imposed considering they need to respect the following conditions:

$$T_{d1}^* < T_r^* ; T_{d2}^* \ll T_4 \text{ and } T_{d2}^* > T_{d1}^* \quad (18)$$

The design the proportionality coefficient between the eigenvalues of the motor and the eigenvalues of the Luenberger observer is made by using the Routh-Hurwitz stability criteria [9], [19].

The proportionality coefficient of the PI controller within the adaptive mechanism:

$$k_R = 1 / (K_u \cdot T_{d1}^*) ; K_u = z_p \cdot \psi_{r0}^2 \cdot a_{14} \quad (19)$$

The integration time of the PI controller within the adaptive mechanism is calculated based on the following relations:

$$T_R = \begin{cases} T_{d1}^* / \alpha(k) & \text{if } \alpha(k) > 0 \\ T_{d1}^* / -\alpha(k) & \text{if } \alpha(k) < 0 \\ T_{d1}^* / \alpha(1.2) & \text{if } \alpha(k) = 0 \end{cases} \quad (20)$$

where:  $\alpha(k) = (1-k) \cdot (a_{11} + a_{33}) - a_{11}$  and the constant  $T_{d1}^*$  the same value as in the case of the current controller.

The proportionality coefficient between the eigenvalues of the motor and the eigenvalues of the Luenberger observer is chosen on the following algorithm [19] (figure 2), where:

$$k_1 = \frac{n_c \omega_{r0} + n_d \omega_{e0} + \sqrt{n_c^2 \omega_{r0}^2 + n_f \omega_{r0} \omega_{e0} + n_d^2 \omega_{e0}^2}}{3n_b \omega_{r0}} ; n_b = R_s L_r^2 z_p (R_s L_r + R_r L_s) ;$$

$$k_2 = \frac{n_c \omega_{r0} + n_d \omega_{e0} - \sqrt{n_c^2 \omega_{r0}^2 + n_f \omega_{r0} \omega_{e0} + n_d^2 \omega_{e0}^2}}{3n_b \omega_{r0}} ; n_c = R_r R_s L_r z_p (L_s L_r - L_m^2) ;$$

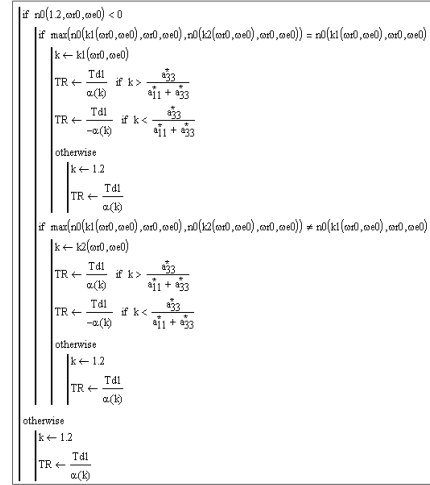


**Fig. 2.** The algorithm of choice of the  $k$  coefficient and  $T_R$  time

$$n_0 = \frac{k \left[ -n_b \omega_r \omega_e k^2 + (n_c \omega_r \omega_e + n_d \omega_e^2) k - n_e \omega_e^2 \right]}{L_r (T_{d1}^*)^2 (L_s \cdot L_r - L_m^2)^2}; n_d = L_r (R_s L_r + R_r L_s)^2$$

$$n_f = 2 \cdot n_c \cdot n_d - 3 \cdot n_b \cdot n_e; n_e = R_r (L_s L_r - L_m^2) (R_s L_r + R_r L_s).$$

### 3. THE ANALYSIS OF THE CONTROL SYSTEMS STABILITY

In order to analyse the stability sequently we shall realise the mathematic model of the vectorial control system. This model is written in an orthogonal axis system  $d\lambda_r - q\lambda_r$  bound to the rotor flux modulus in which the state vector will have fourteen elements:

$$x = [x_i]^T; i = 1 \dots 14 \quad (21)$$

where:  $x_1 = i_{ds\lambda_r}$ ;  $x_2 = i_{qs\lambda_r}$ ;  $x_3 = i_{dr\lambda_r}$ ;  $x_4 = i_{qr\lambda_r}$ ;  $x_5 = \omega_r$ ;  $x_{11} = \hat{i}_{ds\lambda_r}$ ;  $x_{12} = \hat{i}_{qs\lambda_r}$ ;  $x_{13} = \hat{\psi}_{dr\lambda_r}$ .

Within the mathematic model of the control system, the induction motor is modeled based on the stator currents - rotor currents model. The input vector is:

$$u = [u_1 \quad u_2 \quad u_3]^T \quad (22)$$

where:  $u_1 = \psi_r^*$ ;  $u_2 = \omega_r^*$ ;  $u_3 = M_r$ .

In these conditions, the mathematic model of the vectorial speed control system is given by the expression:

$$dx/dt = f(x, u) \quad (23)$$

where:  $f(x, u) = [f_i(x, u)]_{i=1, \dots, 14}$  and the  $f_i$  functions are:

$$f_1 = \alpha_{11}x_1 + (\hat{\omega}\lambda_r + \alpha_{12}z_p x_5)x_2 + \alpha_{13}x_3 + \alpha_{14}z_p x_5 x_4 + \beta_{11}g_1 \quad (24)$$

$$f_2 = -(\hat{\omega}\lambda_r + \alpha_{12}z_p x_5)x_1 + \alpha_{11}x_2 - \alpha_{14}z_p x_5 x_3 + \alpha_{13}x_4 + \beta_{11}g_2 \quad (25)$$

$$f_3 = \alpha_{31}x_1 - \alpha_{32}z_p x_5 x_2 + \alpha_{33}x_3 + (\hat{\omega}\lambda_r - \alpha_{34}z_p x_5)x_4 + \beta_{31}g_1 \quad (26)$$

$$f_4 = \alpha_{32}z_p x_5 x_1 + \alpha_{31}x_2 - (\hat{\omega}\lambda_r - \alpha_{34}z_p x_5)x_3 + \alpha_{33}x_4 + \beta_{31}g_2 \quad (27)$$

$$f_5 = K_{m1}(x_3 x_2 - x_4 x_1) - K_{m2}x_5 - K_{m3}u_3 \quad (28)$$

$$f_6 = u_2 - x_{13} \quad (29)$$

$$f_7 = K_\omega/T_\omega \cdot x_8 + K_\omega \cdot (u_1 - g_3) - K_a \cdot x_{13} \cdot x_{12} \quad (30)$$

$$f_8 = u_1 - g_3 \quad (31)$$

$$f_9 = K_\psi/T_\psi \cdot x_6 + K_\psi \cdot (u_2 - x_{13}) - x_{11} \quad (32)$$

$$f_{10} = K_M (K_\omega/T_\omega \cdot x_8 + K_\omega(u_1 - g_3) - K_a \cdot x_{13} \cdot x_{12}) + K_M/T_M \cdot x_7 - x_{12} \quad (33)$$

$$f_{11} = a_{11}^* x_{11} + \widehat{\omega}_{\lambda r} x_{12} + a_{13}^* x_{13} + b_{11}^* g_1 + l_{11}(x_1 - x_{11}) - l_{12}(x_2 - x_{12}) \quad (34)$$

$$f_{12} = -\widehat{\omega}_{\lambda r} x_{11} + a_{11}^* x_{12} - a_{14}^* z_p g_3 x_{13} + b_{11}^* g_2 + l_{12}(x_1 - x_{11}) + l_{11}(x_2 - x_{12}) \quad (35)$$

$$f_{13} = a_{31}^* x_{11} + a_{33}^* x_{13} + l_{21}(x_1 - x_{11}) - l_{22}(x_2 - x_{12}) \quad (36)$$

$$f_{14} = -x_{13} \cdot (x_2 - x_{12}) \quad (37)$$

Under these circumstances the mathematical model of the speed vector control system is fully determined as being defined by the non-linear differential equations system given by (23) whose initial condition is:

$$x(0) = [0 \ 0 \ 0 \ 0 \ 0 \ 0 \ 0 \ 0 \ 0 \ 0 \ 0 \ 0 \ 0 \ x_{130} \ 0]^T \quad (38)$$

where:  $x_{130} = 10^{-9}$ .

Within the expressions above the following notations were made:

$$v_{ds} = K_i/T_i \cdot x_9 + K_i \cdot f_9; \quad v_{qs} = K_i/T_i \cdot x_{10} + K_i \cdot f_{10} \quad (39)$$

$$h_1 = a_{13}^* \cdot x_{13} + a_{31}^* \cdot x_{12}^2/x_{13} + z_p \cdot g_3 \cdot x_{12} \quad (40)$$

$$h_2 = a_{14}^* \cdot z_p \cdot g_3 \cdot x_{13} + a_{31}^* \cdot x_{11} \cdot x_{12}/x_{13} + z_p \cdot g_3 \cdot x_{11} \quad (41)$$

$$g_1 = (b_{11}^* \cdot v_{ds} - h_1)/b_{11}^*; \quad g_2 = (b_{11}^* \cdot v_{qs} - h_2)/b_{11}^* \quad (42)$$

$$g_3 = -k_R \cdot x_{13} \cdot (x_2 - x_{12}) + k_R/T_R \cdot x_{14} \quad (43)$$

$$\widehat{\omega}_{\lambda r} = 1/x_{13} \cdot [l_{22} \cdot (x_1 - x_{11}) + l_{21} \cdot (x_2 - x_{12})] + z_p \cdot g_3 + a_{31}^* \cdot x_{12}/x_{13} \quad (44)$$

$$l_{11} = (1-k) \cdot (a_{11}^* + a_{33}^*); \quad l_{12} = z_p \cdot g_3 \cdot (1-k) \quad (45)$$

$$l_{22} = -\gamma \cdot l_{12}; \quad l_{21} = (a_{31}^* + \gamma \cdot a_{11}^*) \cdot (1-k^2) - \gamma \cdot l_{11} \quad (46)$$

The study of the stability control system for discrete case, suppose the discretization of the nonlinear system (23). After the discretization, we get:

$$x(k+1) = f(x(k), u(k)) \quad (47)$$

where:  $x(k) = [x_i(k)]^T$ ;  $u(k) = [u_1(k) \ u_2(k) \ u_3(k)]^T$

The equations defining the induction motor and equations defining the extended Luenberger estimator will be discretization using the transition matrix of the canonical system. The automatic controllers of the composition of the control system and the adaptation mechanism will be discretization using the Tustin method:

$$\begin{bmatrix} f_1 \\ f_2 \\ f_3 \\ f_4 \end{bmatrix} = F_d \cdot \begin{bmatrix} x_1 \\ x_2 \\ x_3 \\ x_4 \end{bmatrix} + H_d \cdot \begin{bmatrix} g_1 \\ g_2 \end{bmatrix} \quad (48)$$

$$f_5 = x_5 + T_s \cdot [K_{m1} \cdot (x_3 \cdot x_2 - x_4 \cdot x_1) - K_{m2} \cdot x_5 - K_{m3} \cdot u_3] \quad (49)$$

$$f_6 = x_6 + T_s \cdot [u_2 - x_{13}] \quad (50)$$

$$f_7 = x_7 + T_s \cdot K_\omega / T_\omega \cdot [x_8 + T_s / 2 \cdot (u_1 - g_3)] + T_s \cdot K_\omega \cdot [u_1 - g_3] - K_a \cdot x_{12} \cdot x_{13} \quad (51)$$

$$f_8 = x_8 + T_s \cdot [u_1 - g_3] \quad (52)$$

$$f_9 = x_9 + T_s \cdot K_\psi / T_\psi \cdot [x_6 + T_s / 2 \cdot (u_2 - x_{13})] + T_s \cdot K_\psi \cdot [u_2 - x_{13}] - x_{11} \quad (53)$$

$$f_{10} = x_{10} + T_s \cdot K_M / T_M \cdot [x_7 + T_s / 2 \cdot g_4] + T_s \cdot K_M \cdot g_4 - x_{12} \quad (54)$$

$$\begin{bmatrix} f_{11} \\ f_{12} \\ f_{13} \end{bmatrix} = \begin{bmatrix} 2 \\ \sum_{i=0}^2 \frac{A_e^i \cdot T_s^i}{i!} \end{bmatrix} \cdot \begin{bmatrix} x_{11} \\ x_{12} \\ x_{13} \end{bmatrix} + \begin{bmatrix} 1 \\ \sum_{i=0}^1 \frac{A_e^i \cdot T_s^{i+1}}{(i+1)!} \end{bmatrix} \cdot B_e \cdot \begin{bmatrix} g_1 \\ g_2 \end{bmatrix} + \begin{bmatrix} 1 \\ \sum_{i=0}^1 \frac{A_e^i \cdot T_s^{i+1}}{(i+1)!} \end{bmatrix} \cdot L_e \cdot \begin{bmatrix} x_1 - x_{11} \\ x_2 - x_{12} \end{bmatrix} \quad (55)$$

$$f_{14} = x_{14} - T_s \cdot [(x_2 - x_{12}) \cdot x_{13}] \quad (56)$$

$$F_d = \sum_{i=0}^7 (A^i \cdot T_s^i / i!); \quad H_d = \sum_{i=0}^6 (A^i \cdot T_s^{i+1} / (i+1)!) \cdot B \quad (57)$$

$$v_{ds} = K_i / T_i \cdot x_9 + [K_i + T_s / 2 \cdot K_i / T_i] \cdot K_\psi / T_\psi \cdot [x_6 + T_s / 2 \cdot [u_2 - x_{13}]] + [K_i + T_s / 2 \cdot K_i / T_i] \cdot K_\psi \cdot [u_2 - x_{13}] - x_{11} \quad (58)$$

$$v_{qs} = K_i / T_i \cdot x_{10} + [K_i + T_s / 2 \cdot K_i / T_i] \cdot K_M / T_M \cdot [x_7 + T_s / 2 \cdot g_4] + [K_i + T_s / 2 \cdot K_i / T_i] \cdot K_M \cdot g_4 - x_{12} \quad (59)$$

$$h_1 = a_{13}^* \cdot x_{13} + a_{31}^* \cdot x_{12}^2 / x_{13} + z_p \cdot g_3 \cdot x_{12} \quad (60)$$

$$h_2 = a_{14}^* \cdot z_p \cdot g_3 \cdot x_{13} + a_{31}^* \cdot x_{11} \cdot x_{12} / x_{13} + z_p \cdot g_3 \cdot x_{11} \quad (61)$$

$$g_1 = (b_{11}^* \cdot v_{ds} - h_1) / b_{11}^*; \quad g_2 = (b_{11}^* \cdot v_{qs} + h_2) / b_{11}^* \quad (62)$$

$$g_3 = k_R / T_R \cdot [x_{14} - T_s / 2 \cdot [(x_2 - x_{12}) \cdot x_{13}]] - k_R \cdot [(x_2 - x_{12}) \cdot x_{13}] \quad (63)$$

$$g_4 = K_\omega / T_\omega \cdot [x_8 + T_s / 2 \cdot [u_1 - g_3]] + K_\omega \cdot [u_1 - g_3] - K_a \cdot x_{12} \cdot x_{13} \quad (64)$$

$$\hat{\omega}_{\lambda r} = 1 / x_{13} \cdot [l_{22} \cdot (x_1 - x_{11}) + l_{21} \cdot (x_2 - x_{12})] + z_p \cdot g_3 + a_{31}^* \cdot x_{12} / x_{13} \quad (65)$$

$$la_{11} = (1 - m) \cdot (a_{11}^* + a_{33}^*) \quad (66)$$

$$la_{12} = z_p \cdot g_3(k) \cdot (1 - m) \quad (67)$$

$$la_{22} = -\gamma \cdot la_{12} \quad (68)$$

$$la_{21} = (a_{31}^* + \gamma \cdot a_{11}^*) \cdot (1 - m^2) - \gamma \cdot la_{11} \quad (69)$$

$$A = \begin{bmatrix} \alpha_{11} & \alpha_{12} & \alpha_{13} & \alpha_{14} \cdot z_p \cdot x_5 \\ -\alpha_{12} & \alpha_{11} & -\alpha_{14} \cdot z_p \cdot x_5 & \alpha_{13} \\ \alpha_{31} & -\alpha_{32} \cdot z_p \cdot x_5 & \alpha_{33} & \alpha_{34} \\ \alpha_{32} \cdot z_p \cdot x_5 & \alpha_{31} & -\alpha_{34} & \alpha_{33} \end{bmatrix} \quad (70)$$

$$B = \begin{bmatrix} \beta_{11} & 0 & \beta_{31} & 0 \\ 0 & \beta_{11} & 0 & \beta_{31} \end{bmatrix}^T \quad (71)$$

$$A_e = \begin{bmatrix} a_{11}^* & \hat{\omega}\lambda_r & a_{13}^* \\ -\hat{\omega}\lambda_r & a_{11}^* & -a_{14}^* \cdot z_p \cdot g_3 \\ a_{31}^* & 0 & a_{33}^* \end{bmatrix} \quad (72)$$

$$B_e = \begin{bmatrix} b_{11}^* & 0 & 0 \\ 0 & b_{11}^* & 0 \end{bmatrix}^T; L_e = \begin{bmatrix} la_{11} & -la_{12} \\ la_{12} & la_{11} \\ la_{21} & -la_{22} \end{bmatrix} \quad (73)$$

where:  $\alpha_{12} = \hat{\omega}\lambda_r + \alpha_{12} \cdot z_p \cdot x_5$ ;  $\alpha_{34} = \hat{\omega}\lambda_r - \alpha_{34} z_p x_5$

As the analysed control system, is non-linear, we can not speak of the system stability only about the equilibrium point's stability.

For this reason after solving the non-linear equation system:

$$f_i(x, u) = x_i; i = 1 \dots 14 \quad (74)$$

obtained from the vectorial functions that define the system (47), we obtain the equilibrium point of the non-linear system.

In order to solve the non-linear equation system (74) we shall apply Newton's method, and the equilibrium point obtained for an imposed input vector is noted:

$$b = [b_i]^T; i = 1 \dots 14 \quad (75)$$

Sequently we shall note by  $b_{ma}$  the equilibrium points' throng obtained for an input vector like:

$$u_{ma}^* = [u_{1m} \quad u_2 \quad u_{3a}]^T \quad (76)$$

The rotor angular speed within the input vector (76) is imposed based on the following mathematical relation:

$$u_{1m}^* = \omega_{rm}^* = n_m \cdot \pi / 60 [\text{rad/s}]; \quad n_m = m [\text{rpm}]; \quad m = \overline{-n_N, n_N} \quad (77)$$

and the rotor flux modulus is given by the expression:

$$u_2 = \psi_r^* = \frac{T_s \cdot L_m}{L_s} \cdot \frac{U_N}{\sqrt{1 + T_r^2 \cdot z_p^2 \cdot \omega_{rN}^2}} [\text{Wb}] \quad (78)$$

The moment of resistance within the input vector (76) is imposed based on the following mathematical relation:

$$u_{3a} = a; a = -\overline{[M_N]}, \overline{[M_N]} \quad (79)$$

where  $\overline{[M_N]}$  is the whole part of the expression:

$$M_N = P_N / \omega_{rN} [\text{N} \cdot \text{m}]; \quad \omega_{rN} = 2 \cdot \pi \cdot n_m / 60 [\text{rad/s}] \quad (80)$$

Sequently for the analysis of the stability we shall linearise the non-linear system (47), around the equilibrium point (75).

The linearised model is given by the expression:

$$\Delta x(k+1) = F_D \cdot \Delta x(k) + H_D \cdot \Delta u(k) \quad (81)$$

where:

$$F_D = \left[ \frac{\partial f_i}{\partial x_j}(x_0, u_0) \right]_{i,j=\overline{1,14}}; \quad H_D = \left[ \frac{\partial f_i}{\partial u_k}(x_0, u_0) \right]_{i=\overline{1,14}; k=\overline{1,3}}$$

$x_0 = b$  and  $u_0$  is the input vector whose components are assumed to be known and invariant in time.

The main problem of this study method is choosing the start point of the Newton's method, on which depends this method's convergence. In this case the start point is:

$$x^* = [x_{10} \quad x_{20} \quad 0 \quad x_{40} \quad x_{50} \quad 0_{1 \times 5} \quad x_{10} \quad x_{20} \quad x_{130} \quad 0]^T \quad (82)$$

where:

$$x_{10} = \frac{u_2}{L_m}; \quad x_{20} = \frac{H_{m2} \cdot u_{1m} + H_{m3} \cdot u_{3a}}{H_{m1} \cdot u_2}; \quad x_{50} = u_{1m}; \quad x_{40} = -\frac{K_{m2} \cdot u_{1m} + K_{m3} \cdot u_{3a}}{K_{m1} \cdot x_{10}}; \quad x_{130} = u_2$$

The field of all eigenvalues that are obtained based on the proceeding above will be noted by  $F_D^{ma}$ , the indexes having the same signification as in the equilibrium points' case.

The study of the non-linear system's stability is made in the low and medium speed area without using the flux weakening method. The tuning relations used are the ones presented in this paper and the constants that occur in the automated controllers' tuning coefficients' calculus, are  $T_{d1}^* = 0.1 \text{ ms}$ ;  $T_{d2}^* = 0.75 \text{ ms}$ .

Taking into account the mentioned ones, sequently we present the eigenvalues' field  $F_D^{ma}$  for the motor type using as a start point the vector (82).

Sequently we shall study the internal structural stability of the non-linear system analysed above, determining the parametric stability field of the identified rotor resistance for which the equilibrium points  $b = b_{ma}$  remain asymptotic stable.

In order to determin the variation field of the identified rotor resistance for which the equilibrium points  $b = b_{ma}$  remain asymptotic stable, we shall modify the identified rotor resistance of the motor based on the following mathematical relation:

$$R_r^* = (R_r + k/100 \cdot R_r) [\Omega]; \quad k \in \mathbb{Z}_+ \quad (83)$$

where  $R_r$  is the resistance of the induction motor.

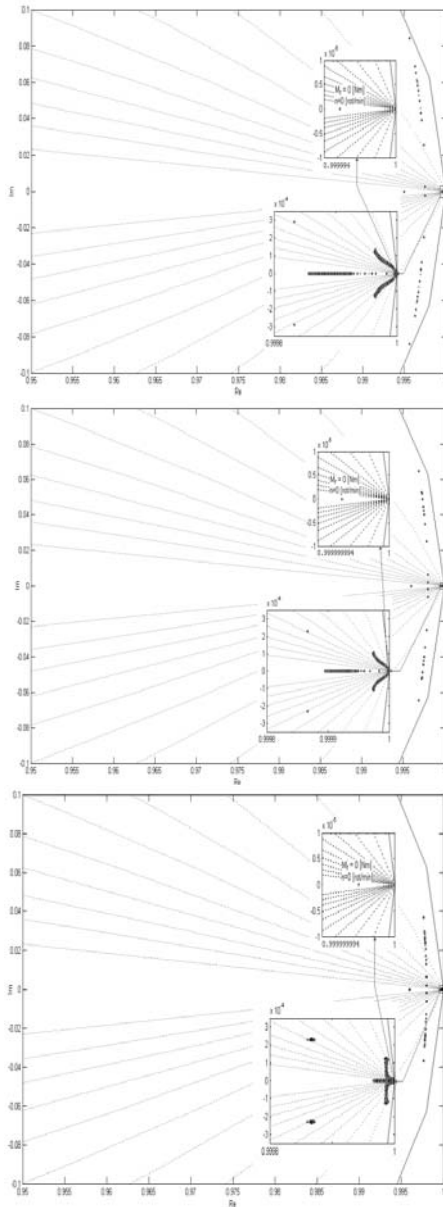


**Fig. 3.** The eigenvalues  $F_D^{ma}$  for the equilibrium point  $b = b_{ma}$ , using the algorithm (fig.2) - motors 1, 2 and 3

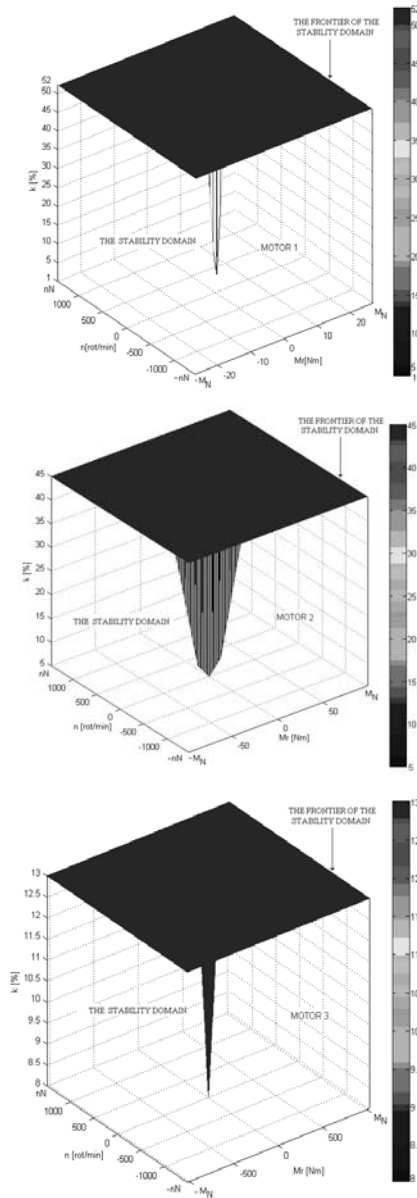


**Fig. 4.** The stability parametric field of the identified rotor resistance - motors 1, 2 and 3

The tuning parameters of the automated controllers, within block B2, will be the same for all the testing period of the structural stability, being determined based on the relations shown in this paper for a rotor resistance equal to the  $R_r$  resistance value of the induction motor.

From those mentioned above we observe that for a specific input vector  $u_{ma}^*$  we shall have  $k$  equilibrium points. For this reason the equilibrium points will be noted:  $b = b_{mak}$ . On the other hand in order to determine the parametric stability field, for each equilibrium point  $b = b_{mak}$  we shall evaluate the eigenvalues of the matrix  $F_D$ , so that the field of these eigenvalues will be noted  $F_D^{mak}$ . The values of the coefficient  $k$  within the expression (83) for which the module of the eigenvalues, that make up the  $F_D^{mak}$  field, becomes greater than unity, define the frontier of the parametric stability field of the identified rotor resistance of the induction motor.

Thus sequentially within figure 4 we present the parametric stability fields for all the three control systems corresponding to the three motor types shown in the annex.

From those mentioned above we observe that the frontier of the stability field of the identified rotor resistance decreases with the increase of the induction motor's power.

This conclusion remains valid both in case the induction machine works in motor mode as in regenerating mode.

In case the motor's revolution and the its resistive moment are close to zero, the stability limit of the identified rotor resistance increases with the induction motor's power.

This study was conducted for a sampling time of  $T_s = 0.4 \mu s$ . Thus the image below will present the graphics for the real and estimated rotors fluxes and also the graphics for the imposed speed, real speed and the estimated speed for small, imposed speeds.

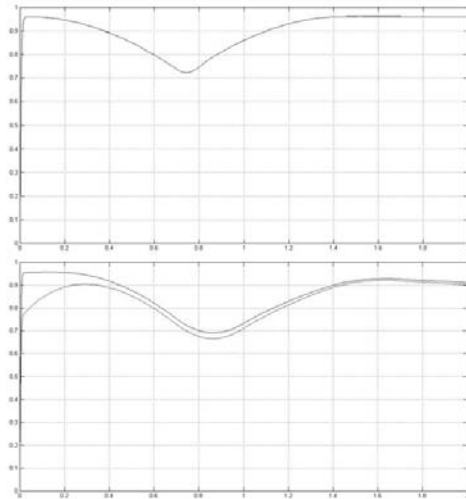


**Fig. 5.** The  $\psi_{dr}$  real flux compared to the  $\hat{\psi}_{dr}$  estimated flux:  $\omega_r^* = 5 \cdot \pi / 30$  [rad/s];  $M_r = 0$ ;  $R_r$  and:  $\omega_r^* = 5 \cdot \pi / 30$  [rad/s];  $M_r = 0$ ;  $R_r^* = 1.7 \cdot R_r$

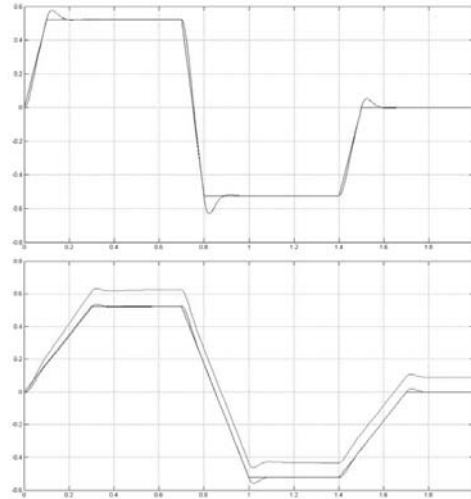


**Fig. 6.** The  $\omega_r$  real speed compared to the  $\hat{\omega}_r$  estimated speed:  $\omega_r^* = 5 \cdot \pi / 30$  [rad/s];  $M_r = 0$ ;  $R_r$  and:  $\omega_r^* = 5 \cdot \pi / 30$  [rad/s];  $M_r = 0$ ;  $R_r^* = 1.7 \cdot R_r$

#### 4. CONCLUSIONS

The use of the formula of the controllers' tuning, shown in this paper, has the advantage of eliminating the experimental methods used so far in the controllers' tuning within the vectorial control systems of an induction motor. The design of the controllers, using the method presented in this paper, ensures the control system with a very good dynamics and robustness. These clear advantages, recommend the successful use of these formula, in common practice.

The stability degree of the speed control systems, sensorless type, decreases with the increase of the motor's power. The closest eigenvalue to the imaginary axis is obtained in null resistant couple and zero speed.

The frontier of the stability domain of the identified rotor resistance decreases with the increase of the induction motor's power. This conclusion remains valid both in case the induction machine works in motor mode as in the case of the regenerating mode. In case the motor's speed and the resistance moment are close to zero, the stability limit of the identified rotor resistance increases with the induction motor's power.

#### REFERENCES

- [1] **Luenberger D.G.**, *An introduction to observers*, IEEE Trans. Ind. on Automatic Control, vol. 16, No. 6, pp.596-602, 1971.
- [2] **Briz F., et al.**, *Analysis and design of current regulators using complex vectors*, IEEE Trans. Ind. Applicat., vol.36, No. 3, pp. 817-825, 2000.
- [3] **Briz F., et al.**, *Current and flux regulation in field-weakening operation of induction motors*, IEEE Trans. Ind. Applicat., vol. 37, No. 1, pp. 42-50, 2001.
- [4] **Yang G., Chin T.H.**, *Adaptive - speed identification scheme for a vector controlled speed sensorless inverter - induction motor drive*, IEEE Trans. Ind. Applicat., vol. 29, No. 4, pp. 820-825, 1993.
- [5] **Kubota H., et al.**, *New adaptive flux observer of induction motor for wide speed range motor drives*, Proc. Int. Conf. IEEE IECON, pp. 921-926, 1990.
- [6] **Kubota H., et al.**, *DSP - based speed adaptive flux observer of induction motor*, IEEE Trans. Ind. Applicat., vol. 29, No. 2, pp. 344-348, 1993.
- [7] **Holtz J.**, *Methods for Speed Sensorless Control of AC Drives*, Proc. Int. Conf. IEEE PCC, pp. 415-420, 1993.
- [8] **Maes J., Melkebeek J.A.**, *Speed sensorless direct torque control of induction motors using an adaptive flux observer*, IEEE Trans. Ind. Applicat, vol. 36, No. 3, pp. 778-785, 2000.
- [9] **Ohyama K., et al.**, *Experimental verification for stability improvement of sensorless vector control system of induction motor using real-time tuning of observer gain*, Electrical Engineering in Japan, vol. 166, No 1, pp. 67-81, 2009.
- [10] **Harnefors L., Nee H.P.**, *Full - order observer for flux and parameter estimation of induction motors*, Proc. EPE, vol. 3, pp. 375-381, 1997.
- [11] **Harnefors L., Nee H.P.**, *Model - based current control of AC machines using the internal model control method*, IEEE Trans. Ind. Applicat., vol.34, No. 1, pp. 133-141, 1998.

- 
- [12] **Hinkkanen M., Luomi J.**, *Stabilization of regenerating - mode operation in sensorless induction motor drives by full - order flux observer design*, IEEE Trans. Ind. Electron., vol. 51, No.6, pp. 1318-1328, 2004.
- [13] **Tsuji M., et al.**, *A sensorless vector control system for induction motor using q-axis flux with stator resistance identification*, IEEE Trans. Ind. Electron., vol. 48, No.1, pp. 185-194, 2001.
- [14] **Stoicuta O., Pana T.**, *Asymptotic stability study of induction motor vector control systems with Luenberger observer*, Proc. Int. Conf. IEEE AQTR, pp. 242-247, 2008.
- [15] **Hamajima T., et al.**, *Sensorless vector control of induction motor stabilized in the whole region with speed and stator resistance identification based on augmented error*, Electrical Engineering in Japan, vol. 155, pp. 52-63, 2006.
- [16] **Suwankawin S., Sangwongwanich S.**, *A speeds - sensorless IM drive with decoupling control and stability analysis of speed estimation*, IEEE Trans. Ind. Electron, vol.49, No.2, pp. 444-455, 2002.
- [17] **Sastry S.**, *Nonlinear systems - analysis, stability, and control*, Springer - Verlag, 1999.
- [18] **Pana T., Stoicuta O.**, *Small speed asymptotic stability study of an induction motor sensorless speed control system with extended Luenberger estimator*, Proc. Int. Conf. IEEE OPTIM, pp: 175-180; 2008.
- [19] **Pana T., Stoicuta O.**, *Design of an extended Luenberger observer for sensorless vector control of induction machines under regenerating mode*, Proc. Int. Conf. IEEE OPTIM, 2010.
- [20] **Pana T., Stoicuta O.**, *Controllers tuning for the speed vector control of induction motor drive systems*, Proc. Int. Conf. IEEE AQTR, 2010.
- [21] **Tamura Y., et al.**, *Design of an adaptive observer for sensorless vector control induction machines under regenerating condition*, Electrical Engineering in Japan, vol. 145, No. 4, pp. 790-798, 2003.

---

**APPENDIX**

- **Motor1** :  $P_N = 4[\text{kW}]$ ;  $U_N = 400[\text{V}]$ ;  $n_N = 1430[\text{rpm}]$ ;  $f_N = 50[\text{Hz}]$ ;  $z_p = 2$ ;  $R_s = 1.405[\Omega]$ ;  $R_r = 1.395[\Omega]$ ;  $L_s = 0.178039[\text{H}]$ ;  $L_r = 0.178039[\text{H}]$ ;  $L_m = 0.1722[\text{H}]$ ;  $J = 0.0131[\text{kg} \cdot \text{m}^2]$ ;  $F = 0.002985[\text{N} \cdot \text{m} \cdot \text{s}/\text{rad}]$ .
- **Motor2** :  $P_N = 15[\text{kW}]$ ;  $U_N = 400[\text{V}]$ ;  $n_N = 1460[\text{rpm}]$ ;  $f_N = 50[\text{Hz}]$ ;  $z_p = 2$ ;  $R_s = 0.215[\Omega]$ ;  $R_r = 0.2205[\Omega]$ ;  $L_s = 0.065181[\text{H}]$ ;  $L_r = 0.065181[\text{H}]$ ;  $L_m = 0.06419[\text{H}]$ ;  $J = 0.102[\text{kg} \cdot \text{m}^2]$ ;  $F = 0.009541[\text{N} \cdot \text{m} \cdot \text{s}/\text{rad}]$ .
- **Motor3** :  $P_N = 160[\text{kW}]$ ;  $U_N = 400[\text{V}]$ ;  $n_N = 1487[\text{rpm}]$ ;  $f_N = 50[\text{Hz}]$ ;  $z_p = 2$ ;  $R_s = 0.0138[\Omega]$ ;  $R_r = 0.007728[\Omega]$ ;  $L_s = 0.007842[\text{H}]$ ;  $L_r = 0.007842[\text{H}]$ ;  $L_m = 0.00769[\text{H}]$ ;  $J = 2.9[\text{kg} \cdot \text{m}^2]$ ;  $F = 0.05658[\text{N} \cdot \text{m} \cdot \text{s}/\text{rad}]$ .

## **ANGULAR SPEED MEASUREMENT USING FPGA TECHNOLOGY**

**NICOLAE PĂTRĂȘCOIU<sup>1</sup>, ADRIAN MARIUS TOMUȘ<sup>2</sup>**

**Abstract:** This paper presents a virtual instrument built in LabVIEW used like a software solution to implement an angular speed measurement for a mobile that is moving in a circular direction. For this, first is determined the function through which is possible to detect the direction of movement and this is implemented through the graphical programming language used in LabVIEW

**Key words:** angular speed, encoder, LabVIEW, FPGA.

### **1. INTRODUCTION**

The movement is defined, as a physical quantity of a mechanical change through is possible to provide information about position of a material point or mobile against a reference system. Quantities derived from this, which may be considered, are position, distance or proximity.

Considering the physical relationship between displacement and velocity, by determining the size of displacement using an incremental sensor, are obtained methods for determining the size of velocity. Most used such methods are based on measurement of elapsed time between successive pulses or counting of pulses number during the prescribed time. As with the displacement case, are frequently situations where the velocity should be considered a vector so it besides determining its value, is necessary to determine direction of movement [4].

### **2. CONNECTING ENCODERS TO DATA ACQUISITION BOARD**

There are data acquisition boards (DAQ) such as the NI 622x, NI 625x, NI 628x (M series devices) or NI USB6211 that have direct support for quadrature encoder measurements so that these devices accept at their input counters signals provided by quadrature encoder. Values counter increases or decreases depending on

the relative time of occurrence of the two trains of pulses. So, when channel A (Ch A) leads channel B (Ch B) in a quadrature cycle, the counter increments and when channel B leads channel A in the same quadrature cycle, the counter decrements. The amount of increments and decrements per cycle depends on the type of encoding – X1, X2, or X4. Fig.1 shows a quadrature cycle and the resulting increments and decrements for X1 encoding. When channel A leads channel B, the increment occurs on the rising edge of channel A. When channel B leads channel A, the decrement occurs on the falling edge of channel A.

There are also data acquisition boards, which have no specific inputs for quadrature signals - E series devices.

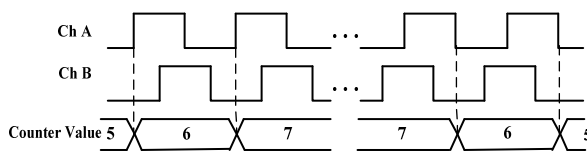


Fig.1. The input signals for data acquisition board

In this case, it is necessary to build a logical system that detects the direction of motion and also increments or decrements a counting value depending on the direction of movement.

Such a system can be achieved through hardware structure, but also can be done by a software solution using digital inputs and counters on the data acquisition board.

If the hardware solution will be chosen, specialized circuits for signal conditioning may be used. For example, the LS7084 quadrature clock converter from LSI Computer Systems, Inc. converts the A and B signals from an encoder into a clock signal and up/down signal that can connect directly to the data acquisition board [4].

Another way to connect and use quadrature encoders with a data acquisition board is to use data acquisition systems using reconfigurable I/O such as PCI-7831R and PXI-7831R or other systems in this class (R series devices).

In this paper is used PCI-7831R data acquisition board to measure the period, frequency and velocity of an induction motor.

The NI 7831R is an R Series device with 96 digital I/O (DIO) lines, eight independent, 16-bit analog output (AO) channels, and eight independent, 16-bit analog input (AI) channels [5].

A user-reconfigurable FPGA (Field-Programmable Gate Array) controls the digital and analog I/O lines on the NI 7831R. The FPGA on the R Series device allows you to define the functionality and timing of the device [6].

Every FPGA chip is made up of a finite number of predefined resources with programmable interconnects to implement a reconfigurable digital circuit.

FPGA chip specifications are often divided into configurable logic blocks like slices or logic cells, fixed function logic such as multipliers, and memory resources like embedded block RAM. There are many other parts to an FPGA chip, but these are typically the most important when selecting and comparing FPGAs for a particular application.

At the lowest level, configurable logic blocks like slices and logic cells are made up of two basic things: flip-flops and look-up tables (LUTs). The various FPGA

families use different architectures based on the way flip-flops and LUTs are packaged together. Virtex-II FPGAs have slices with two LUTs and two flip-flops, whereas Virtex-5 FPGAs have slices made up of four LUTs and four flip-flops [5], [6].

### 3. SYSTEM IMPLEMENTATION WITH VIRTUAL INSTRUMENT

A program developed in LabVIEW is called a virtual instrument (VI) and it has two components the block diagram that represent program itself and the front panel that is user interface.

It can change the functionality of the FPGA on the R Series device in LabVIEW using the LabVIEW FPGA Module to create and download a custom virtual instrument (VI) to the FPGA. Using the FPGA Module, you can graphically design the timing and functionality of the R Series device.

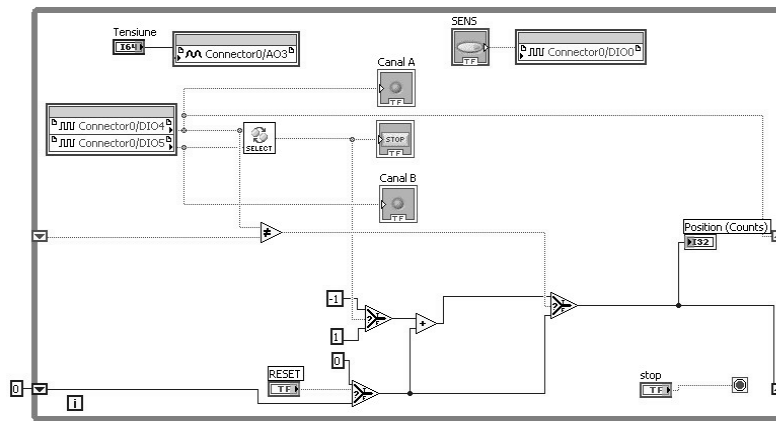


Fig.2. Bloc diagram of FPGA virtual instrument

For measure the angular speed in LabVIEW, first is created a FPGA virtual instrument through which are used the resources of the PCI 7831R acquisition board. Thus, digital inputs DIO3, DI4 and DIO5 are used for acquisition of Channel A, Channel B and Channel Z signals from incremental sensor, digital output DI0 and analog output AO3 are used to command the motor. Also, there is a button to stop the motor and one to stop the program. The diagram block of the FPGA VI is shown in figure 2.

After compilation, virtual instrument is downloaded to the FPGA.

Next, is created host virtual instruments which control the FPGA virtual instrument already created. The diagram block of the Host VI is presented in figure 3.

Loading the FPGA virtual instrument, we have access to all his resources.

To measure the angular speed is used a method that is based on measurement o of elapsed time between successive pulses. For that, is used a Case structure which, on rising edge, is calculate the period of signal from Channel Z of the encoder. Once the period of signal is calculated, we can obtain the frequency and the angular speed with

some simple calculations as can be seen in figure 4.

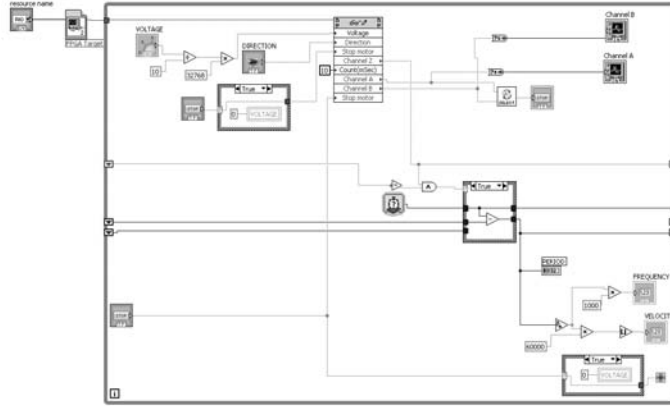


Fig.3. Diagram block of Host virtual instrument

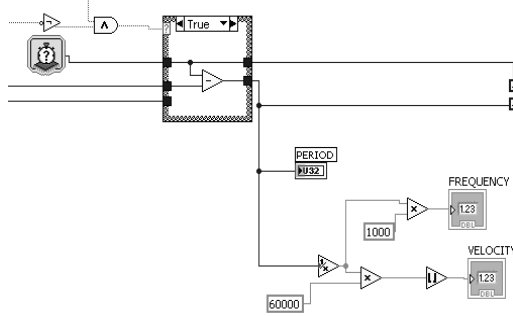


Fig.4. Virtual Instrument for frequency and velocity

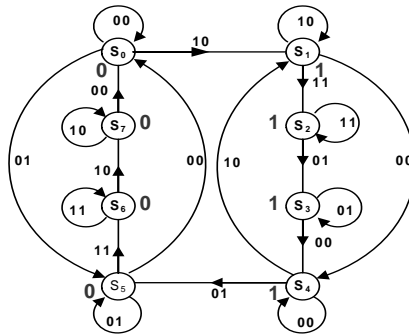


Fig.5. Transition graph of states

To determine the movement direction is chosen the software solution.

For synthesizing the command control signal is considered a chart signals that identify all the possibilities of combining the two pulse trains according to the direction of rotation. Based on this chart, 8 distinct states denoted by  $S_i$  ( $i = 0 \dots 7$ ), can be identified and is constructed the states transition graph shown in figure 5 [3].

Based on the transition graph is built the primitive matrix that contain on the columns the correlation between combination of the input signals (Channel A and Channel B) and on the rows contains all possible transitions from one internal stable state. This is accompanied by full matrix of the output that contains the values of output variable during both states and transitions. Columns are cyclic coded using Gray code [1], [3].

To identify a minimal configuration of the sequentially system is built a reduced matrix of states. Technique used to reduce the number of states from primitive

		State $x_1$				Counting Selection
		00	01	11	10	
$x_1x_2$	00	0	1	x	0	0
	01	1	0	0	0	1
	11	1	1	x	0	1
	10	0	1	1	1	0

		State $x_2$				Counting Selection
		00	00	00	00	
$x_1x_2$	00	0	0	x	1	0
	01	1	1	1	1	1
	11	1	0	x	1	1
	10	0	0	0	0	0

Fig.6. State transition matrix

matrix, is based only on the equivalence from the theory of sequential automatic and reduction of state is through merger or annexation in compliance with specific rules.

To construct the excitation functions, represented by logic functions for states  $x_1$  and  $x_2$  is necessary to build matrices of transition for reduced states and their number must be equal to the number of state variables. These matrices are shown in figure 6 in which notation X means states impossible during

operation.

Applying the method of synthesis of logical functions based on Karnaugh diagrams it can identify the logical functions of the excitation variables (states)  $x_1$ ,  $x_2$  respectively for function of output signal *Counting Selection* as follows [3]:

$$\begin{aligned}
 x_1 &= B \cdot x_1 + \bar{A} \cdot \bar{B} \cdot x_2 + B \cdot \bar{x}_1 \cdot \bar{x}_2 + A_1 \cdot x_1 \cdot \bar{x}_2 \\
 x_2 &= \bar{x}_1 \cdot x_2 + A_1 \cdot \bar{x}_1 + \bar{B} \cdot x_2 \\
 \text{Counting Selection} &= x_2
 \end{aligned}
 \tag{1}$$

From equations (1) can be seen that the output signal is identical to the state  $x_2$  which simplifies implementation with logic gates for the scheme that generate the control signal for counting direction.

Based on logical functions (1) can create a logical diagram of the system through which make selection for direction of counting and LabVIEW have built-in the logical operations through which can be implemented the logical functions above. In this case are used Compound Arithmetic/Logic functions through which can select basic arithmetic or logical operations with two or more variables [2].

This will be a sub-structure, SubVI called *SELECT*, in the main program used to determine the displacement and angular speed values.

To control the movement, stopping and changing engine speed are used a button-type control, a switch and a knob-type control.

Views of the front panel that is user interface, corresponding to the two directions of movement corresponding to two states of operation for the virtual instrument are presented in figure 7, where it can observe the direction identified by signals Channel A and Channel B.

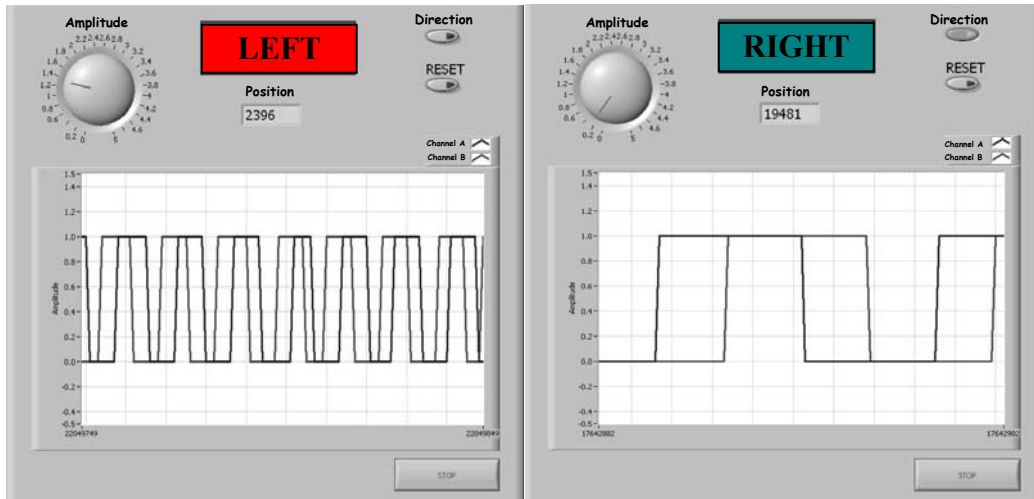


Fig.7. Front panel of Host VI

#### 4. CONCLUSIONS

The solution presented can be applied to any data acquisition boards which do not accept their input signals in quadrature but have a FPGA chip embedded that makes it possible to implement the logic functions.

Such a data acquisition board has no counter, because the user has direct access to the resources board, he can create as many counters as needed with 16, 32 and 64 bits, depending on the number of digital channels of the acquisition board.

#### REFERENCES

- [1]. **Carroll J., Long D.** *Theory of Finite Automata*. Prentice Hall, New Jersey, 1989
- [2]. **Patrascoiu N.** *Sisteme de achizitie si prelucrare a datelor. Instrumentatie Virtuala*. Ed. Didactica si Pedagogica, Bucuresti, 2004
- [3]. **Patrascoiu N, Poanta A, Tomus A, Sochirca B.** *Detection of motion direction implemented by virtual instrumentation*. Recent Advanced in Automation & Information WSEAS Proceeding (ICAI'10)
- [4]. **Webster.G.J.** *The measurement, Instrumentation and Sensors Handbook*. CRC Press LLC, 2000
- [5]. \* \* \*, *Reconfigurable I/O Devices for PCI/PXI/CompactPCI Bus Computers*, National Instruments Corporation, 370489B-01, april 2004
- [6]. \* \* \*, *Quadrature Encoder Velocity and Acceleration Estimation with CompactRIO and LabVIEW FPGA*, National Instruments Corporation

## DESIGNING, MODELING AND SIMULATION OF A PICO-HYDRO POWER PLANT CONTROLLER

CAMELIA BARBU<sup>1</sup>, ROXANA BUBATU<sup>2</sup>, ADRIAN DINOIU<sup>3</sup>,  
LORAND BOGDANFFY<sup>4</sup>

**Abstract:** The objective of this paper is to design a Pico-hydro power plant controller based on his mathematical model. First, the natural hydro process is considered consisting of water lake, supply pipe, hydro turbine, DC generator and controller. Second, for each part of the Pico-hydro is written the mathematical model and after that the entire system is simulated in open loop. Then the controller is designed and the system is simulated in closed loop. These two control modes are compared and presented the advantages of each of them. The simulation results are as expected and can be used to design and validate the controller.

**Key words:** renewable energy, mathematical model, simulation

### 1. INTRODUCTION

The Pico-hydro means a plant of small power, having no more 10 kW representing lately the biggest challenges in clean energy generation, due to the following advantages:

- Use sources of low water flow and fall and are environment friendly ;
- Can autonomously function and useful for isolated areas;
- The initial investments are low.

The Pico-hydro plant has the following important elements: water lake and vane; supply pipe; hydro turbine; DC generator and controller.

---

<sup>1</sup> Lecturer Eng., Ph.D. at the University of Petrosani, [tabacarucamelia@yahoo.com](mailto:tabacarucamelia@yahoo.com)

<sup>2</sup> Ph. D. Student at the University of Petrosani, [roxana.bubatu@yahoo.com](mailto:roxana.bubatu@yahoo.com)

<sup>3</sup> Ph. D. Student at the University of Petrosani, [adidinoiu@yahoo.com](mailto:adidinoiu@yahoo.com)

<sup>4</sup> Ph. D. Student at the University of Petrosani, [lorandbo85@yahoo.com](mailto:lorandbo85@yahoo.com)

In this analysis we will consider the above case of a DC generator with a common power bus. The Pico-hydro plant can be considered as a system with the block diagram from fig.1.

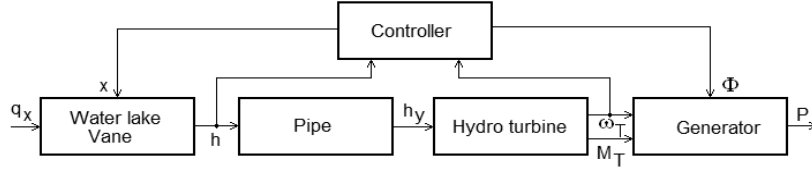


Fig.1. Pico-hydro system block diagram

The water lake has as input a  $q_x$  uncontrollable flow and as output a vane that controls the  $h$  water level in the lake, producing a  $q_v$  controllable flow. There are two water levels: the minimum  $N_0$  level and the maximum  $N_1$  level. The water level  $h$  must be controlled by the on/off position  $x$  of the vane between these two levels.

The second component is the hydro turbine, which is a nonlinear element, having as input the  $h_y$  pressure and as outputs the  $M_T$  torque and the  $\omega_T$  speed. The DC generator is a nonlinear element, too. The inputs of the generator are the  $M_T$  torque, the  $\omega_T$  speed, the  $\Phi$  control flux and the output is the DC power  $P$ . The controller has two inputs, the  $h$  pressure and the  $\omega_T$  speed and two outputs, one for on/off control of the vane and the other for generator flux  $\Phi$  control [1].

## 2. MATHEMATICAL MODEL FOR HYDRAULIC PROCESS

In this section we will model and simulate the hydraulic process of power plant and we will present the simulation results [1].

Considering the volume  $V$ , surface  $S$  and level  $h$  of the tank, we can write the relationship:

$$\frac{dV}{dt} = q_x - q_v \quad (1)$$

In order to model the on-off control principle of the vane we will introduce in the above relation the step distribution  $\theta(x)$ , resulting:

$$q_v = \frac{1}{k_v} \cdot \Delta h_v \cdot \theta(x) \quad (2)$$

With  $V = S \cdot h$ ,  $\Delta h = h$ ,  $T_v = k_v \cdot S$ , we get the mathematical model of the process and the transfer function:

$$T_v \cdot \frac{dh}{dt} + h \cdot \theta(x) = k_v \cdot q_x \quad (3)$$

$$G_w = \frac{h(s)}{q_x(s)} = \frac{k_V}{\theta(x) + T_V \cdot s}$$

$$= \begin{cases} \frac{k_V}{T \cdot s}; & \theta(x) = 0 \text{ (closed vane)} \\ \frac{k_V}{1 + T_V \cdot s}; & \theta(x) = 1 \text{ (opened vane)} \end{cases} \quad (4)$$

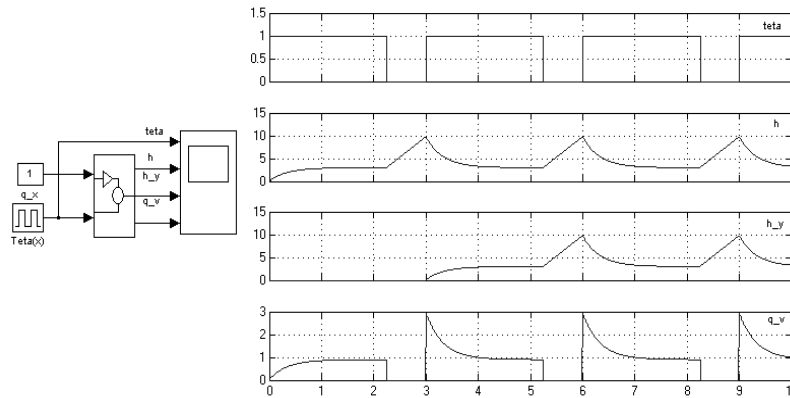


Fig.2. Simulation of hydraulic process: a) model; b) simulation results

### 3. MATHEMATICAL MODEL OF THE DC GENERATOR

We begin from the hydraulic turbine equations, in linear form, where  $a$  and  $b$  are constants [1]. When only the  $q_T$  flow and the  $\omega_T$  speed are modified, we get the mathematical relations for torque:

$$M_T = a \cdot q_T - b \cdot \omega_T \quad (5)$$

In dynamic regime the dependence between torque  $M_T$  and pressure  $h_y$  can be written to a linear differential equation:

$$T_T \cdot \frac{dM_T}{dt} + M_T = k_T \cdot h_y \quad (6)$$

where:  $T_T$  is time constant and  $k_T$  is the steady state gain.

Results the transfer function of the turbine:

$$G_{MT}(s) = \frac{M_T(s)}{h_y(s)} = \frac{k_T}{1 + T_T \cdot s} \quad (7)$$

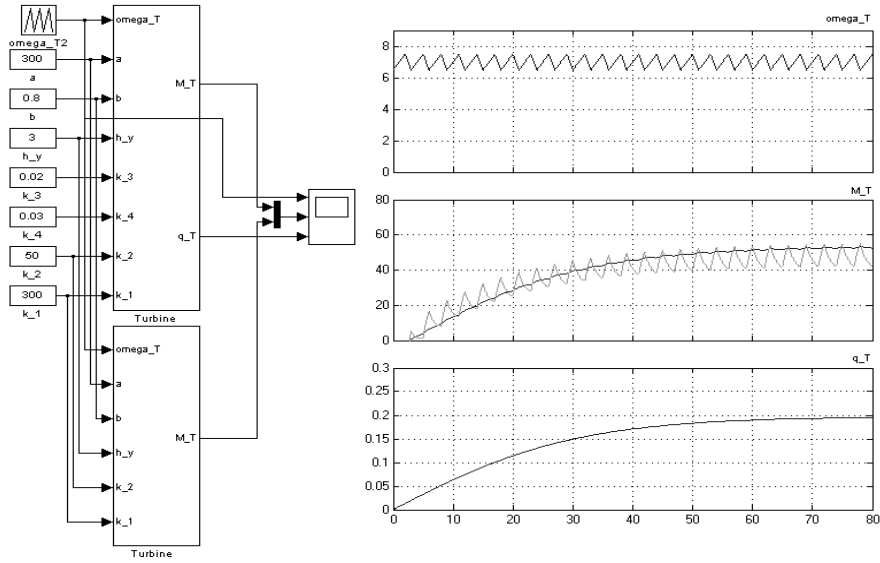


Fig.3. Hydro turbine, model and simulation results

In fig.3 are presented the modeling and simulation results for the nonlinear and linear approach, having the following data:  $a=400$ ,  $b=1.5$ ,  $k_1=300$ ,  $k_2=50$ ,  $k_3=0.02$ ,  $k_4=0.03$ .

In this simulation we will consider the input  $h_y$  constant of 5 m and the input  $\omega_T$  fluctuating between 7 and 8 rad/s. As outputs we will represent the  $M_T$  torque and the  $q_T$  flow.

Second, we will write the DC generator mathematical model. This because the Pico-hydro generally use the DC solution in order to charge the batteries. The generator equations for the input torque  $M_T$  and the outputs voltage  $U$  and power  $P$  are as follows:

$$U = k_e \cdot \Phi \cdot \omega_T - (R_G + R_L) \cdot i - L_G \cdot \frac{di}{dt} \quad (8)$$

$$M_T = k_m \cdot \Phi \cdot i \quad (9)$$

$$P = Ui = M_T \omega_T - \frac{R_G + R_L}{k_m^2 \cdot \Phi^2} M_T^2 - \frac{L_G}{k_m^2 \cdot \Phi^2} M_T \frac{dM_T}{dt} \quad (10)$$

where:  $\Phi$ ,  $i$  and  $U$  are generator's flux, current and voltage;  $R_G$  and  $L_G$  are internal generator's resistance and impedance and  $R_L$  is the load. In this case  $L_G$  can be neglected.

In order to maintain an approximately constant output voltage, there can be introduced a loop on speed. In fig.4 are presented the model and simulation results for the two cases, open loop and closed loop.

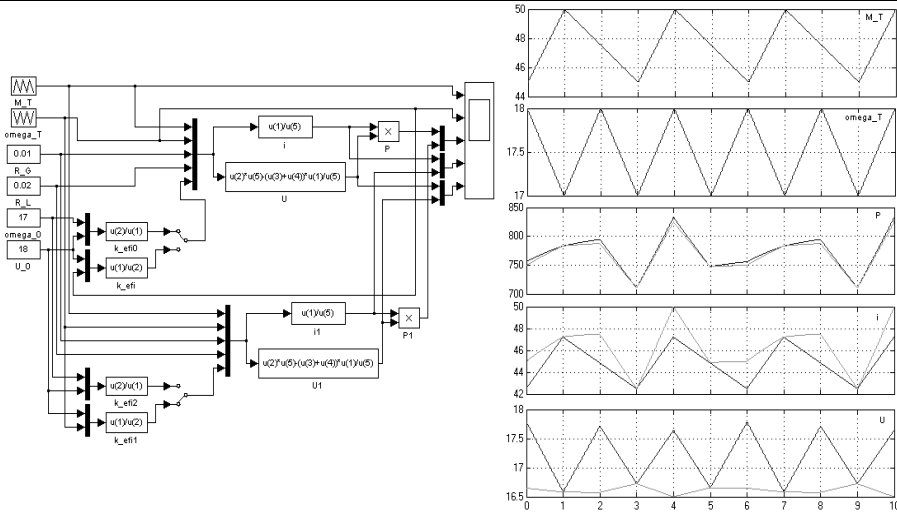


Fig.4. DC generator: model and simulation results

#### 4. MODELING THE ENTIRE PLANT

For modeling and simulation of the plant we consider the hydraulic and electrical parts together with the dedicated controller. This controller is based on on/off principle and controls the input flow of the turbine and stabilizes the output voltage of the DC generator. First, we will design the controller that has two inputs and two outputs. The inputs are the pressure  $h$  and the speed  $\omega_T$ , [2] [3].

The outputs are the on/off control signal for the lake vane and the DC generator flux  $\Phi$ . In fig.5 is presented the controller model and simulation results.

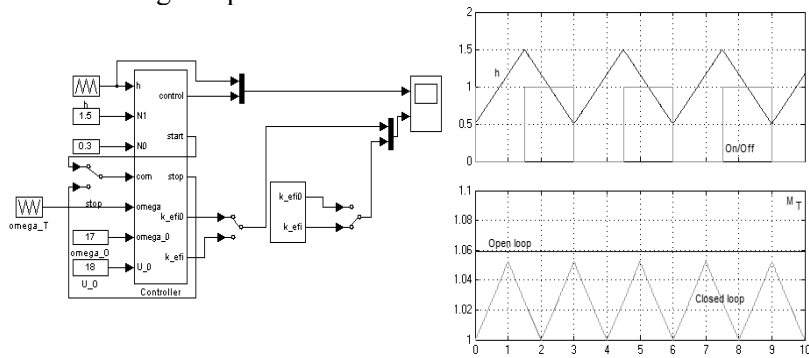


Fig.5. Controller: a) block model; b) simulation results

The plant complete model was obtained connecting all the elements presented above and the controller.

In fig.6 are shown the simulation model and results for this system. There were used the following data:  $q_x = 6 \text{ m}^3/\text{s}$ ;  $S = 12 \text{ m}^2$ ;  $N_1 = 1.5 \text{ m}$ ;  $N_0 = 0.4 \text{ m}$ ;  $\omega_0 = 15 \text{ rad/s}$ ;

$U_0 = 18 \text{ V}$ ;  $h_0 = 8 \text{ m}$ ;  $R_L = 0.02 \ \Omega$ ;  $R_G = 0.01 \ \Omega$ ;  $T_p = 5 \text{ s}$ ;  $k_T = 7.5$ ;  $T_T = 5 \text{ s}$ ;  $h = 0.5 \dots 2 \text{ m}$ ;  $\omega_T = 18 \dots 20 \text{ rad/s}$ .

The system can run in two modes that are open loop and speed closed loop. In fig.6.b there can be noticed the very good results in closed loop control.

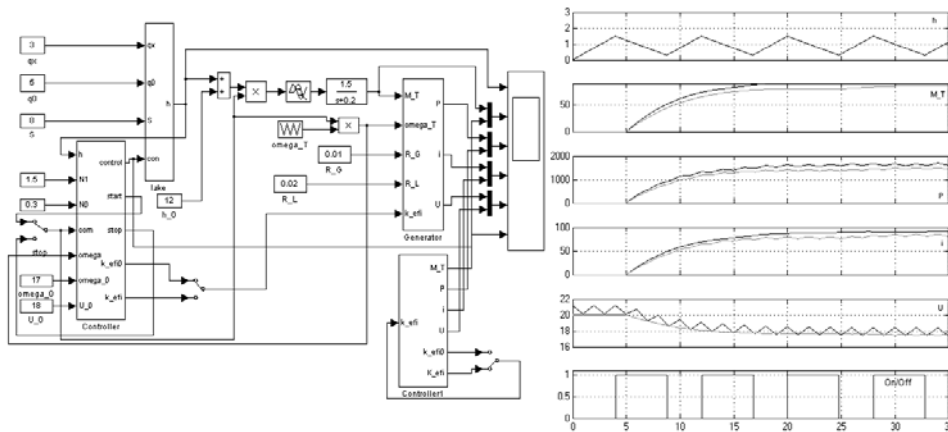


Fig.6. Complete plant: a) model; b) simulation results

## 5. CONCLUSIONS

Many years the small rivers and the fresh running water were an important life resource for the little communities around them. Today, due to the technology of Pico-hydro, this running water represents also an important clean energy resource too.

This paper presents a systemic approach on the Pico-hydro plant, starting with the achievement of the process and continuing with the controller design.

The hydraulic part and the electrical part were modeled and simulated. Then, there is designed, modeled and simulated the controller and are obtained the simulation results for the plant.

The results of this paper prove the correctness of this solution and can be used in practical applications, like controllers design for Pico-hydro plants.

## REFERENCES

- [1]. Fraile-Ardanuy J., Wilhelmi J.R., Fraile-Mora J., Pérez J.I., Sarasúa I., *A Dynamic Model of Adjustable Speed Hydro Plants*, 9 Congreso Hispano Luso de Ingeniería Eléctrica, Marbella, Spain, 2005
- [2]. Pop E., Leba M., Tabacaru Barbu I.C., Pop M., *Modeling, Simulation and Control of Pico-Hydro Power Plant*, Control Systems, Proceedings of the 4<sup>th</sup> WSEAS/IASME Corfu, GREECE, October 26-28, 2008, ISBN 978 960 474 014 7, ISSN 1790 2769, pp. 103-108
- [3] Tabacaru-Barbu I. C., *Contributions Regarding the Modeling, Simulation and Implementation of Methods and Techniques of a Sustainable Integrated Renewable Energetic System Achievement*, Ph.D. Thesis, University of Petrosani, 2009

## SOFTWARE APPLICATION APPLICATION FOR DETERMINING THE MINIMUM TRIP LENGTH ON MAP

ANGELA EGRI<sup>1</sup>, VALI-CHIVUTA SIRB<sup>2</sup>

**ABSTRACT:** *This software application shows how identifying the roads on a map over time, selection the minimum trip, creating a map and using the intuitive interface for determining the minimum trip length on map . In addition, the software may open new maps, which are separate from the source code, and create new maps.*

**KEY WORDS:** *Minimum trip length, source code, intuitive interface, map search algorithm.*

### 1. INTRODUCTION

The basic functionality (fig.1.) of the program is to identify roads on a map over time. In addition, the program may open new maps (which are separate from the source code) and create new maps.

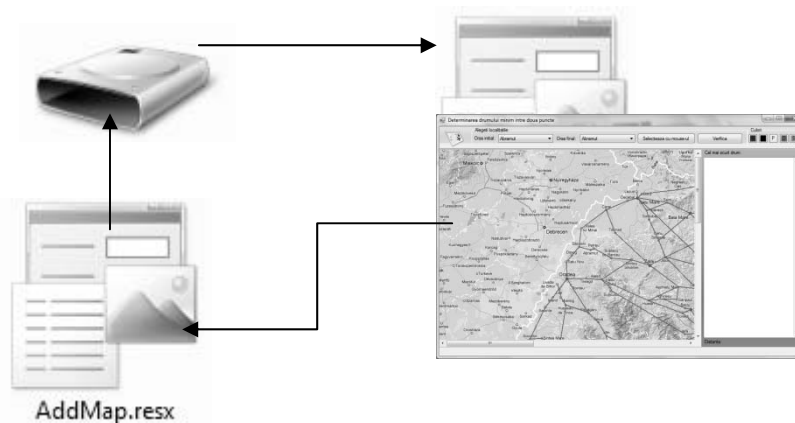


Fig. 1. Software working principle

<sup>1</sup> *Assoc. prof. eng., phd. at the University of Petroșani;*

<sup>2</sup> *Lecturer eng. ,phd. at the University of Petroșani;*

## 2. MINIMAL TRIP SELECTION

Once a map is loaded (fig.2.), you can find the minimum path between two nodes [1]. Nodes can be chosen from lists available, or may be selected by clicking “*Selectează cu mouse-ul*”. Once you press this button, first click on the map to select the city closest to where you clicked as the original city and the second click will set the final city (destination).

In lists, cities are displayed in alphabetical order, regardless of the order in which they were introduced when the map was created.



Fig.2. City selection panel

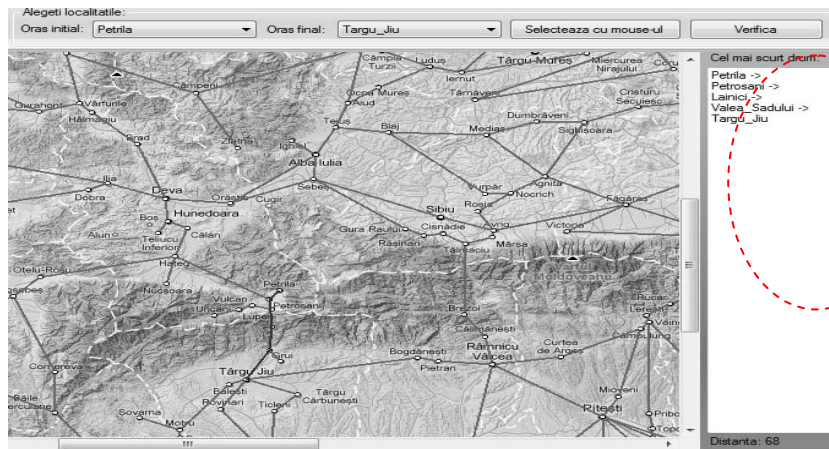


Fig. 3. Representation and display the shortest path and distance

Pressing the Check button, the program will be served with the task of calculating the minimum path between two points. The optimal solution will be colored differently, and the road will be displayed in the text box available. The total distance is also displayed. Efficiency of the total number of nodes depends on the values map and the distances between them.

### 3. CREATING A MAP

The program provides the opportunity to create new maps and open them to calculate various roads [2]. Thus, a user may place the maps to meet their needs. To create a map, the client must have an image of the map (fig.4.) in a format supported by the program (jpg, bmp, png). Initially it will enter the selected image (using the utility program) and points to their name, then the distances between points, where there is direct link.

Map Resources must be saved in the application directory. Three files will be automatically generated with the same name (fig.5.) and different extensions, each of which contains part of the data needed to run the program on paper

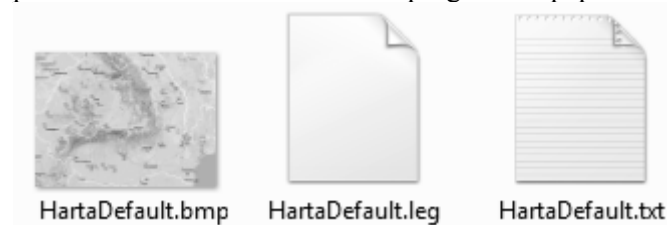


Fig. 4. Files required by a map

**nume\_hartă.txt** contains information about the number of nodes on the front line and following lines are present name and coordinates of nodes on which the point is on the map (in pixels)

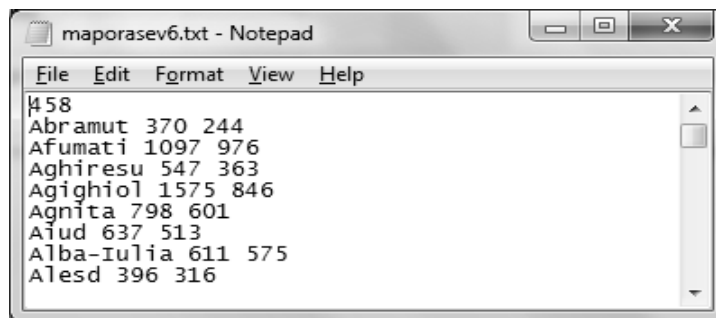


Fig. 5. Text file structure of map file maporasev6

**nume\_hartă.leg** adjacency matrix is formed. Each line is a line array, with elements separated by a space

**nume\_hartă.bmp** is the map image.

These files are automatically generated by the utility provided by the program when saving (fig.6.).



Fig. 6. Application window to create maps

After being selected image may be entered either by typing node point coordinates manually or by clicking with the mouse on the image. After that point the name was introduced, it can be saved. When all nodes have been introduced, is the next step, namely the introduction of road between nodes.

#### 4. USER INTERFACE

The program has an intuitive interface (fig.7.), easy to use. It starts with a default map, or final map open. If the required files to open the map files are not found, then an error will be generated and the program will start without a map, the user will open the map he wants.

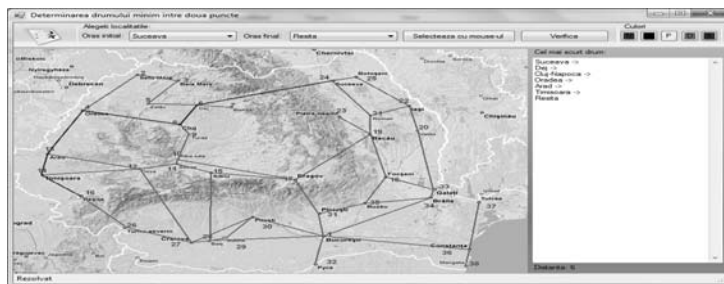


Fig. 7. Main screen

Pressing the button on the top left will show the application menu, which will be explained below:

- " **Deschide hartă** " will display the dialog box (fig.8.) for opening a file with a map. Resources are files in the directory of the application directory;
- " **Creează hartă** " will display a window, the user can create new maps, using an existing image and selecting nodes and roads, and the name of nodes and distances from roads;

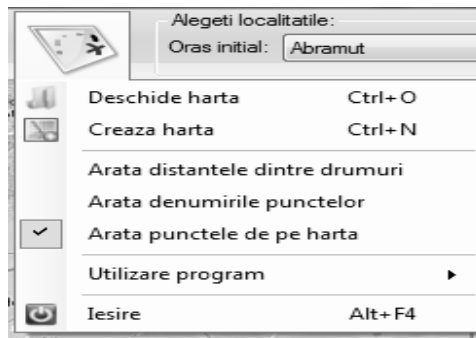


Fig. 8. Program menu

- **Display Options.** The program is possible that the names of nodes (i.e. cities) are already on the map. In this case, uncheck the option that will show the names. Each of the three options can be activated when necessary;
- **" Utilizare program "** contains a submenu that provides information about how to use the program. 3 video tutorials are present: the search road map, open map, creating newmap;
- **" Ieisre "** will close the program

## 5. INTERNAL STRUCTURE

The program was developed in Visual Studio 2010. NET Framework 3.5 using C#. The base is represented by a class that applies the algorithm on a map stored Floyd as I said earlier [3].



Fig. 9. Basic classes used in the program

These classes are separate programs (fig. 9.) and are used in these forms. It has three forms, one for users, one for those who want to add maps and one that will be shown the contents of the documentation required by the client (one of three video tutorials available that will explain to users how to use all the functionality ). As a program developed in Visual Studio 2010, NET Framework 3.5 must be installed on the pc to be able to use (fig. 10.) the program, which can be downloaded free from Microsoft's official site.



Fig. 10. The project files in Visual Studio 2010

Because the functionality is separated from the interface, then it can be improved without affecting the client or his work. By changing the grade of the road map search algorithm can be streamlined, and other algorithms can be implemented, such as [3] Dijkstra's algorithm or Bellman-Ford.

The program features three video tutorials. These can be accessed from the menu. At the request of a tutorial, you'll see a form in which we find a media player that plays the tutorial specified.



Fig. 11. Help window with video tutorial

## REFERENCES

- [1]. **Egri A.** : *Artificial intelligence and robotic*. Focus Publishing, ISBN 973 -8367 - 48 – 4, Petrosani, Romania, 2002.
- [2]. **Egri A.** : *The simulation of time-optimal control for robotic arms*. Control Engineering and Applied Informatics, CEAI, vol.6, nr.2, ISSN 1454-8658, 2004 .
- [3]. **Manber U.** : *Introduction to Algorithms. A Creative Approach*, Addison Wesley, 1989.
- [4]. **Whitby, B.** : *Artificial intelligence* . Oneworld Publications, ISBN 1851683224, London, England, 2003.
- [5]. **\*\*\*** : *Google map Free Download* , google.brothersoft.com.

## INDEX OF AUTHORS

<b>B</b>	<b>P</b>
<b>BARBU C., 49, 77</b>	<b>PANĂ C.L., 11</b>
<b>BOGDANFFY L., 77</b>	<b>PĂTRĂSCOIU N., 71</b>
<b>BUBATU R., 49, 77</b>	<b>POP E., 49</b>
	<b>POPESCU F.G., 11, 29</b>
<b>D</b>	<b>S</b>
<b>DINOIU A.N., 77</b>	<b>SAMOILĂ B.L., 17, 29, 43</b>
	<b>SÎRB V.C., 83</b>
<b>E</b>	<b>STOCHIȚOIU M.D., 5, 37</b>
<b>EGRI A., 83</b>	<b>STOICUȚA O., 55</b>
	<b>T</b>
<b>M</b>	<b>TĂBĂCARU T., 17, 43</b>
<b>MÂNDRESCU C, 55</b>	<b>TOMA A.I., 11, 29</b>
<b>MITITICA T., 29</b>	<b>TOMUȘ A.M., 71</b>
	<b>U</b>
<b>N</b>	<b>UȚU I., 5, 37</b>
<b>NICULESCU T., 23</b>	

## REVIEWERS

Assoc. Prof. dr. ing. Susana Arad  
Prof. dr. ing. Ion Fotau  
Assoc. Prof. dr. ing. Corneliu Mandrescu  
Assoc. Prof. dr. ing. Nicolae Patrascoiu  
Prof. dr. ing. Aron Poanta  
Prof. dr. ing. mat. Emil Pop  
Assoc. Prof. dr. ing. Ilie Utu